Formulation and process development of biodegradable microparticles for controlled parenteral drug delivery

Inaugural-Dissertation
to obtain the academic degree
Doctor rerum naturalium (Dr. rer. nat.)

submitted to the Department of Biology, Chemistry and Pharmacy
of Freie Universität Berlin

by

LISA BESSLICH

2020

Die vorliegende Arbeit wurde von März 2015 bis Juni 2020 unter der Leitung von Prof. Dr. Roland Bodmeier am Institut für Pharmazie angefertigt.

1. Gutachter: Prof. Dr. Roland Bodmeier
2. Gutachter: Prof. Dr. Philippe Maincent

Disputation am: 16.07.2020

Selbstständigkeitserklärung

Hiermit erkläre ich, dass ich diese Arbeit selbständig verfasst habe und keine anderen als die angegebenen Quellen und Hilfsmittel in Anspruch genommen habe. Ich versichere, dass diese Arbeit in dieser oder anderer Form keiner anderen Prüfungsbehörde vorgelegt wurde.

Berlin, den 03.08.2020

Lisa Beßlich

To my family

Acknowledgements

Table of Contents

1. INTRODUCTION

The present thesis discusses the formulation and process development, optimization and characterization of biodegradable drug-loaded microparticles intended for controlled parenteral drug delivery. In the following chapter, available drug delivery systems are described and compared. The greatest attention is being paid to biodegradable microparticles, with focus on formulation, manufacturing techniques, their characterization and associated challenges.

1.1 Drug delivery systems for controlled parenteral drug delivery

Parenteral drug delivery has received a growing attention in the past decades. It is applicable for drugs which are not suitable for gastrointestinal administration, e.g. due to stability, solubility, or permeability problems, or, more importantly, if a prolonged release is aimed [1-4].

Drug delivery forms based on polymers able control the drug release show certain advantages. A reduced frequency of injections leads to an enhanced patient compliance especially in the treatment of chronic diseases. Additionally, reduced fluctuations in the drug plasma concentration profile may increase safety and efficacy of the drug product [5]. Despite the long approval time of polymers for parenteral use and the aforementioned advantages, only 19 different drugs in long-acting PLGA depot formulations have been approved by the U.S. Food and Drug Administration (FDA) [6]. The major concern is the high effort of research and development, and multi-step manufacturing processes requiring extensive process control [6, 7].

Common polymer-based dosage forms are solid implants and microparticles, achieving controlled release up to 3-6 months (Table 1). Small, rod-shaped solid implants are usually administered with the help of a syringe under local anesthesia [8]. They can be prepared by hot-melt extrusion (HME) [9], compression [10], compression molding [11], injection molding [12] or RAM-extrusion [13]. Among these, HME is the preferred preparation method, because the continuous process under screw extrusion facilitates a more uniform drug distribution within the matrix and is scalable to industrial

processes [14]. Several drawbacks are associated with solid implants. The preparation processes commonly involve high temperature and pressure, possibly causing drug instabilities. Additionally, the requirement of a surgery under local anesthesia may reduce the patient compliance.

Table 1 Examples of marketed solid drug delivery systems with controlled drug release in Germany [15].

API	Exemplary commercial product (manufacturer)	Dosage form	Polymer	Duration of action
Buserelin acetate	Profact® (Apogepha)	Implant	PLGA	2-3 m
Carmustin	GLIADEL (Kyowa)	Implant	Polifeprosan 20	~ 1 m
Dexamethasone	Ozurdex® (Allergan)	Implant	PLGA	3-6 m
Exenatide	Bydureon® (AstraZeneca)	Microparticles	PLGA	1 w
Goserelin	Zoladex® (AstraZeneca)	Implant	PLGA	1-3 m
Leuprorelin	Leuprolin-ratiopharm (Ratiopharm)	Implant	PLA/PLGA	3 m
Leuprorelin acetate	Enantone depot® (Takeda)	Microparticles	PLA/PLGA	1-3 m
Octreotide acetate	Sandostatin LAR Depot® (Novartis)	Microparticles	PLGA	1 m
Risperidone	Risperdal Consta® (Janssen)	Microparticles	PLGA	2 w
Triptorelin acetate	Decapeptyl® Gyn (Ferring)	Microparticles	PLGA	1 m
Triptorelin embonate	Pamorelin® LA (Ipsen)	Microparticles	PLGA	1 m
Triptorelin pamoate	Decapeptyl® N (Ferring)	Microparticles	PLGA	1 m

Microparticles address this problem, as they can be injected with a smaller syringe and thus do not require a surgery [16]. However, organic solvents are used during the preparation process. Detailed information on biodegradable microparticles is given in section 1.2.

In situ forming implants (ISI) and microparticles (ISM) were developed to reduce the manufacturing process complexity [17]. For both systems, a biocompatible polymer solvent is used. After injection, the solvent diffuses out and water (non-solvent) stemming from body fluids diffuses in, ultimately leading to polymer precipitation and thereby incorporating the drug after the administration to the patient [18, 19]. For ISM, the solution is emulsified in a biocompatible outer phase, while for ISI the polymer solution containing the drug is used directly [18]. However, a drawback of these systems is the high burst driven by the polymer precipitation delay and the solvent diffusion towards the body fluids, which limits the applicability of such systems with special regard on narrow therapeutic index (NTI) drugs [20].

To control the drug release, polymers are used as the matrix former. The polymer as well as its degradation products must not evoke immune reactions (biocompatibility). Biocompatible polymers can be divided by their biodegradability, i.e. whether they can be degraded under physiological conditions after administration.

Non-biodegradable polymers commercially used for solid implants include silicone, poly(vinyl alcohol)/silicone, ethylene vinyl acetate and polyimide. Release from these drug delivery systems may be up to 5 years but require a removal by surgery.

Biodegradable polymers are for example poly(lactide), poly(glycolide), poly (lactide-co-glycolide), poly(ethylene glycol)-poly(lactide), polycaprolactone, tri(ethylene glycol) polyorthoester and polyanhydrides.

Of these, only the three polymers poly(lactic acid), poly(lactide-*co*-glycolide) and polifeprosan 20 (polyanhydride) are currently available in solid drug delivery systems on the German market (Table 1).

1.2 Microparticles for parenteral controlled drug delivery

Microparticles are, as defined by the International Union of Pure and Applied Chemistry (IUPAC), particles sized between 0.1 and 100 µm [21]. The lower limit between micro- and nanosizing is still a matter of debate according to IUPAC. Due to their small size, a parenteral (i.e. s.c. or i.m.) administration without, in opposite to solid implants, the need of a surgery or local anesthesia is feasible with a 20-gauge needle [16, 22]. Microparticles are commonly composed of a biodegradable, biocompatible matrix, a drug, and possible additive excipients. One distinguishes between different forms of microparticles depending on the drug distribution within the particulate, the architecture of which has a great influence on the drug release.
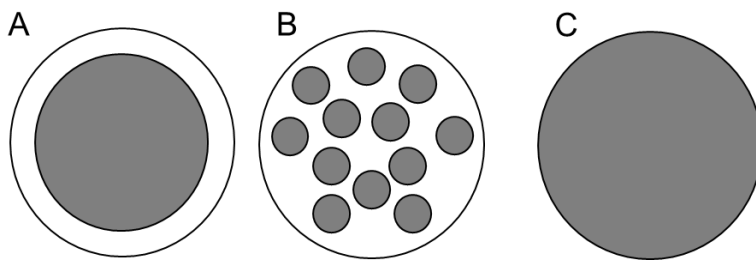
Figure 1 Schematic display of different microparticle morphologies depending on the drug distribution (A: microcapsule, B: multivesicular structure, C: microsphere) (adapted from [23]).

Microcapsules are hollow microparticles, with a solid shell comprising the polymer and eventually further excipients enclosing a core, which comprises the drug in form of a reservoir system (Figure 1, A). The core itself can be liquid, gaseous, semi-solid or in solid state, while the shell represents the solid barrier for drug diffusion [23-25].

In contrast to this, microspheres are characterized by a homogeneous drug dispersion (Figure 1, C). A distinction is drawn between solid and molecular dispersion of the drug, which also can have an influence on the later drug product characteristics like drug release and stability.

Additionally, intermediate forms between microspheres and microcapsules exist, characterized by many accumulates of the drug homogeneously distributed within the polymer matrix (Figure 1, B). By careful choice of the matrix and microparticles architecture determined by polymer chemistry and preparation process, a controlled drug release over hours up to several months can be designed.

The preparation method is chosen according to physicochemical properties of the drug to be encapsulated. Available methods comprise bottom-up or top-down methods. Bottom-up methods are generally based on the polymer precipitation (e.g. solvent evaporation, solvent extraction, spray drying, spray congealing, phase separation/ coacervation, melt emulsification) or by interfacial polymerization methods. Challenges of those methods include low encapsulation efficiencies, complex process setups and commonly the use of organic solvents as processing aids. Low drug loadings and encapsulation efficiencies can be optimized by choosing suitable manufacturing conditions, which is desirable especially for cost-intensive drugs like e.g. peptides or proteins [26, 27].

Top-down methods comprise the preparation of solid matrices (e.g. by extrusion, compression or melting/cooling) followed by diminution [28, 29]. Despite the omission of organic solvents and high drug loadings, there are sound disadvantages. Uncontrollable high burst due to high surface area, low control on particle shape and high energy input resulting in possible drug instabilities are expected.

Major research interest focusses therefore on bottom-up preparation methods like organic phase separation or solvent evaporation, which is given more detailed information on in section 1.2.2.

1.2.1 Poly(lactide-*co*-glycolide) as biodegradable matrix

Due to its biodegradability and biocompatibility, poly(lactide-*co*-glycolide) (PLGA) is commonly used as the matrix of polymer-based biodegradable drug delivery systems (Table 1).

The degradation of the aliphatic polyester PLGA is governed by acid- or base-catalyzed hydrolysis of the ester backbone [30]. Oligomers and monomers of increasing water-solubility are formed, while critical average molecular weight of water-soluble PLGA-oligomers range from 1050 to 1150 [31]. Degradation products are the monomers lactic acid and glycolic acid.

The degradation rate of the copolymer determines the drug release onset, which is affected by the physicochemical properties of the polymer. The formulation and manufacturing process of the polymer controls the polymer attributes. PLGA can be synthesized by ring-opening polymerization of lactide and glycolide monomers with the help of catalysts and initiators [32]. The microstructure of the copolymer (monomer distribution along the polymer backbone) determines the thermal properties, acidic

microclimates and ultimately the degradation rate [33, 34]. The ratio between the monomers lactide and glycolide determines the hydrophilicity and thus the solubility and degradation of the polymer [6, 35]. Lactide monomers contain methyl groups which increase the hydrophobicity, increasing the polymer degradation time. By end-capping the polymer, i.e. shielding the terminal acid function by esterification, the hydrophilicity decreases, resulting in increased degradation times [36]. The molecular weight determines additionally the polymer degradation [37]. With increasing molecular weight, the time until soluble oligomers or monomers are formed increases, thus increasing the time for degradation. Furthermore, the molecular weight distribution may influence the solubility profile and ultimately the drug release.

Additionally, the physicochemical properties of the polymer may have a strong influence on solubilities in organic solvents, which is of importance during formulation and process development [6].

1.2.2 Common preparation methods for PLGA microparticles

1.2.2.1 Organic phase separation: Methodological aspects and associated challenges

Drug-loaded microparticles can be prepared by organic phase separation (Figure 7). First, the drug is suspended, emulsified, or dissolved in an organic phase with a biodegradable polymer and a suitable solvent. By the addition of a suitable non-solvent for the polymer, a liquid-liquid phase separation is induced, causing the formation of a polymer-poor (continuous phase) and a polymer-rich phase (dispersed phase). Prerequisites have been described and studied elsewhere to successfully incorporate the drug within the polymer-rich phase which is then covered by the polymer-poor phase [38, 39]. In short, for a successful encapsulation of the dispersed phase, the interfacial tension between drug and polymer-poor phase must be high, while it must be low between drug and polymer-rich phase. Additionally, the surface tension between drug and polymer-poor phase must be higher than the surface tension between polymer-rich and polymer-poor phase.

The nascent microdroplets are then transferred to a hardening bath comprising a hardening agent, which solidifies the droplets. After rinsing to remove adhering non-)solvent or drug, microparticles are dried and sieved.

In general, a liquid-liquid phase separation in a polymer solution can be triggered by a variation in its composition [40]. By addition of a suitable non-solvent for the polymer, i.e. silicon oil, the mixture becomes thermodynamically unstable. The separation of the mixture into two separate liquid phases, of which one is a polymer-rich and the other a polymer-poor phase, decreases the free energy and a thermodynamically stable equilibrium is reached [41]. The theoretical basics regarding thermodynamics during the phase separation process were intensely described and reviewed in the literature, which focused on the description of solubilities and enthalpic and entropic interactions in the ternary phase systems [7, 40]. By this, good solvents for polymers, suitable non-solvents (high polymer-solvent interaction parameter) and hardening agents may be predicted. Based on the Flory-Huggins theory [42], who introduced a lattice model to describe solubilities, polymers will only dissolve in solvents if the interaction parameter is lower than a critical interaction parameter value χ_c. This parameter is at a given temperature

$$\chi_c = 0.5 \left(1 + \frac{1}{\sqrt{x}} \right)^2 \tag{1}$$

with x the polymerization degree of the polymer [43]. Considering very high molecular weights of the polymer, the critical value can be approximated with

$$\lim_{x \to \infty} 0.5 \left(1 + \frac{1}{\sqrt{x}} \right)^2 = 0.5 \tag{2}$$

and concluded, that at interaction values $\chi_c > 0.5$ a phase separation will occur. Though this approach is only applicable for binary systems, it helps to understand the basis of phase separation by interaction potential between solvent and polymer.

The solubility of polymers was also described by Hansen et al. [44], who stated that the solubility of polymers in solvents is influenced by hydrogen-bonding δ_h, polar forces δ_p and dispersive forces δ_d. Another approach is the Hildebrand solubility parameter, which is directly linked to the cohesive energy density (CED), being the energy required to separate the molecules of the material to an infinite distance [7, 44]. Clearly, the solubility of a material correlates with the lattice energy, as this energy needs to be overcome to dissolve the respective material.

The knowledge about the mutual affinities between components of the ternary phase system is important for a successful preparation of microparticles [7]. A liquid-liquid phase separation is aimed, which, in contrast to a solid-liquid phase separation, leads to a viscous coacervate phase which can be processed into free-flowing microparticles by a final hardening step. If the interaction between polymer and solvent is too high, the desolvation of the polymer is too weak and the coacervate phase will thus be too liquid for microencapsulation. If in contrast the interaction between the polymer and the solvent is too low, the desolvation of the polymer will be too strong and a solid-liquid phase separation (precipitation) will occur. Thus, only a moderate polymer desolvation driven by a slightly lower interaction between polymer-solvent than between solvent-coacervating agent and polymer-coacervating agent will lead to a sufficient viscosity of the coacervate phase [7].

Additionally, the desolvation depends on component concentrations in the mixture. During phase separation, the coacervation agent is added subsequently changing solvent and non-solvent distribution between the phases dynamically. Upon an increasing non-solvent concentration, the polymer solvent is extracted from the polymer-rich phase to the polymer-poor phase, causing a concentration of the polymer-rich phase indicated by a volume decrease [45]. Additionally, the viscosity of the polymer-rich phase increases with increasing non-solvent amount [46]. Against this background, the amount of non-solvent is essential to obtain polymer-rich droplets of a viscosity sufficient for transfer, but not yet in a sticky state. This critical non-solvent concentration is described by the "stability window".

For the solidification of the nascent microdroplets, high interaction parameters between the polymer solvent and the hardening agent are required. Moreover, the non-solvent must be miscible with the hardening agent for sufficient dilution.

The water-free phase separation process is particularly suitable for water-soluble drugs, achieving high encapsulation efficiencies and low burst. Nevertheless, the preparation method is associated with various challenges. Lack of process robustness is a major drawback, with a high tendency to agglomeration of microparticles upon transfer to the hardening bath. There is only limited information on process development and optimization available, and the complex, multi-step batch-process results in a product by process, which lacks scalability and transferability to industrial manufacturing processes. For example, the stability window is conventionally

determined by optical microscopy [47]. Visual examination of the microscopical appearance of a phase-separated mixture depending on formulation parameters is then used to define the amount of non-solvent needed to meet the stability window in the preparation process. The method lacks accuracy, as the interpretation depends on the operator. The robustness is expected to be low as the sample composition can be affected due to evaporation of the polymer solvent. Additionally, the results have to be interpreted carefully as they do not fully represent the actual conditions of the microparticle preparation process.

Furthermore, residual solvents represent a major drawback of the preparation method, which have to be controlled and minimized in accordance with official guidelines [2, 3]. It is thus expected that detailed information on the phase separation process can support process optimization for future development studies. For example, *in situ* visualization tools (e.g. Crystalline®) which are currently gaining attention regarding dynamic systems like crystallization processes [48] may improve the characterization of the phase separation process. Additionally, the influence of formulation and process parameters on quality attributes like agglomeration, particle size, encapsulation efficiency and residual solvents should be considered.

1.2.2.2 Solvent evaporation: Methodological aspects and associated challenges

To prepare microparticles by solvent evaporation method, a drug is dissolved, dispersed, or emulsified in a polymer solution [49, 50] (Figure 2). The organic phase is then emulsified in an aqueous outer phase comprising a stabilizer. The polymer solvent is evaporated under stirring, and the nascent microdroplets solidify upon polymer precipitation. After collection, particles are dried and sieved.
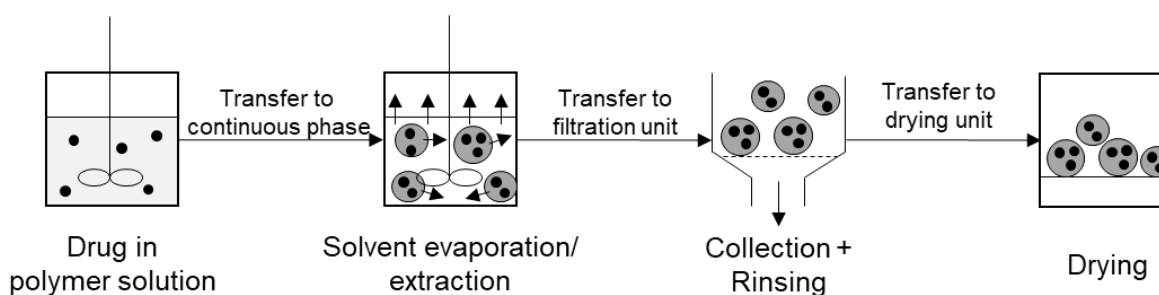
Figure 2 Schematic overview of the microparticle preparation by solvent evaporation/ extraction process.

Formulation and process parameters have a critical influence on the quality attributes of the microparticles. A major challenge of the preparation process is to decrease the initial drug release and increase the encapsulation efficiency, which applies especially to water-soluble drugs diffusing out to the aqueous phase until polymer precipitation occurs.

Decreasing the drug solubility in or increasing the osmotic pressure of the aqueous phase [51, 52] and using W/O/W or S/O/W processes [53, 54] decreased the drug diffusion to the outer aqueous phase, resulting in increased encapsulation efficiencies. Decreasing the solubility of the polymer in the solvent [55], increasing the solubility of the solvent in the outer phase [56], increasing the polymer concentration [56-58], increasing the amount of outer phase [58] or increasing the solvent removal rate [59, 60] accelerated the polymer precipitation, resulting in increased encapsulation efficiencies.

However, increasing the precipitation speed may lead to an increased porosity, which can alter drug release mechanism [61].

As a drawback, processing times of several hours are needed to completely remove the organic solvent in solvent evaporation processes. By increasing the amount of the aqueous phase (solvent extraction method), processing times can be reduced; however, too high volumes are often unfavorable in industrial processes as they reduce processable batch sizes.

1.2.3 Drug release from PLGA microparticles

PLGA biodegrades into biocompatible, water-soluble monomers, releasing incorporated drugs in a controlled manner upon contact with biological fluids [62]. PLGA matrices are degraded via bulk erosion (Figure 3), which is characterized by several steps. Starting with the hydrolysis of the backbone, the molecular weight decreases, while the mass remains constant in the beginning. With decreasing molecular weight the glass transition temperature decreases, which is further supported by an increasing water influx acting as a plasticizer. Thus, loss of mechanical properties is caused. After reaching a certain molecular weight threshold, mass loss is initiated. In contrast to this, other polymers like poly(orthoesters) show surface erosion (Figure 3) [63].
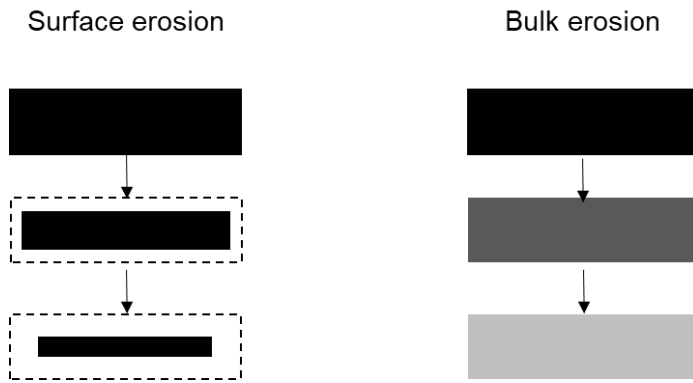
Figure 3 Surface erosion versus bulk erosion of a biodegradable polymeric matrix (adapted from [64]).

The mechanism of degradation results in typical triphasic drug release patterns of PLGA drug delivery systems (Figure 4) [65].
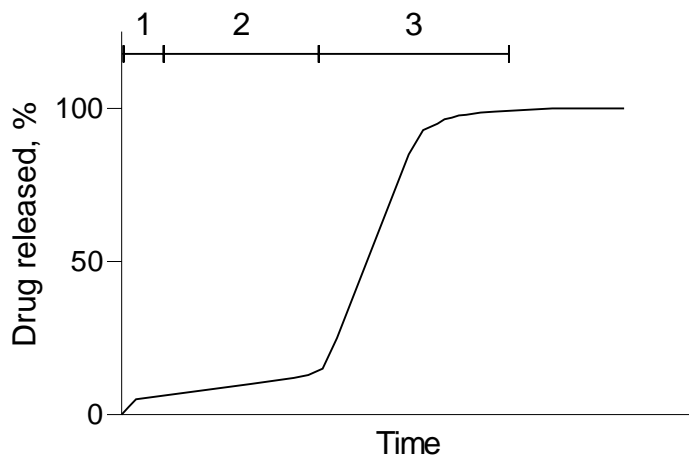
Figure 4 Typical triphasic release pattern of PLGA drug delivery systems with initial release (1), lag-phase (2) and fast release (3).

Release starts with an initial drug release (burst) (Figure 4, 1) [66, 67]. The burst is attributed to drug present on or close to the surface, which is a major concern during the drug release from microparticles, as the surface area is higher compared to implants. After this, a lag-time follows which is dominated by drug diffusion through interconnected, water-filled pores of the matrix or the polymer matrix (Figure 4, 2) [68, 69]. The diffusion depends also on the physicochemical properties of the drug, e.g. solubility in the matrix or molecular weight [70, 71]. After the lag-phase, the third release phase starts with comparatively fast drug release (Figure 4, 3). In general, the

onset of the third release phase can be altered by choice of the physicochemical properties of the polymer [72]. However, the physicochemical properties of the drug (e.g. solubility, solid state), interactions between drug and polymer as well as the formulation and morphology of the microparticles (e.g. drug loading, particle size, surface morphology, porosity and drug distribution) have a strong influence on all release phases, which has been extensively studied and summarized elsewhere [65]. As the numerous release mechanisms may overlay, prediction of the release pattern is a major concern in research and development.

1.3 Emulsification and emulsion stability upon processing

Independent of the preparation method, both organic phase separation and solvent evaporation/extraction include the formation of emulsions, where a dispersion of two immiscible or partially miscible liquid phases is formed. The key parameters for the droplet formation are the operating conditions, the resulting flow conditions in the mixing device geometry and the physicochemical properties of the dispersed and continuous phase, e.g. viscosity and density for liquids [73], which have to be considered during formulation and process development. Emulsions are thermodynamically instable systems. The instability mechanism of coalescence, which is relevant to the coacervate stability during microparticle preparation by organic phase separation, is thus summarized in the following. Additionally, pharmaceutical mixing technologies are described, which are commonly used in the preparation of polymer-based microparticles for parenteral drug delivery.

1.3.1 Stability of emulsions upon processing

Emulsions are thermodynamically instable systems, tending to decrease the interfacial area to lower the system energy [74], which can be achieved, amongst other mechanisms, by coalescence and gravitational separation [75]. These physicochemical instabilities may already occur during emulsification steps in the phase separation process.
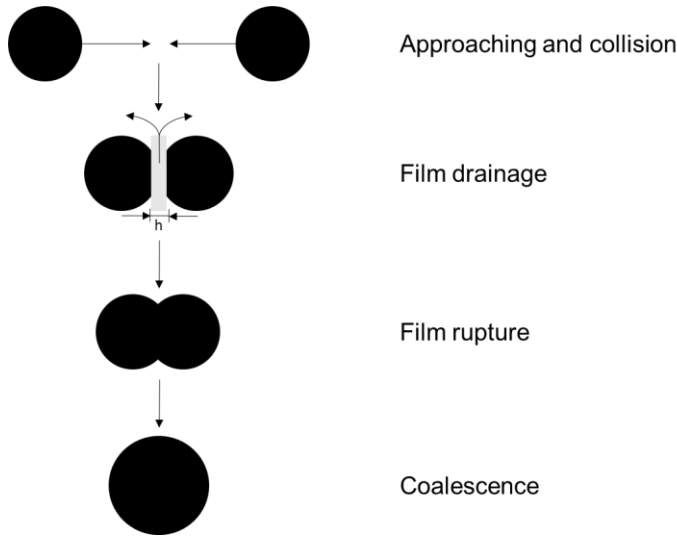
Figure 5 Schematic representation of single steps occurring during coalescence (adapted from [76, 77]).

The mechanism of coalescence can be divided in distinct steps (Figure 5) according to the film drainage model, which is the most popular theory among others regarding the coalescence process [77, 78]. After the approaching and collision of two droplets, a drainage of the interfacial film, more particularly the dispersed phase between the two adjacent droplets, occurs. If the distance between the two droplets decreases to a critical rupture thickness, attracting intermolecular forces like van der Waal's forces occur and if the interaction time is sufficient, droplets will coalesce [79, 80].

For a coalescence occurrence, both the frequency of collisions and the probability of a coalescence in the case of collision have to be considered. First, from the collision frequency N

$$N = \left(\frac{8\pi}{3}\right)^{\frac{1}{2}} d^2 n^2 (\varepsilon d)^{\frac{1}{3}} \tag{3}$$

with ε the energy dissipation rate of the fluid per unit mass, d the droplet diameter, and n the number of droplets per volume it can be concluded that the collision frequency of droplets is decreased with decreasing energy dissipation rate, droplet size and decreasing volume concentration of the dispersed phase [81].

Second, the coalescence efficiency is given by

$$\lambda = \exp\left(-\frac{t_{drainage}}{t_{contact}}\right) \tag{4}$$

with $t_{drainage}$ the drainage and $t_{contact}$ the contact or interaction time. The interaction time is mainly influenced by the flow during stirring, while the drainage time is the sum of interaction forces between the droplets and the mobility of the interphase, which is itself dominated by the viscosity of the continuous phase [77, 82, 83]. The probability of coalescence is thus decreased with decreasing the interaction forces between the droplets and decreasing the mobility of the interphase.

Emulsion stabilization approaches follow additionally Stoke's Law regarding the terminal velocity of a sphere falling in a fluid

$$v_p = \frac{2}{9} \frac{r^2 g (\rho_{DP} - \rho_{CP})}{\eta} \tag{5}$$

with r the droplet diameter, g the gravitational filed strength, ρ_{DP} the density of the dispersed phase, ρ_{CP} the density of the continuous phase and η the dynamic viscosity [84]. With decreasing terminal velocity of the droplets, the emulsion stability is increased, which is achieved by reduced droplet sizes, equalization of the densities of dispersed and continuous phase and increasing the viscosity of the continuous phase.

1.3.2 Mixing in pharmaceutical applications

Depending on the specific user requirement specification according to physicochemical properties of the phases and mixture, the desired dispersion quality (droplet size distribution) or flexibility in set-up, a suitable mixer has to be critically chosen. In the following, the most important mixers used for mixing in pharmaceutical applications are listed and described regarding their set-up, mixing mechanism and associated advantages or drawbacks.

1.3.2.1 Rotor-Stator-Mixing

The high-shear rotor-stator mixer is commonly used in the preparation process of pharmaceutical products [85-88]. In rotor-stator mixers, a high velocity spinning rotor is located within a static stator screen, while the distance between rotor and stator screen, the rotor stator gap clearance δ, is kept short. Upon movement, the rotor accelerates the fluid tangentially and forces it through the stator slots [89]. By decreasing the stator slot widths, the hydrodynamic forces increase [90]. The high shear stress characteristic for the rotor-stator mixers explains the high dispersing

efficiency of these mixers, leading to fast and efficient droplet and particle size reductions even for demanding preparation processes of e.g. nano-dispersions or -emulsions [91]. A further advantage is the scalability of the process, as well as the feasibility of operation in continuous mode by the installation of in-line rotor-stator mixers [89, 92-94].

1.3.2.2 Ultrasonication

The application of ultrasonic irradiation is commonly used in the preparation of dispersions and emulsions [95, 96]. A sonication probe (sonotrode) contains piezoelectric transducers and is connected to a power supply unit. The ultrasonic vibrations are transmitted directly to the medium. The ultrasound irradiation generates an acoustic cavitation, which is the formation, growth and implosive collapse of bubbles in the medium causing, locally, extreme conditions. Shockwaves or jets cause mechanical stress, which is able to disrupt droplets of the dispersed phase or cause interparticle collisions. Dispersion efficiency increases generally with dispersion time, ultrasonic radiation intensity and ultrasonic frequency, but depends also on physicochemical properties of the dispersed and continuous phase [95, 97, 98]. The emulsification efficiency was comparable to homogenization of PMMA solutions in methylene chloride emulsified in PVA solutions [99]. Ultrasonication was superior compared to mechanical agitation, as smaller average droplet sizes, less energy consumption and improved droplet size distribution uniformity were found, while reducing the required amount of stabilizer [100].

However, the local high temperatures and pressures are known to cause harmful damages to sensitive drugs like peptides and proteins leading to activity loss [101]. Additionally, an ultrasound-induced polymer degradation occurred in the case of PLA and PLGA dispersions, leading to decreased molecular weight which might influence drug release [102]. As the dispersion efficiency decreases with increasing distance to the sonication probe, scalability is difficult [97, 99, 103]. Furthermore, shedding may cause sample contamination with metallic particles stemming from the sonication probe [103].

1.3.2.3 Impeller

Overhead stirrers equipped with impellers are commonly used at development and production stages for the preparation of dispersions, emulsions and solutions. Upon movement of the impeller in a vessel comprising the mixture, a certain flow is achieved. The flow pattern may be radial or axial, while the latter is preferred as higher mixing efficiencies are achieved [104, 105].

To describe and compare different stirrers, the dimensionless power number N_p can be used, defined by

$$N_p = \frac{P}{\rho n^3 d^5} \tag{6}$$

with P the power, ρ the fluid density, n the stirring speed and d the stirrer diameter [106]. With increasing power number, the actually available fraction of the introduced power to the system increases.

Both flow pattern and power number highly depend on the impeller geometry and the vessel wall [107].

Scale-up has been described for stirred tanks and already successfully performed for the preparation of emulsions or microparticles [108]. However, as the scale-up of discontinuous processes is commonly conducted by dimensional analysis (geometric scale up), the flexibility of batch sizes is limited, which has to be considered already at development stages.

1.3.2.4 Static mixers

Static mixers are motionless and composed of mixer elements of different shape and geometry which are fitted in a housing tube. By pumping the phases to be mixed at a certain phase ratio through the mixer, phases are combined and thus a mixing is achieved (Figure 6).

Feeds　　　Pumps　　　Static mixer　　　Reservoir
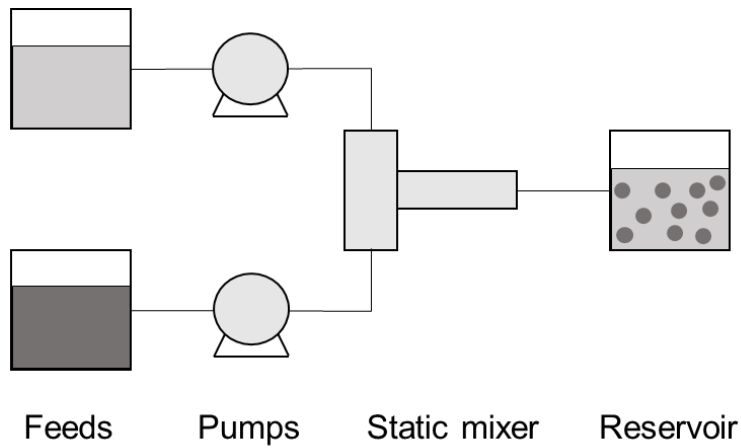
Figure 6 Set-up of a static mixer combining two phases resulting in an emulsion (adapted from [109]). Feed solutions are transferred by pumps to a T-piece connected to the static mixer and collected in a reservoir tank.

Two mixing mechanisms may occur upon mixing with a static mixer [110]. First, upon passing a mixing element, the phases are divided, possibly rotated, and recombined after the element [110-112]. Thus, the number of striations N increases exponentially with the number of elements n following the correlation

$$N = N_{start} k^n \tag{7}$$

with N_{start} the number of layers at the beginning and k the number of channels created by one element. The stretching and folding mechanism is decisive in the laminar flow regime [110]. Second, a radial mixing may occur in the mixer, which applies for laminar and turbulent mixing. By rotations during passing the element, additional mixing is achieved [110].

The fluid dynamics (laminar or turbulent) can be described with the dimensionless Reynolds number Re

$$Re = \frac{\rho v d}{\eta}$$

with ρ the fluid density, v the flow rate, d the characteristic diameter and η the dynamic viscosity of the fluid. The characteristic diameter is specified for different geometries of the mixer elements. If the Reynolds number reaches a critical value Re_{crit}, the flow regime changes from laminar to turbulent.

Mixing efficiency and underlying mechanism depend strongly on the fluid dynamics [109], the static mixer geometry [113, 114], number of elements or number of passes [109, 115], flow rate [109] and physicochemical properties of the dispersed and

continuous phase [109, 113, 116]. In general, with increasing Reynolds numbers, increasing flow rates and increasing number of elements, mixing efficiency is improved.

Static mixers are of high importance in industrial applications, as they require significantly less space compared to stirred tanks. Due to the lack of moving parts, the maintenance effort in terms of time and costs are comparatively low [110], with less space needed, lower product residence time and lower energy consumption compared to stirred vessel processes [117]. The process was scalable [109]. Additionally, the continuous process facilitates a high flexibility in batch size meeting industrial needs, and numbering up represents an efficient way to scale-up in a fast and robust manner. However, high equipment demands raise especially for highly viscous mixtures and mixtures comprising organic solvents regarding the materials and set-up of static mixers and high pressure pumps. A further drawback is the increasing pressure with decreasing tubing diameter, limiting the downscaling of static mixers particularly for highly viscous materials. Furthermore, comparatively high material consumption has to be considered for small batches as tubings have to be filled completely to allow processing.

1.4 Residual solvents in pharmaceutical products

Only few preparation methods like hot-melt extrusion or direct compression for PLGA drug delivery systems are available which do not require the use of organic solvents. For the majority of microparticle preparation methods, the polymer must be processed in dissolved state prior to controlled precipitation and drug microencapsulation. Due to the respective solubility of polyesters, the choice of solvents is limited, and approaches are currently under investigation to replace or limit the solvents used.

Methylene chloride is commonly used as the polymer solvent for the preparation of microparticles by solvent evaporation and organic phase separation [118-121]. For the latter, a non-solvent is needed to induce the liquid-liquid phase separation. A common non-solvent is the non-volatile silicon oil polydimethylsiloxane [7, 47]. For solidification, the phase-separated emulsion is transferred to a hardening bath, comprising a hardening agent which extracts the solvent. Common hardening agents are the volatile silicon oil octamethylcyclotetrasiloxane or alkanes like hexane or heptane [122].

Excipients used as processing aids should be removed to minimum in the products, which applies in particular for organic solvents in polymer-based drug formulations because of two major reasons.

First, for toxicological reasons assuring the patient's safety, pharmaceutical products must comply with official limits recommended by the current ICH guideline [123] (Table 2). The guideline applies to all dosage forms and administration routes and categorizes solvents in three different classes by risk assessment regarding their potential risk to human health.

Class 1 solvents should be avoided, as they are known or strongly suspected human carcinogens, and represent environmental hazards. Class 2 solvents can be used but must be limited to given values according to the guideline. They are non-genotoxic animal carcinogens or possible causative agents of other irreversible toxicity (i.e. neurotoxicity, teratogenicity), or suspected of other significant but reversible toxicities. Limits for these solvents are given by the term permitted daily exposure (PDE), which corresponds to a pharmaceutically acceptable daily intake of the residual solvent. Class 3 solvents should be preferably used. No health-based exposure limit is needed, and the PDE of class 3 solvents is > 50 mg per day. Classification is conducted according to a permanent review of currently available safety data, thus the list is not exhaustive and classification of solvents can be adjusted whenever necessary [123].

Second, critical quality attributes of microparticles may be altered by the presence of residual solvents. Residual solvents are small molecules acting as plasticizers in the polymeric matrix, thus reducing the glass transition temperature and potentially affecting the drug release and/or raising stability issues during the shelf-life [124-127]. Thus, residual solvents have to not only to be minimized but also to be controlled.

Table 2 Common organic solvents of classes 2 and 3 used as processing aids for pharmaceutical products with their classification according to the ICH guideline and the permitted daily intake (PDE) (adapted from [123]).

Solvent	PDE (mg/day)
Class II	
Acetonitrile	4.1
Chloroform	0.6
Dichloromethane	6.0
N,N-Dimethylformamide	8.8
Hexane	2.9
Methanol	30.0
N-Methylpyrrolidone	5.3
Tetrahydrofuran	7.2
Toluene	8.9
Class III	
Acetic acid	50
Acetone	50
Butanol	50
Dimethyl sulfoxide	50
Ethanol	50
Ethyl acetate	50
Ethyl ether	50
Heptane	50
Propanol	50

One of the first approaches to detect and quantify methylene chloride in microparticles was thermogravimetry (TG) and chlorine analysis [128]. Meanwhile, the most common method to quantify volatile organic solvents is gas chromatography (GC), usually coupled with flame ionization detector (FID). GC involves a high effort of sample

preparation. As matrix effects are common for the detection of volatile residual solvents, the compendial method recommends the standard addition method for quantification [129].

As non-volatile residual solvents cannot be quantified by GC, a further analytical method is needed for the quantification of polydimethylsiloxane appearing in microparticles prepared by phase separation method. Only few results have been reported on polydimethylsiloxane residuals [122], and, to our knowledge, no information is available in the scientific literature on polydimethylsiloxane residuals when microparticles were hardened with the silicon oil octamethylcyclotetrasiloxane. Due to their similar molecular structure, interferences were expected in FT-IR and H-NMR [122].

Numerous studies focused on the reduction of volatile residual solvents, which was mainly achieved by improving the extraction or the drying method [122, 130, 131]. Increasing the temperature close to the glass transition temperature in combination with decreased pressure was the most promising approach to lower methylene chloride residuals [122]. However, only few studies are available on the influence of formulation and process parameters on residual volatile and non-volatile solvents in PLGA microparticles prepared by the organic phase separation method.

1.5 Research Objectives

- To investigate the effect of formulation and process parameters on the critical quality attributes of microparticles prepared by an organic phase separation method

- To improve the process robustness of an organic phase separation method to reduce agglomeration, increase yield and decrease process complexity

- To develop and prove the suitability of an H-NMR method to simultaneously quantify volatile and non-volatile residual solvents in drug-loaded PLGA microparticles prepared by an organic phase separation method, and to compare it to compendial and other available methods

- To investigate the effect of formulation and process parameters on the residual solvent levels in microparticles prepared by an organic phase separation process

- To investigate the effect of the process temperature on the solvent evaporation and on critical quality attributes of blank and drug-loaded PLGA microparticles prepared by a solvent evaporation method

2. MATERIALS AND METHODS

2.1 Materials

<u>Drugs and polymers</u>

Water-soluble peptide drug, micronized minocycline-HCl (D_{50} 1.8 µm, Zhejiang Hisun, China), risperidone (Wuxi Jida Pharmaceutical Co. Ltd., Jiangyin, Jiangsu, China), acid-terminated 50:50 poly(lactide-*co*-glycolide) (PLGA) (RG 504H, Resomer, Evonik Industries AG, Essen, Germany), polyvinyl acetate (Mowiol 4-88, Merck KGaA, Darmstadt, Germany)

<u>Solvents and others</u>

Methylene chloride (Emsure, Merck KGaA, Darmstadt, Germany), polydimethylsiloxane (360 med, Dow Corning Inc., Midland, Michigan, USA), octamethylcyclotetrasiloxane (Cyclomethicone 5-NF, Dow Corning Inc., Midland, Michigan, USA), heptane (Carl Roth GmbH + Co. KG, Karlsruhe, Germany and VWR International GmbH, Darmstadt, Germany), toluene (Suprasolv® for gas chromatography, Merck KGaA, Darmstadt, Germany), N,N-dimethyl formamide (Pestinorm®, VWR International GmbH, Darmstadt, Germany), deuterated chloroform (99.8 atom %D, stabilized with Ag, Carl Roth GmbH + Co. KG, Karlsruhe, Germany). All other salts and buffers were of analytical grade.

2.2 Methods

2.2.1 Characterization of materials

2.2.1.1 Determination of drug solubility

Drug solubility was tested by a method adapted from WHO protocol [132]. In short, an overage solid amount was added to the medium to be tested and shaken at 150 rpm on an orbital shaker at the indicated temperature. The dissolved amount in aqueous media was determined by measuring the UV absorbance of the centrifuged supernatant. For methylene chloride, an aliquot of the supernatant was sampled, the solvent was evaporated, and the residual solids were then dissolved in aqueous media for UV analysis. Shaking and analysis of the supernatant every 24 hrs was continued until the drug concentration did not change anymore (NMT 5% difference to the prior time point).

2.2.1.2 Viscosity measurements

After motor adjustment, a sample of 1.0 mL was placed on a rotational rheometer (MCR 302, Anton Paar GmbH, Austria) and measured at a shear rate of 10 s^{-1} (1 measurement per second, measurement time 100 s). Temperature was controlled automatically, gap size between plate and cone (50 mm/ 1°) was 0.102 mm. The mean ± SD of 100 measurements is reported.

2.2.1.3 Static methylene chloride diffusion of methylene chloride from a 6 % PLGA solution to different solvents

To graduated reagent tubes comprising 2 mL of a 6 % w/w PLGA solution in methylene chloride, 2 mL of ethanol, octamethylcyclotetrasiloxane or heptane were added carefully. The static diffusion of methylene chloride from the polymer solution to the solvents was then investigated by following the volume change of the PLGA solution over 60 min (n=1).

2.2.2 Characterization of the phase-separation process and intermediates

2.2.2.1 Stability window with conventional method by optical microscopy

To accurately weighed aliquots of PLGA solutions (3, 6 or 9 % w/w) in methylene chloride, different polydimethylsiloxane amounts were added resulting in different pre-determined polydimethylsiloxane concentrations. The reagent tubes were carefully closed with screwing caps and mixed for 30 sec at 1200 rpm (MS2 Minishaker, IKA®-Werke GmbH & CO. KG, Staufen im Breisgau, Germany). A droplet was placed on an objective slide with a well, covered and the appearance of the mixture was observed with an optical microscope (Axioskop, Carl Zeiss AG, Oberkochen, Germany).

2.2.2.2 Volume trend investigation and resuspendability study

To accurately weighed aliquots of PLGA solutions (6 % w/w) in methylene chloride, polydimethylsiloxane was added resulting in different polydimethylsiloxane concentrations. The reagent tubes were carefully closed with screwing caps, mixed for 60 sec at 1200 rpm (MS2 Minishaker, IKA®-Werke GmbH & CO. KG, Staufen im Breisgau, Germany) and then shaken horizontally at 175 rpm for 1 h (KS 501 D, IKA®-Werke GmbH & CO. KG, Staufen im Breisgau, Germany). After centrifugation for 10 min at 3800 rpm (Mega Star 1.6R, VWR International, Radnor, Pennsylvania, United States), the volumes of the separated phases were determined. The resuspendability was then investigated by testing the vortex speed (MS2 Minishaker, IKA®-Werke GmbH & CO. KG, Staufen im Breisgau, Germany) needed to fully resuspend the coacervate phase.

2.2.2.3 Coacervate stability

To accurately weighed solutions of PLGA (3 or 6 % w/w) in methylene chloride, pre-determined amounts of polydimethylsiloxane were added, resulting in different polydimethylsiloxane concentrations. The total weight of the mixture was 4.0 g, while polymer concentration and ratios between solvent and polydimethylsiloxane were varied. Mixtures were vortexed for 10 sec (MS2 Minishaker, IKA®-Werke GmbH & CO. KG, Staufen im Breisgau, Germany), and the time until a complete phase separation occurred was measured. Samples were prepared in triplicate.

2.2.2.4 In-situ investigation of coacervate formation: Appearance, transmissivity and droplet size distribution with Crystalline®

In-situ investigations of the coacervation process were made with the help of Crystalline® (Technobis Crystallization Systems, Netherlands). An accurately weighed amount of a PLGA solution (3 or 6 % w/w) in methylene chloride was filled into an analysis cell equipped with a hook stirrer and closed carefully with an anti-solvent-screwing-cap. The non-solvent polydimethylsiloxane was added continuously through a silicon tubing (3 mm ID) with the help of a syringe pump (Harvard Apparatus, Holliston, Massachusetts, United States) and a glass syringe. Stirring speed and temperature were controlled automatically by the system. The samples were observed, *in situ*, with a camera installed perpendicular to the cell. Pictures were taken automatically every 4 sec. The transmissivity of the sample was measured continuously. Pictures were processed with ImageJ (ImageJ 1.52a, National Institutes of Health, United States) for droplet size measurements.

2.2.2.5 Solvent distribution profile

To accurately weighed aliquots of PLGA solutions (6 % w/w) in methylene chloride, different polydimethylsiloxane amounts were added resulting in different polydimethylsiloxane concentrations. The reagent tubes were carefully closed with screwing caps, vortexed at 1200 rpm for 60 sec (MS2 Minishaker, IKA®-Werke GmbH & CO. KG, Staufen im Breisgau, Germany), centrifuged at 3800 rpm for 10 min (Mega Star 1.6R, VWR International, Radnor, Pennsylvania, United States), and volumes of the separated phases were determined. Samples from the supernatant and the coacervate phase were diluted with CDCl$_3$ containing 0.2 % w/v toluene serving as an internal standard and the composition was quantified by H-NMR (Avance III, Bruker Corporation, Billerica, Massachusetts, USA). The mean polydimethylsiloxane and methylene chloride recoveries were 109.62 % and 71.29 %, respectively.

2.2.2.6 Droplet size distribution analysis by laser diffraction analysis (LD)

Droplet size distribution of an aqueous phase in a PLGA solution was determined by laser diffraction analysis (1000 rpm, dispersant: 3 % PLGA in methylene chloride,

0.5-1 % obscuration, RI 0.94, Mastersizer 2000 with Hydro 2000µP, Malvern Panalytical Ltd., Malvern, United Kingdom).

2.2.3 Characterization of the methylene chloride removal in emulsified state

2.2.3.1 Determination of the methylene chloride removal profile by weight loss study

To determine the solvent removal profiles, 2.0 g of methylene chloride were injected in a stirred 1 % w/v PVA solution controlled at a certain temperature (IKAMAG RCT, IKA®-Werke GmbH & CO. KG, Staufen im Breisgau, Germany). The weight was determined initially and followed over-time and the weight loss was attributed to methylene chloride evaporation during heating. As the phase temperatures were below the boiling point of the aqueous outer phase, water loss was negligible (0.1 % w/w during heating to 80 °C at 4 K/min).

2.2.3.2 Detection of the limit of superheat by hot stage microscopy

Methylene chloride or a PLGA solution in methylene chloride was emulsified for 60 sec in a 1 % w/v PVA solution with a vortexer (MS2 Minishaker, IKA®-Werke GmbH & CO. KG, Staufen im Breisgau, Germany) and a droplet was placed on an objective slide with well. After covering with a glass plate, the emulsion was observed with an optical microscope (Axioskop, Carl Zeiss AG, Oberkochen, Germany) under application of a temperature ramp of 5-10 K/min with a hot stage (FP82HT, Mettler-Toledo International Inc., Columbus, United States). Pictures were taken and processed with the software Zen (Carl Zeiss AG, Oberkochen, Germany). Determination of the limit of superheat was performed at least in triplicate.

2.2.4 Preparation of microparticles

2.2.4.1 Preparation of microparticles by organic phase separation (batch process) – S/O/O method

830 mg PLGA were dissolved in methylene chloride reaching a polymer concentration of 2.5-6 % w/w. Micronized minocycline HCl (drug loadings of 0, 5 or 10 %) was dispersed in the PLGA solution with a homogenizer (Ultraturrax T-25 basic, IKA Werke

GmbH & Co. KG, Staufen im Breisgau, Germany) at 17,500 rpm for 2 min. The non-solvent polydimethylsiloxane was added under stirring with a propeller stirrer (tip speed 4147 cmmin^{-1}, Eurostar 60 control, IKA Werke GmbH & Co. KG, Staufen im Breisgau, Germany) to induce coacervation, reaching polydimethylsiloxane concentrations of 35-60 % w/w in the ternary mixture. This emulsion was injected under stirring (propeller stirrer, tip speed 14,137 cmmin^{-1}, Eurostar 60 control, IKA Werke GmbH & Co. KG, Staufen im Breisgau, Germany) at 5-10 mlmin^{-1} into the hardening bath containing between 195 g and 390 g of the volatile silicone oil octamethylcyclotetrasiloxane or heptane, corresponding to methylene chloride to hardening agent ratios of 1:15 to 1:25. After hardening for 30 min, microparticles were collected by vacuum filtration (stainless-steel sieve, 10 µm) and rinsed with 70 g octamethylcyclotetrasiloxane. The microparticles were dried under vacuum at 100 mbar or 0.05 mbar under application of a temperature ramp program (Epsilon 2-4 LSCplus, Martin Christ Gefriertrocknungsanlagen GmbH, Osterode am Harz, Germany). Starting from 20°C, the temperature was held for 24 h and increased by 10 K afterwards, until 40°C were reached (total drying time 72 h).
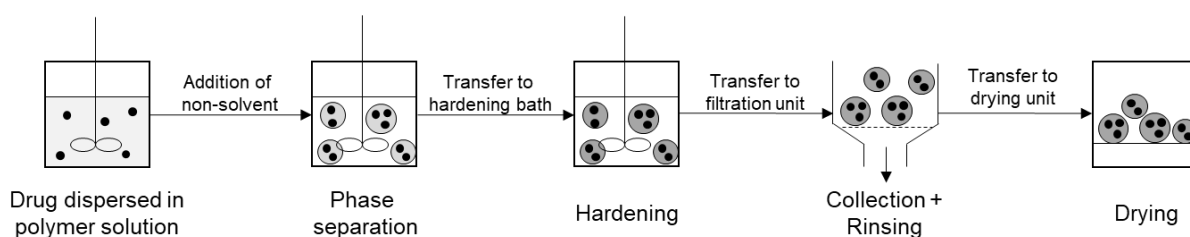
Figure 7 Scheme of the microparticle preparation process by organic phase separation (S/O/O method, batch process).

2.2.4.2 Preparation of microparticles by organic phase separation (batch process) – W/O/O method

172 mg PLGA were dissolved in 2.7 g methylene chloride (6 % w/w). Then, 130 mg of the aqueous drug solution (solid content 11 % w/w) were dispersed in the PLGA solution with a rotor-stator-dispersing tool (21,500 rpm, 2 min, Ultraturrax, IKA®-Werke GmbH & CO. KG, Staufen im Breisgau, Germany) or with a sonication probe (50 % amplitude, 30 sec, HD 200, Sonopuls, BANDELIN electronic GmbH & Co. KG). After addition of 2 g of the non-solvent polydimethylsiloxane under stirring with a homogenizer (21,500 rpm, 2 min, Ultraturrax, IKA®-Werke GmbH & CO. KG, Staufen

im Breisgau, Germany) to induce phase separation, the emulsion was injected under stirring with a propeller stirrer (500 rpm, Eurostar 60 control, IKA Werke GmbH & Co. KG, Staufen im Breisgau, Germany) into the hardening bath containing 70 g heptane. After hardening for 1 h, microparticles were collected by vacuum filtration (stainless-steel sieve, 10 µm) and rinsed with heptane, ethanol and water. The microparticles were dried in a desiccator for 72 h.
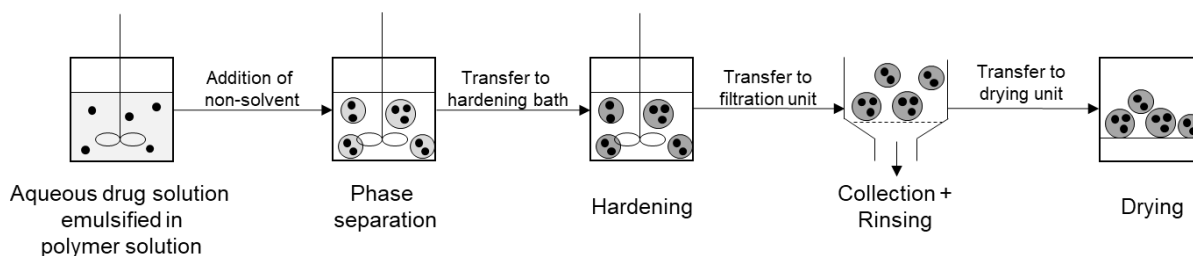
Figure 8 Scheme of the microparticle preparation process by organic phase separation (W/O/O method, batch process).

2.2.4.3 Preparation of microparticles by organic phase separation with a static mixer (continuous process)

A PLGA solution in methylene chloride (1.5-6% w/w) was combined and mixed with polydimethylsiloxane in a static mixer (Promix Solutions AG, Switzerland). If a drug was present, the micronized hydrophilic model drug was added to the PLGA solution and dispersed for 60 sec with a rotor-stator disperser (Ultraturrax T25, IKA) at 17,500 rpm. Dispersion was continued during the preparation process. The emulsion was then injected in a stirred hardening bath comprising octamethylcyclotetrasiloxane (methylene chloride to octamethylcyclotetrasiloxane ratio 1:20 w/w). Stirring of the hardening bath was performed with an overhead stirrer (IKA Eurostar 60 control, IKA) at a stirring rate of 500 rpm (5 cm propeller) for the small scale and 250 rpm (10 cm propeller) for the large scale (tip speed: 7854 cm/min). Transfer of solutions/ dispersion was performed at a total flow rate of 100-200 mL/min with two piston pumps (Ismatec FMI RH Piston Pump, ETFE pump head, Cole Parmer) through PTFE tubings (4.48 x 6.00 mm, Cole Parmer). Phase ratios of the polymer solvent and coacervating agent (methylene chloride to polydimethylsiloxane ratio, w/w, from 1.0:0.5 to 1.0:1.0) were adjusted by flow rates of the single phases. Time of injection was adjusted according

to PLGA solution flow rate to inject 10.0 g of PLGA solution. Particles were collected by vacuum filtration, washed with octamethylcyclotetrasiloxane and dried at 100 mbar for 48 hrs.
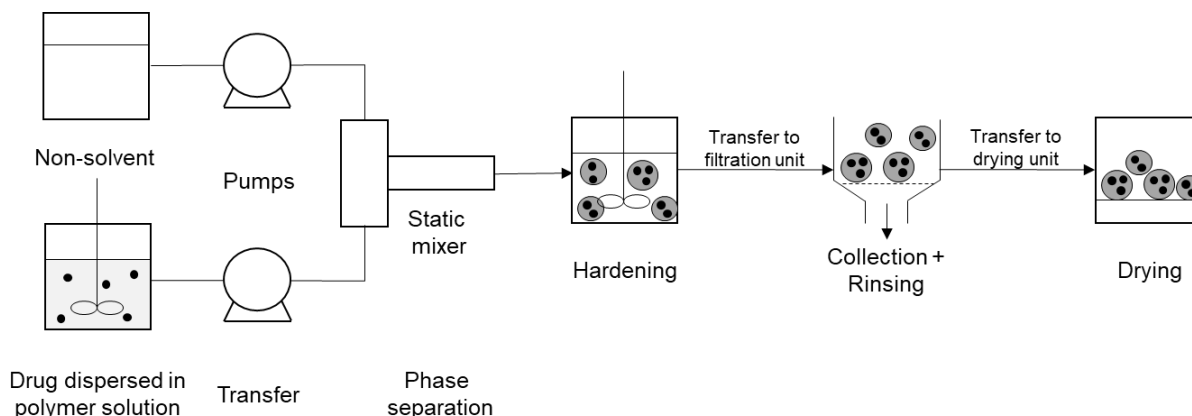
Figure 9 Scheme of the microparticle preparation process by organic phase separation (S/O/O, continuous process with a static mixer).

2.2.4.4 Preparation of microparticles by solvent evaporation method

Batches with 0, 10 and 30 % theoretical drug loading were prepared at different aqueous phase temperatures.

PLGA was dissolved together with risperidone in methylene chloride and emulsified at ambient temperature in a 1 % w/w PVA solution to form a primary emulsion (O:W ratio 1:2, w/w). The PLGA concentration in the organic phase was kept constant at 10 % w/w while the amount of drug was adapted resulting in 0, 10 or 30 % drug loading, based on the total microparticle weight. Stirring was performed with a magnetic stirrer (Electronicrührer Multipoint HP, Variomag, Fisher Scientific GmbH, Schwerte, Germany) at 400 rpm. The primary emulsion was then injected with a glass syringe through a stainless steel tubing (3 mm ID) beneath the surface of a 1 % PVA solution (O:W 1:40) under stirring at 700 rpm and controlled temperature (IKAMAG RCT, IKA®-Werke GmbH & CO. KG, Staufen im Breisgau, Germany). Depending on the preparation temperature, the dispersion was stirred for 12 hrs (25°C), 1 h (55 °C), 10 min (75 °C) or 1 min (95 °C) to evaporate methylene chloride. Thereafter, the suspension was poured into a stirred iced 0.5 % PVA solution (W:W 1:3) to cool the microparticles. The hardened microparticles were immediately separated by vacuum

filtration and washed 3 times with 300 mL deionized water before drying for 12 hrs in a desiccator followed by drying under vacuum at ambient temperature for 48 hrs.
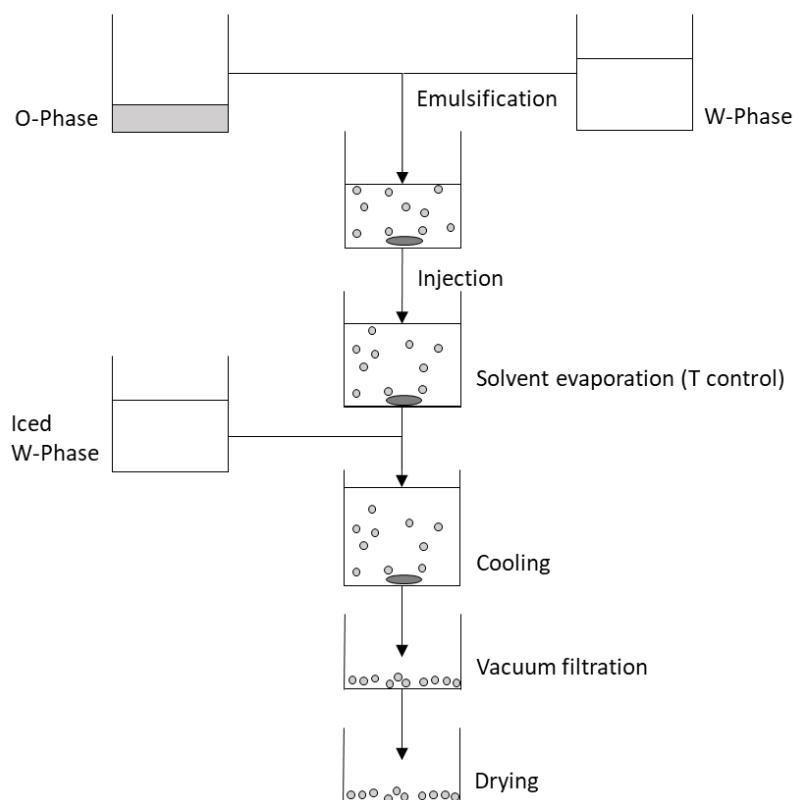
Figure 10 Scheme of the preparation process of microparticles by solvent evaporation prepared at different aqueous phase temperatures.

2.2.5 Microparticle characterization

2.2.5.1 Surface morphology, microscopical and macroscopical appearance and particle size distribution by scanning electron microscopy and optical microscopy

Microparticle appearance and surface morphology was investigated by scanning electron microscopy (REM FEI QUANTA 200, Hillsboro, USA). Dry samples were mounted on aluminum stubs and sputtered with gold (85 sec at 40 mA under Argon, 0.05 to 0.1 mbar, table distance of 6 cm to the target, SCD 040, Balzers Union, Balzers, Liechtenstein). Samples were observed under high vacuum and high voltage (15.0 kV). To observe cross-sections, microparticles were embedded in a solvent-free glue (UHU® Alleskleber ohne Lösungsmittel, Bolton Adhesives, Rotterdam, Netherlands) and cut after drying with a razor blade.

Pictures for microscopical appearance were taken with an optical microscope (Axioskop, Carl Zeiss AG, Oberkochen, Germany), pictures for macroscopical appearance were taken with an IPhone SE (Apple Inc., Cupertino, California, USA).

Droplet and particle size distributions were measured by optical imaging with an optical microscope (Axioskop, Carl Zeiss AG, Oberkochen, Germany). The number of droplets or particles counted was n=100, measurement was performed with the software Zen (Carl Zeiss AG, Oberkochen, Germany).

Pore sizes in cross-sections were measured with ImageJ (ImageJ 1.52a, National Institutes of Health, United States). A minimum of 10 pores was measured.

2.2.5.2 Determination of assay and encapsulation efficiency by UV-Vis and HPLC

For the peptide drug, about 40.0 mg microparticles were accurately weighed and dissolved. The assay was determined by HPLC.

For minocycline HCl, to an accurately weighed amount of microparticles 0.5 N NaOH was added and shaken for 2 hrs (KS 501 D, IKA®-Werke GmbH & CO. KG, Staufen im Breisgau, Germany). Aliquots were then measured by UV-Vis spectroscopy (Agilent 8453, Agilent Technologies Inc., Santa Clara, United States) at 247 nm with a background correction at 550 nm. Drug stability was proven by UV signal stability in the solvent up to 24 hrs (recovery 94-100 %). Concentrations were calculated with the help of previously established standard curves.

For risperidone, the actual drug loading was determined by dissolving an accurately weighed amount of microparticles in acetonitrile (ACN) and diluting 1:1, v/v, with deionized water. The absorbance of the solution was then measured by UV-Vis spectroscopy (Agilent 8453, Agilent Technologies Inc., Santa Clara, United States) at 277 nm with a background correction at 400 nm. Concentrations were calculated with previously established standard curves.

For all drugs, the assay was calculated by

$$dl\ (\%) = 100\% * \frac{c * V}{m_{MP}}$$

with dl the drug loading, c the concentration of risperidone in the solution, V the volume of the microparticle dilution and m_{MP} the weight of the microparticles under test.

The encapsulation efficiency was calculated by

$$EE\ (\%) = 100\% * \frac{dl_{act}}{dl_{theo}}$$

with EE the encapsulation efficiency, dl_{act} the actual drug loading based on dry weight, and dl_{theo} the theoretical drug loading.

2.2.5.3 Determination of residual solvents

2.2.5.3.1   Fourier-transform infrared spectroscopy (FT-IR)

FT-IR spectra were generated with an Excalibur 3100 FTIR spectrophotometer (Varian Inc., Palo Alto, USA). Liquid (polydimethylsiloxane, octamethylcyclotetrasiloxane) and solid (PLGA, minocycline HCl) samples were placed directly on a horizontal attenuated total reflectance (ATR) accessory with a single reflection diamond crystal (Pike Miracle, Pike Technologies, Madison, USA). The crystal was flushed with dry air for a minimum of 5 h prior to measurements. The average of 64 scans at 4 cm^{-1} resolution was analyzed after blank correction by the Varian software (Resolution Pro 4.0).

2.2.5.3.2   H-NMR Method Validation

The samples were filled into NMR tubes and closed carefully with a stopper. Measurement was performed with a Bruker Avance III (Bruker Corporation, Billerica, Massachusetts, USA) at 500 MHz. The spinning rate was 20 Hz, pulse sequence program was Avance zg30, tip angle of 30°, spectral width was 20 ppm and data acquisition was set to 3.2 s. Peak integration was performed manually after Fourier transformation and automated baseline correction with the software MNova 10.0 (Mestrelab Research S.L., Santiago de Compostela, Spain). Toluene served as the reference (peak area was normalized to 1) and solvent peaks were related to the toluene peak (integral ratio).

Samples for the calibration curves were prepared in CDCl$_3$ in presence of PLGA with 0.2 % m/v toluene as an internal standard. Certain amounts of solvents were weighed and dissolved in a stock solution, followed by dilution to obtain the respective concentrations. The PLGA concentration was kept constant at 20 mg/ml.

The LOD and LOQ were determined based on signal-to-noise ratios of 2:1 and 9:1. The blank sample with PLGA serving as the matrix in presence of toluene was used to

determine the noise at the respective chemical shift and the concentrations of the residual solvents were calculated with the help of standard curves.

Samples for the specificity were prepared by dissolving the respective materials (PLGA, methylene chloride, polydimethylsiloxane, and toluene) in CDCl$_3$ together.

Samples for the accuracy and precision for the solvents were prepared in CDCl$_3$ in presence of PLGA with 0.2 % m/v toluene as internal standard. The percent recovery of the assay in the sample was calculated for three replicates per concentration level to express the closeness of agreement between nominal and actual value. With the normalized integral ratio

$$\widetilde{PA} = \frac{PA_{Sol}}{PA_{Tol}} \times \frac{Conc_{Tol,act}}{conc_{Tol,theo}} \tag{8}$$

the concentration of the residual solvent was calculated with

$$conc_{Sol} = \frac{\left(\frac{PA_{Sol}}{PA_{Tol}} \times \frac{Conc_{Tol,act}}{conc_{Tol,theo}}\right) - b}{a} \tag{9}$$

with $\frac{PA_{Sol}}{PA_{Tol}}$ the integral peak ratio of the solvent based on the internal standard toluene (value set to 1), $conc_{Sol}$ the concentration of the residual solvent, $conc_{Tol,act}$ the actual and $conc_{Tol,theo}$ the theoretical toluene concentration, respectively, and b the y-intercept and a the slope from the linearity studies for the respective residual solvent. To determine the intermediate precision, solutions at three different concentration levels for all solvents were prepared and analyzed on 3 different days.

2.2.5.3.3   Residual solvent quantification by H-NMR

Volatile (methylene chloride, octamethylcyclotetrasiloxane) and non-volatile (polydimethylsiloxane) solvents were quantified by H-NMR. Samples were dissolved in CDCl$_3$ containing 0.2 % toluene (w/v) serving as an internal standard. After filtration (PTFE, 0.45 µm) to eliminate from undissolved drug particles, the filtrate was filled into NMR tubes and measured. Concentration was calculated with previously established calibration curves based on the normalized integral ratio of the compound to toluene. Samples were prepared in triplicate.

2.2.5.3.4   Residual solvent quantification by headspace gas chromatography (GC)

Volatile residual solvents (methylene chloride, octamethylcyclotetrasiloxane) were quantified with a headspace gas chromatography (GC-2014, Shimadzu Corp., Kyoto, Japan) with a method adapted from USP monograph for residual solvents. Standard solutions were prepared containing a known amount of methylene chloride ("Standard solution-methylene chloride") and octamethylcyclotetrasiloxane ("Standard solution-octamethylcyclotetrasiloxane"). About 250 mg microparticles, accurately weighed, were dissolved in 25.0 mL dimethylformamide ("sample solution"). To three GC vials, each 4.0 mL sample solution were filled. To the first, 1.0 mL dimethylformamide was added, to the second, 1.0 mL of the "Standard solution-methylene chloride" was added and to the third, 1.0 mL "Standard solution-octamethylcyclotetrasiloxane" was added and carefully closed by crimping with an aluminum cap sealed with a PTFE layer. Samples were equilibrated automatically under shaking by an autosampler (HT 200 series, HTA S.r.l., Brescia, Italy) for 45 min at 105 °C. Sample volumes of 1.0 mL were injected automatically, the needle temperature was set to 110 °C. The column oven temperature was increased from 40.0 to 230.0 °C at a heating rate of 20 K/min, the carrier gas was N_2. Samples were detected with a flame ionization detector (FID) set to 250.0 °C. Evaluation of the spectra was performed with a software (GCsolution, Shimadzu Corp., Kyoto, Japan). The residual solvent levels in microparticles (% w/w) were calculated according to the formula

$$c_{MP} = 100 \, \% * \left[\frac{c_{SS} * PA_{Test} * V_{MP}}{\left(4PA_{spiked} - 4PA_{Test}\right) * m_{MP}} \right] \tag{10}$$

with c_{SS} the concentration of the standard in the standard solution, PA_{Test} the obtained peak area of the sample diluted with blank dimethylformamide, V_{MP} the volume in which microparticles were dissolved, PA_{spiked} the peak area obtained from the spiked sample with the respective standard solution and m_{MP} the actual weight of microparticles under test. Linearity samples were prepared by dilution series, repeatability samples were obtained by filling similar samples from a stock to five vials followed by injection. The noise signal was obtained from blank dimethylformamide spectra at the respective retention times and LOD and LOQ were calculated by signal-to-noise ratios of 2:1 and 9:1 with the help of standard curves.

2.2.5.3.5   Residual water content by Karl Fischer titration

The water content of microparticles was determined according to the method for coulometric Karl-Fischer determination (Ph. Eur. 2.5.32). About 20.0 mg microparticles were accurately weighed and dissolved in 1.0 g glacial acetic acid. About 150.0 mg of this solution, accurately weighed, were analyzed in triplicate for the water content with a coulometric Karl Fisher titrator (C20, Mettler-Toledo International Inc., Columbus, United States). System suitability was checked with repeatability (RSD < 5 %) and bracketing (0.95-1.05) of a water standard (Honeywell Hydranal™, Fisher Scientific GmbH, Schwerte, Germany). The water content based on total weight was calculated after correction for the water content of the blank.

2.2.5.4 Determination of drug release from microparticles

2.2.5.4.1   Peptide-loaded microparticles

For the peptide drug, a known amount of microparticles was placed in TRIS-buffered medium. Sink conditions were maintained based on maximum achievable drug concentration depending on the drug loading. Samples were incubated in a horizontal shaker at 80 rpm and 37 °C (Incubation shaker 3033, Gesellschaft für Labortechnik, Burgwedel, Germany), and investigation was performed in triplicate. Drug release was tested by sampling aliquots of the supernatant through a needle filter (BD Blunt™ filter, Becton, Dickinson and Company Corp., Franklin Lakes, United States) and fresh medium was backflushed. Drug concentration was quantified by UV-Vis spectroscopy (Agilent 8453, Agilent Technologies Inc., Santa Clara, United States).

2.2.5.4.2   Risperidone-loaded microparticles

The drug release was determined under static and moved conditions.
For the static method, about 5 to 10 mg microparticles were accurately weighed and placed in an Eppendorf tube. After addition of 1.5 mL of pre-warmed dissolution medium (PBS pH 6.8/ 0.02 % Na-azide), the tubes were closed and incubated in an upright position in an incubation shaker (37 °C, 80 rpm) (Incubation shaker 3033, Gesellschaft für Labortechnik, Burgwedel, Germany). At pre-determined time-points, tubes were turned upside-down for three times prior to sampling. Sampling volumes were 0.5 mL, which were sampled through a needle filter (BD Blunt™ filter, Becton,

Dickinson and Company Corp., Franklin Lakes, United States). Fresh, pre-warmed medium was replaced by backflushing through the needle filter to retrieve possibly adhering microparticles. Quantification of the drug concentration was performed by measuring the UV-Vis absorption (Agilent 8453, Agilent Technologies Inc., Santa Clara, United States) at 277 nm with a background correction at 400 nm. Determination of drug release was performed in triplicate.

For the moved method, about 10-20 mg microparticles were accurately weighed and placed in lyophilization vials. After addition of 6.5 mL of pre-warmed dissolution medium (PBS pH 6.8/ 0.02 % Na-azide), vials were closed by crimping with aluminum caps and incubated in a horizontal position in an incubation shaker (37 °C, 80 rpm, Incubation shaker 3033, Gesellschaft für Labortechnik, Burgwedel, Germany). One air bubble was remaining, which moved the suspension upon drug release study. At pre-determined time-points, tubes were turned upside-down for three times prior to sampling. Sampling volumes were 1.0 mL, which were sampled through a needle filter. Fresh, pre-warmed medium was replaced by backflushing through the needle filter to retrieve possibly adhering microparticles. Quantification of the drug concentration was performed by measuring the UV-Vis absorption (Agilent 8453, Agilent Technologies Inc., Santa Clara, United States) at 277 nm with a background correction at 400 nm. Determination of drug release was performed in triplicate.

Sink-conditions were maintained for all drug release studies throughout the experiment (concentration less than 30 % of the saturation solubility in the release medium).

The pH was measured in aliquots of the supernatant with a daily calibrated pH meter (Seven Multi, Mettler-Toledo International Inc., Columbus, United States). For comparability, the pH was normalized by assigning values of 1.0 and 0 to the initial and final pH value, respectively.

2.2.6 Data evaluation and presentation

Data was evaluated and presented with the help of Microsoft® Excel® (Office 365 MSO, Microsoft Corporation, Redmond, Washington, USA) and GraphPad Prism 8.3.0 (GraphPad Software, San Diego, California, USA).

3. RESULTS AND DISCUSSION

3.1 Improving the process robustness of a phase separation method for the manufacturing of PLGA microparticles

PLGA microparticles for a prolonged drug release are commonly prepared by the solvent evaporation/ extraction method [49, 50]. To prepare microparticles, the drug is dispersed, dissolved or emulsified in a PLGA solution in an organic solvent (e.g. methylene chloride), which is then emulsified in an aqueous phase comprising a stabilizer. Microparticles are solidified upon solvent evaporation, collected by sieving and dried. However, low encapsulation efficiency and high burst is a major concern, as water-soluble drugs may diffuse out, which should be avoided especially in the case of high potency and expensive drugs [133, 134].

The phase separation method represents a water-free preparation alternative, facilitating the formulation of low-burst microparticles combined with high encapsulation efficiencies even for highly water-soluble drugs [7, 35, 135-137].

To prepare microparticles, the drug is either suspended, dissolved or emulsified in a polymer solution (e.g. PLGA in methylene chloride). The addition of a non-solvent (e.g. polydimethylsiloxane) changes the solvent-polymer interaction and hence induces a liquid-liquid phase separation to reduce the systems unfavorable internal enthalpy. The polymer-rich phase is emulsified in the polymer-lean phase. Droplets are then hardened by methylene chloride extraction in a hardening bath (e.g. octamethylcyclotetrasiloxane) [7, 46].

The core of the process is the coacervate stability, which depends on the non-solvent concentration and substantially determines the risk of agglomeration. To produce non-agglomerated microparticles of controlled size, the nascent microdroplets can only be transferred during a particular stability window, where the droplets are viscous enough for droplet stabilization in terms of size and shape, but are not yet in a sticky state [46, 47].

Thus, the phase separation process was investigated in the first part of this chapter, followed by an investigation of the effect of formulation and process parameters in

terms of coacervate stability, drug encapsulation, particle size control and agglomeration in the hardening bath.

3.1.1 Influence of the coacervation step

The microparticle preparation is based on the phase separation of the PLGA solution in an organic solvent upon the introduction of a polymer non-solvent [7].

A precise knowledge on the distribution and diffusion directions of the solvent and non-solvent between the two phases (polymer-rich and polymer-poor phase), the determination of the optimum non-solvent concentration, and detailed knowledge on the coacervate stability and its formation is thus important to support the development of a robust preparation process of microparticles.

3.1.1.1 Solvent distribution profile

The solvent distribution upon proceeding phase separation was investigated by quantification of the compounds in the separated phases.
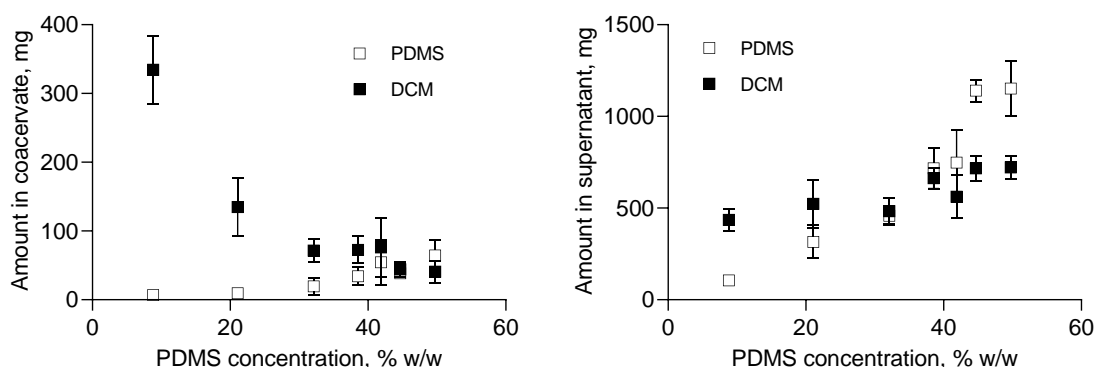
Figure 11 Amount of coacervating agent polydimethylsiloxane (PDMS) and solvent methylene chloride (DCM) in the coacervate (left) and supernatant (right) phase as a function of the polydimethylsiloxane concentration in a mixture with 1.0 g of a 6 % w/w PLGA solution in methylene chloride (n=3, mean ± SD).

At low polydimethylsiloxane concentrations (8.5 % w/w), a distinct interphase was observed after centrifugation, indicating a phase separation into a polymer-rich and a polymer-poor phase. With increasing polydimethylsiloxane concentrations, the

methylene chloride amount in the coacervate phase decreased, which was due to a solvent extraction to the continuous, polymer-poor phase (Figure 11). While at lower polydimethylsiloxane concentrations a steeper slope and hence extraction of methylene chloride was observed, a methylene chloride plateau amount was reached starting from a silicon oil concentration of about 32 %, indicating an equilibrium between the continuous and the dispersed phase. Simultaneously, the methylene chloride amount increased in the supernatant, confirming the results of the concentration change in the coacervate phase reaching its plateau at the same polydimethylsiloxane concentration (Figure 11).

On the one hand, the polydimethylsiloxane amount in the coacervate phase was constant at low polydimethylsiloxane concentrations (about 6.8 mg and 9.6 mg for 8.8 % and 21.1 % silicon oil concentrations, respectively), which indicated a polymer desolvation at low silicon oil concentrations by methylene chloride diffusion in the direction of the continuous phase. On the other hand, the amount of the silicon oil in the polymer-rich coacervate phase noticeably increased at about 38.6 % to 41.9 % silicon oil concentration, which was most probably due to a simultaneous methylene chloride outflow to the supernatant and a non-solvent inflow in the direction of the polymer-rich phase (Figure 11). This might be explained by interactions on molecular level or the higher viscosity of the coacervate phase or a combination thereof.

Constant silicon oil amounts in the coacervate phase with increasing total polydimethylsiloxane concentrations from 8.9 to 40.2 % were also found for PLGA concentrations between 0.6 and 1.1 % in methylene chloride [46]. However, the increasing amount of polydimethylsiloxane in the polymer-rich phase at very high polydimethylsiloxane concentrations was not observed. This might be because the investigated polymer concentration was lower, and the silicon oil grade differed from the one used in the present study (1000 cSt vs. 350 cSt). Furthermore, methodological aspects might have reduced the accuracy of the reported results, as no standard was used for the quantification of the silicon oil, and the quantification of methylene chloride was performed by weight loss.

The increase of silicon oil amount in the coacervate phase from about 40 % onwards correlated with a fast increasing coacervate viscosity based on increasing PLGA concentrations due to solvent extraction. This might explain the increasing affinity of the non-solvent to the coacervate phase. It also seems possible, that the highly viscous coacervate enclosed parts of the outer phase in terms of a multiple emulsion. The

polydimethylsiloxane amount in the supernatant increased in a linear manner with increasing polydimethylsiloxane to methylene chloride ratio, indicating the major fraction of polydimethylsiloxane being present in the polymer-poor phase, thus predominantly determining the polymer-poor phase characteristics (Figure 11).

The solvent distribution profile showed a highly dynamic system as a function of the polydimethylsiloxane concentration, which is expected to determine the emulsion characteristics to a great extent. The observed constant changes in phase compositions underlined the importance of a detailed investigation of the phase-separation process, which is required to obtain a stable coacervate phase needed for the preparation of microparticles.

3.1.1.2 Determination of the stability window and optimization approach of the conventional stability window determination method

The phase separation method for the preparation of PLGA microparticles requires stable coacervate droplets to obtain non-agglomerated microspheres with a narrow particle size distribution in a robust manner. Conventional methods for the determination of the optimum non-solvent amount imply studying the appearance of different coacervate phases by optical microscopy as a function of the non-solvent concentration [47]. Thereby, qualitative information regarding the different coacervation stages is achieved. At a certain non-solvent concentration, a stability window is reached, where the viscosity is high enough for a safe transfer to the hardening bath. The stability window should not be crossed in the direction of higher concentrations, where the coacervate phase viscosity gets too high, and droplets become sticky and tend to coalescence and agglomeration [7].

Interactions between polymer, anti-solvent and solvent determine the position of the stability window. Polymer chemistry is important, as molecular weight, molecular weight distribution, monomer composition and end-groups have a strong influence on the polymer solubility in the organic solvent, which ultimately affects the extent of desolvation as a function of the anti-solvent concentration [46, 47, 138]. Additionally, the polymer concentration is known to influence the position of the stability window [7]. Also, the quality of the solvent and anti-solvent influences the phase separation process [46, 47]. With the introduction of further excipients (e.g. drug, stabilizers or surfactants) a re-evaluation of the ternary phase diagram has to be conducted, as they

might compete for polymer, solvent or anti-solvent within the system, possibly shifting the stability window or changing its width. Even batch-to-batch variabilities of polymers or the change of a supplier (despite the same intrinsic viscosity label) might lead to problems regarding agglomeration due to small changes in e.g. molecular weight distribution [138]. Ternary phase diagrams have therefore to be prepared even upon minor formulation changes on a default basis.

Three different PLGA concentrations were microscopically observed as a function of the added polydimethylsiloxane concentration according to the conventional method by optical microscopy [47] (Figure 12, Figure 13, Figure 14).

For all PLGA concentrations, a distinct liquid-liquid phase separation occurred starting from about 0.5 % polydimethylsiloxane. From about 0.5 to 20 % polydimethylsiloxane, the polymer-rich phase was highly transparent and the droplets were easily deformable and yet unstable (Figure 12 A-B, Figure 13 A-B, Figure 14 A-B). The low amounts of the non-solvent polydimethylsiloxane needed to induce a liquid-liquid phase separation indicated a comparatively high mutual affinity between methylene chloride and the silicon oil [41, 139].

For the lowest PLGA concentration of 3 % in methylene chloride, and polydimethylsiloxane concentrations ranging from about 20 to 35 %, the coacervate phase showed homogeneous droplets, indicating the system being within the stability window (Figure 12 C-D). With increasing polymer concentration, the stability window width decreased. For a PLGA concentration of 6 %, a stable coacervate phase was achieved at polydimethylsiloxane concentrations of about 20 to 25 % (Figure 13-C), while for the highest polymer concentration of 9 % practically no stability window could be determined. At a polydimethylsiloxane concentration of about 29 %, the droplets were not yet stable, while at about 33 %, the coacervate droplets agglomerated (Figure 14 C-D). This observation was most probably due to an increasing coacervate volume and viscosity with the increasing polymer concentration, resulting in a faster transition to the sticky state [120].

However, the determination of the upper limit of the stability window is accompanied with a high risk of interpretation failure due to non-automated microscopic evaluation. Despite the presence of separate droplets at very high polydimethylsiloxane concentrations of about 43 % and 45 % (Figure 12-F, Figure 13-F), the macroscopical observation at these concentrations showed a highly viscous phase sticking to the vial

bottom, which could not be resuspended with a magnetic stirrer (Figure 15). Thus, agglomeration might occur during hardening, ultimately reducing the yield.

The findings from the microscopical study underlined the importance of an interpretation of the obtained appearances only in combination with macroscopical information.

Besides the pronounced dependency of data interpretation from the individual operator and thus a weak inter-and intra-comparability of the results, the microscopical investigation of the microdroplets furthermore showed typical drawbacks of an *off-line* analysis method. First, the time span from sampling to the actual measurement is longer than the time in which the emulsion stability can be ensured. Second, sampling can have a detrimental effect on the appearance, as unstable droplets may be deformed during sample preparation and, driven by the high vapor pressure of methylene chloride, solvent evaporation during the measurement may change the sample composition and thus the droplet appearance. Third, the sample representativeness cannot be assured as soon as the sticky state is reached.

The high risk of misinterpretation of the results may affect critical quality attributes of the microparticles such as particle size distribution, as well as the yield.

Despite sampling being performed immediately after stirring, sticking material to the vial bottom was not available for microscopical analysis because it could not be resuspended starting from a particular polydimethylsiloxane concentration, ultimately decreasing the data quality to an insufficient level.
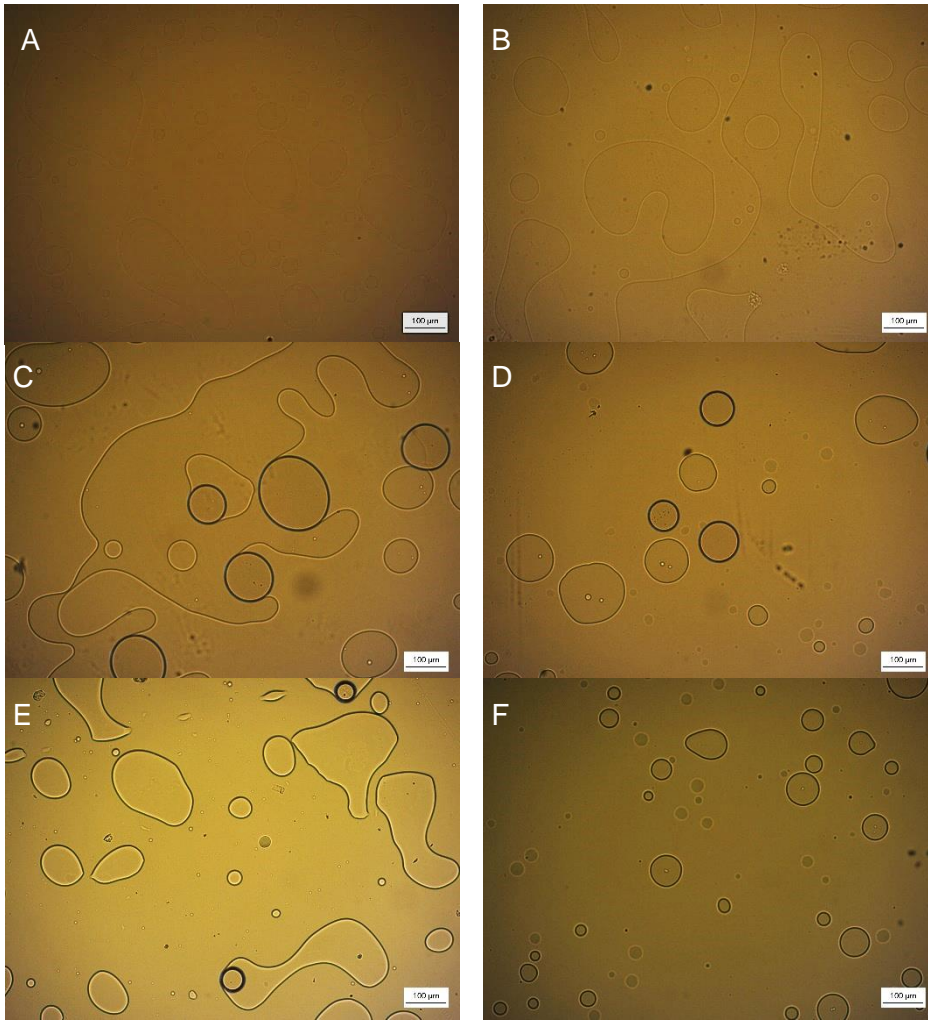
Figure 12 Microscopic appearance of coacervate phase as a function of the polydimethylsiloxane concentration in the system. 3 % w/w PLGA in methylene chloride, scale bar represents 100 μm. Polydimethylsiloxane concentrations: A: 0.6 %, B: 13.2 %, C: 24.5 %, D: 32.3 %, E: 39.1 %, F: 43.1 %.
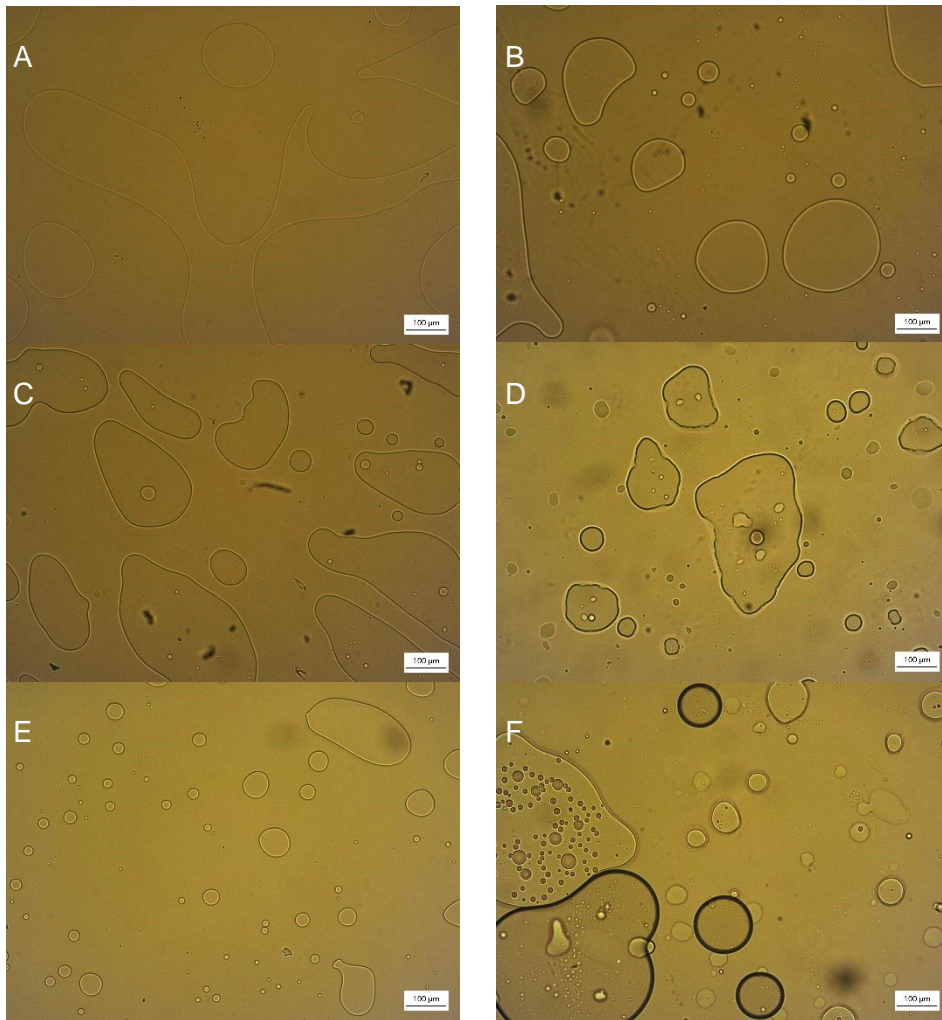
Figure 13 Microscopic appearance of coacervate phase as a function of the polydimethylsiloxane concentration in the system. 6 % w/w PLGA in methylene chloride, scale bar represents 100 μm. Polydimethylsiloxane concentrations: A: 3.7 %, B: 13.0 %, C: 23.5 %, D: 30.2 %, E: 34.9 %, F: 40.9 %
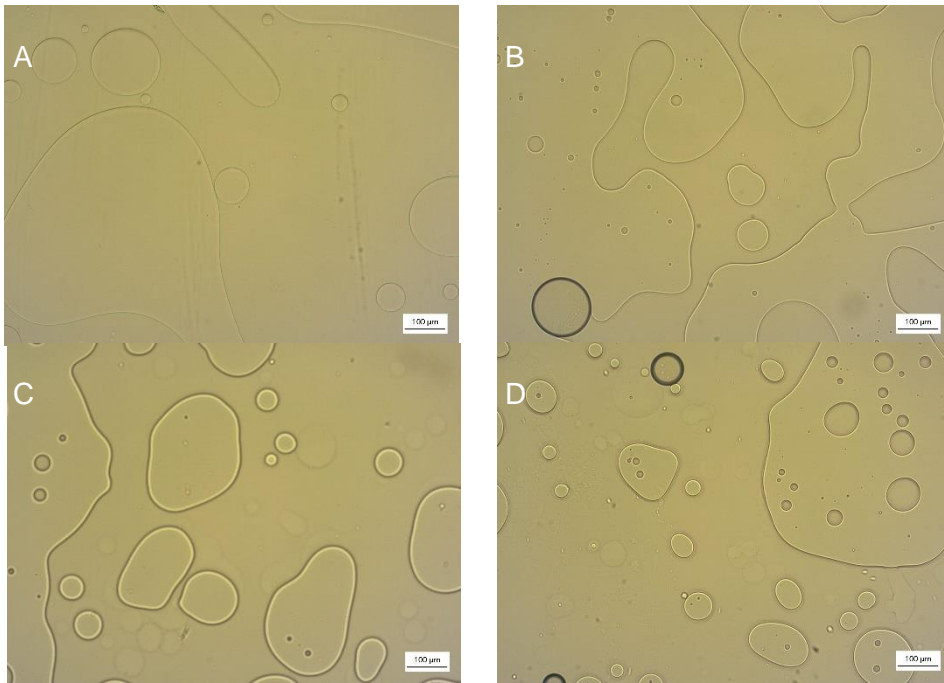
Figure 14 Microscopic appearance of coacervate phase as a function of the polydimethylsiloxane concentration in the system. 9.0 % w/w PLGA in methylene chloride, scale bar represents 100 µm. Polydimethylsiloxane concentrations: A: 10.7 %, B: 20.0 %, C: 28.6 %, D: 33.2 %.

Figure 15 Macroscopical appearances of liquid-liquid phase separated system with 45 % w/w polydimethylsiloxane before (left) and after (right) stirring. To the bottom of the vial, a viscous yellowish layer sticks which cannot be resuspended. 6 % w/w PLGA in methylene chloride.

Thus, there is a need of a method which delivers more detailed information on the coacervate stability to better approximate the stability window. The effect of the polydimethylsiloxane concentration on the total-, the supernatant-and the coacervate volume as well as the resuspendability were expected to indicate the stability window in a more representative way. The closed set-up was expected to increase the test robustness, and operator-independent results were expected to increase the reproducibility and comparability.

Polydimethylsiloxane concentrations from about 20 to 60 % were investigated. At polydimethylsiloxane concentrations of about 21 %, the mixture was liquid-liquid phase separated. With increasing polydimethylsiloxane concentration, the total volume and the supernatant volume constantly increased (Figure 16), which was expected due to the increasing total polydimethylsiloxane amount in the system and the proceeding solvent extraction to the polymer-poor phase. The coacervate phase, on the other hand, showed the highest volume at about 20 % polydimethylsiloxane, and decreased thereafter slowly along with the extraction of the organic solvent methylene chloride to the polymer-poor phase. The major contribution to the increase in the supernatant volume at concentrations up to about 40 % polydimethylsiloxane was attributed to methylene chloride, while the minor change after about 40-45 % polydimethylsiloxane in the system was attributed only to the increasing polydimethylsiloxane amount, as the coacervate volume ran into a plateau.

The stirring speed with a vortex mixer was used to test the dispersibility of the polymer-rich phase as a function of the progressing phase separation. With increasing polydimethylsiloxane concentration, a constantly increasing stirring speed was needed to fully resuspend the coacervate phase, which corresponds to the assumption of a continuous organic solvent extraction from the coacervate phase to the polymer-poor phase. From polydimethylsiloxane concentrations of about 50 % onwards, the coacervate phase could not be resuspended anymore, showing the start of a sticky state and indicating a polymer precipitation, thus the start of a turnover from a liquid-liquid phase separation to a solid-liquid phase separation (Figure 16).
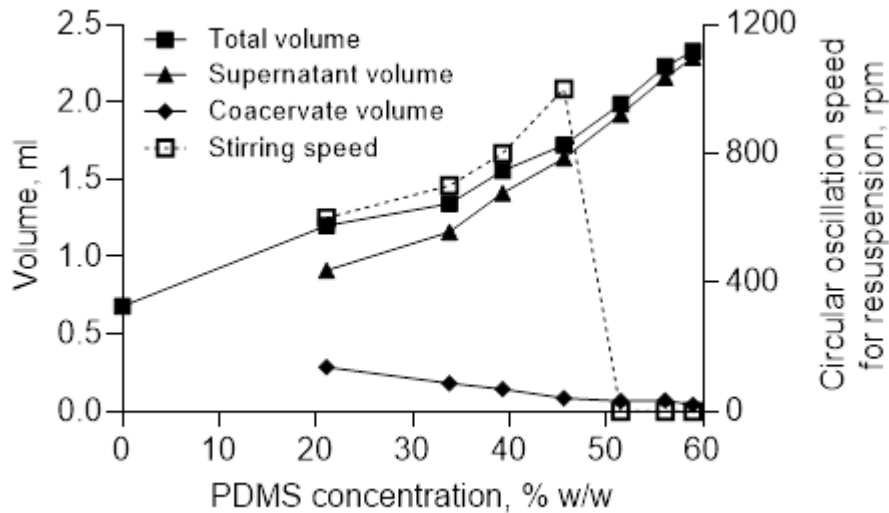
Figure 16 Influence of the polydimethylsiloxane concentration on the total, coacervate and supernatant phase volume and the circular oscillation speed required to fully resuspend the coacervate phase within 10 sec (n=3, mean ± SD). 6 % w/w PLGA in methylene chloride.

Thus, a polydimethylsiloxane concentration range from about 30 to 40 % was found reasonable according to the study (Figure 16). In this concentration range, the coacervate phase volume decreases at a comparatively very low rate due to a very slow methylene chloride extraction. At the same time, the coacervate phase is still resuspendable within seconds, thus assuring a sufficient mixing efficiency and a low risk of sticking. The stability window width per "volume/resuspendability" study was shifted to higher polydimethylsiloxane concentrations and a broader working range than the one obtained from the microscopical appearance per "conventional" method, which showed stable droplets only at polydimethylsiloxane concentrations of about 20 to 25 %.

At these concentrations however, the new method indicated a high coacervate phase volume and hence a high organic solvent amount. This results in a comparatively low viscosity, high density and ultimately a low coacervate droplet stability. The gap regarding width and location of the stability window was attributed to the aforementioned uncertainties associated to the *off-line* method. The microscopical method is fast and easy, however, stages can be missed due to the discontinuous addition manner of polydimethylsiloxane in the measurement set-up.

The combined *off-* and *on-line* stability window determination method still lacked transferability to the actual process. In the actual production process, the non-solvent is subsequently added to the polymer solution under continuous stirring at controlled temperature and in a closed system to exclude solvent evaporation during the process. The suitability of an *in-line* method (Crystalline®) was assessed as it was expected to allow for a continuous *in situ* observation of the droplet formation as a function of increasing polydimethylsiloxane concentrations under simulated process conditions. Up to 6.3 % polydimethylsiloxane, the mixture was clear, indicating a homogeneous ternary system (Figure 17, A). Between polydimethylsiloxane concentrations from 6.3 to 6.8 %, droplet formation started. From 6.8 % polydimethylsiloxane onwards, homogeneous droplets became visible, indicating the critical concentration needed for a clear phase separation of the ternary system (Figure 17, B). The coacervation start can thus be precisely determined by the novel *in situ* observation of ternary phase systems, facilitating the construction of solubility or compatibility charts under controlled process conditions, which is not limited to the present example of liquid-liquid phase separation.

Figure 17 Appearance of a ternary phase system with 6 % w/w PLGA in methylene chloride and different polydimethylsiloxane concentrations (A: 6.3 % w/w, B: 6.8 % w/w). Temperature 20 °C, stirring rate 600 rpm, polydimethylsiloxane addition rate 0.05 mL/min. The scale bar indicates 500 µm.

For increasing polydimethylsiloxane concentrations, the droplets became more distinct, less transparent and the outer layer showed a darker color. This was due to increased molecular interactions between polymer chains, resulting in polymer precipitation at the outer droplet layers causing a decreased light transmission (Figure 18). The visual examination of the mixture showed first signs of agglomeration at a polydimethylsiloxane concentration of 52.4 % (Figure 18, "H", arrow). Two droplets

coalesced, forming one particle which would be expected to cause agglomerates or at least broader particle size distributions of the final microspheres after exposure to the hardening agent.

The herein described *in situ* method was the only one to catch also an "instability" state as well as the onset of the phase separation at a high level of reproducibility and hence raises great potential as novel method for the determination of the stability window under simulated process conditions, thus being strongly relevant for early formulation and process development stages.

According to the obtained results, the stability window of a 6 % PLGA in methylene chloride solution is considerably broader, with a polydimethylsiloxane concentration range from about 6.8 % up to about 50 %.
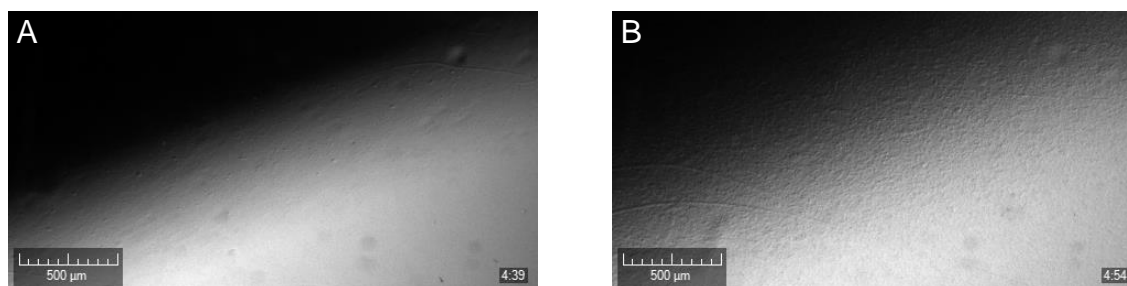
Figure 18 Appearance of a ternary phase system with 6 % w/w PLGA in methylene chloride and different polydimethylsiloxane concentrations (A: 15.0 %, B: 25.0 %, C: 30.0 %, D: 35.0 %, E: 40.0 %, F: 45.0 %, G: 50.0 %, H: 52.4 %). Temperature 20 °C, stirring rate 600 rpm, polydimethylsiloxane addition rate 0.05 mL/min. The scale bar indicates 500 µm.

To assess the optimum polydimethylsiloxane concentration for a safe coacervate droplet transfer to the hardening bath, the results from the phase volume trend study and from the appearance of the droplets, both as a function of the polydimethylsiloxane concentration, were combined and evaluated.

For this, the transmissivity of the sample was simultaneously determined, *in situ*, as a function of the non-solvent concentration in the ternary mixture (Figure 19).
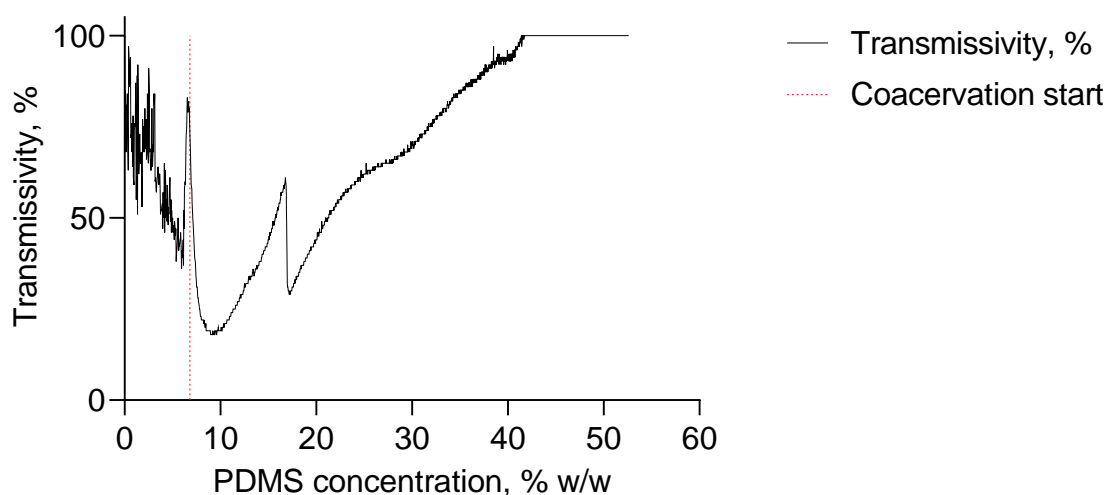
Figure 19 Effect of the polydimethylsiloxane (PDMS) concentration on the transmissivity of a mixture with 6 % w/w PLGA in methylene chloride. Temperature 20 °C, stirring rate 600 rpm, polydimethylsiloxane addition rate 0.05 mL/min.

With increasing polydimethylsiloxane concentration, the transmissivity of the mixture decreased from 100 % transmissivity at 0 % polydimethylsiloxane to 37 % transmissivity at 6.2 % polydimethylsiloxane. The decrease in transmissivity indicated a change of the optical properties of the sample due to the continuous composition change upon the silicon oil addition. Between 6.3 % and 6.8 % polydimethylsiloxane, a peak showed a sudden increase in the transmissivity (Figure 19), which was due to the sudden formation of droplets emulsified in the polymer-poor phase, showing a higher light transmissivity than the mixture. This supported the result from visual examination, where for the similar concentration range the phase separation occurred (Figure 17). After this, the transmissivity decreased to a minimum of 18.0 % transmissivity at 9.0 % polydimethylsiloxane. This was most probably due to the increasing polymer-rich phase volume, where the minimum transmissivity indicated a completed phase separation with the highest volume of dispersed phase and, thus, the

highest droplet number possible, leading to a maximum light reflection caused by the curvature of the droplet surfaces.

Thereafter, the transmissivity increased with increasing polydimethylsiloxane concentrations, reaching 100 % transmissivity at about 42 % polydimethylsiloxane. The increasing transmissivity with increasing non-solvent concentration was due to the solvent extraction from the polymer-rich phase to the polymer-poor phase, leading accordingly to a decreased volume ratio of the coacervate phase based on the total emulsion volume (Figure 16). This caused a lower droplet number, leading to a lower probability of light reflection by the inner phase and thus an increasing transmissivity of the emulsion.

The increased transmission at about 16.8 % polydimethylsiloxane was, according to a visual examination of the respective appearance, due to only a slight variation in the droplet appearance and was thus not related to a certain phase change in the ternary system (Figure 20).

The slight increase in the droplet size due to the increasing coacervate phase viscosity at constant stirring speed adds on the decreasing number of droplets, thus further increasing the transmissivity of the sample. The transmissivity reached a plateau at 100 % transmissivity and did not change upon instabilities of the coacervate phase.
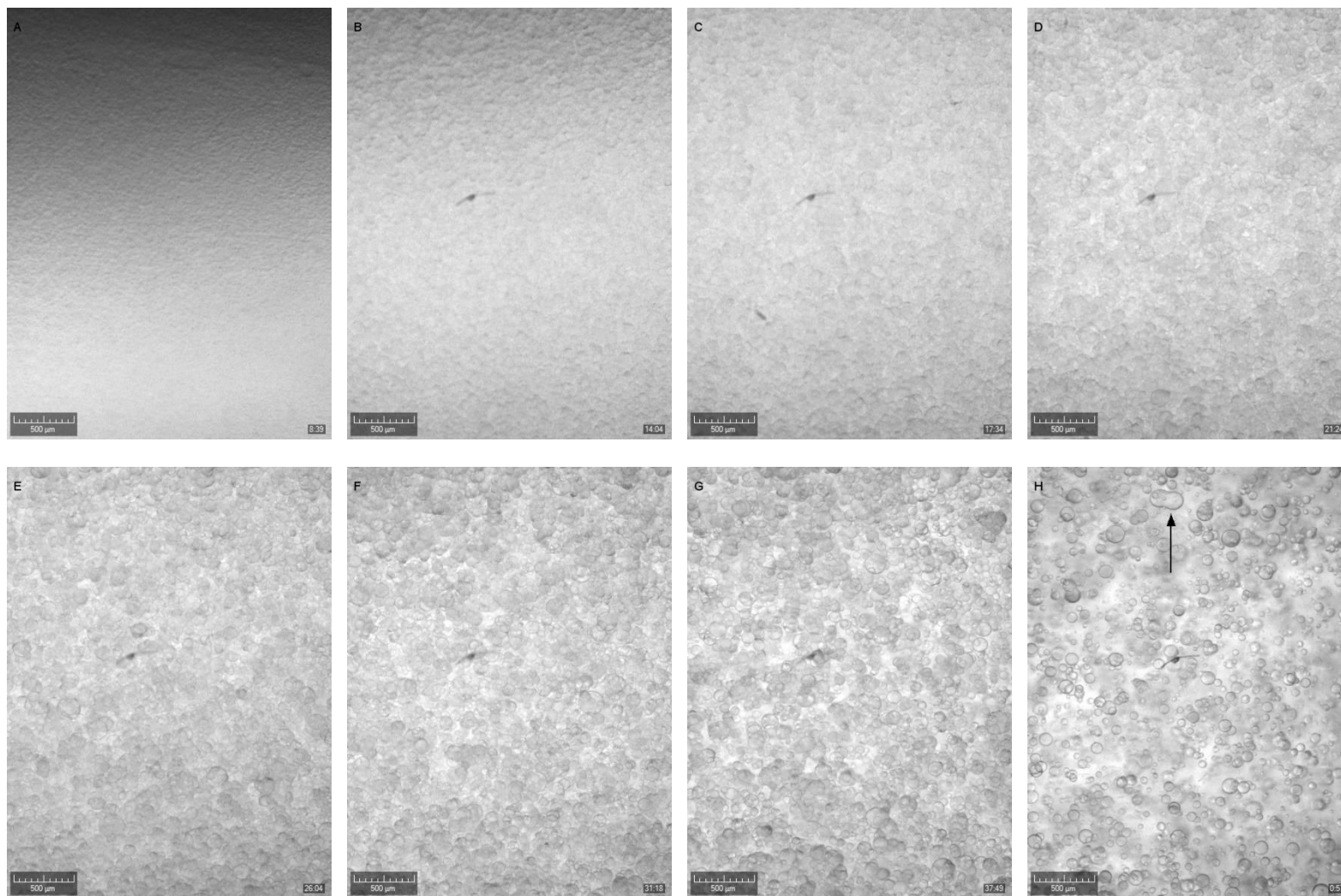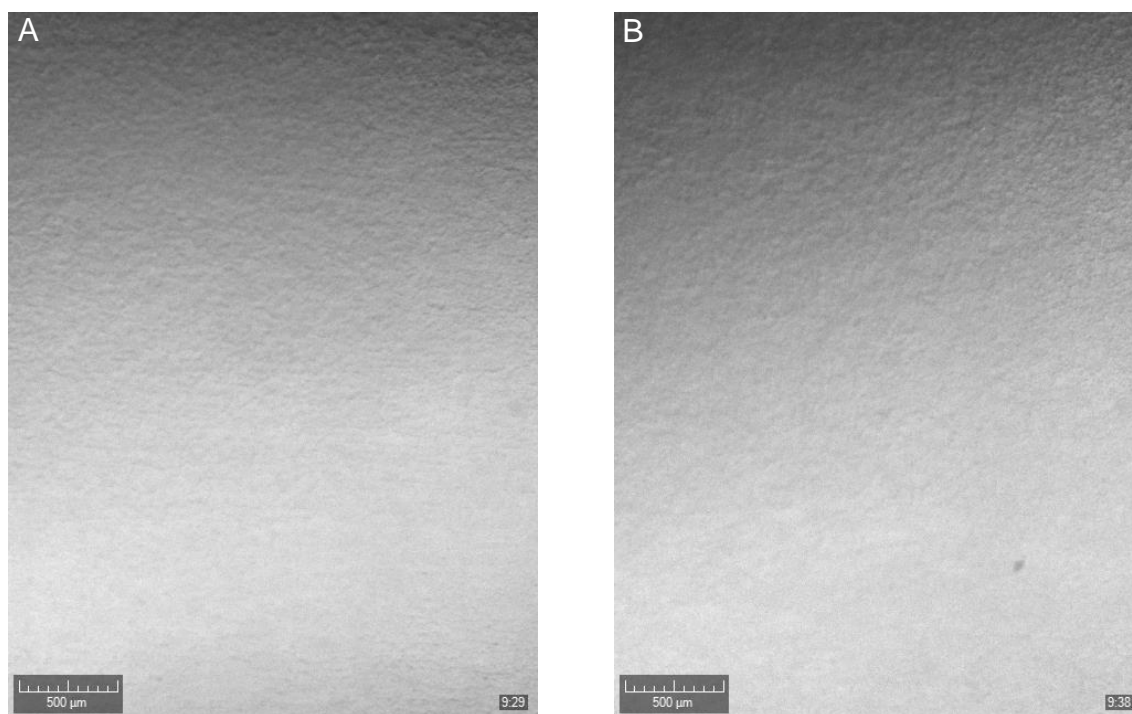
Figure 20 Appearance of a ternary phase system with 6 % w/w PLGA in methylene chloride and different polydimethylsiloxane concentrations. The appearance at lower polydimethylsiloxane concentration (16.8 % w/w, A), corresponding to the peak transmissivity does not differ from higher polydimethylsiloxane concentration (17.2 % w/w, B) corresponding to the valley transmissivity. Temperature 20 °C, stirring rate 600 rpm, polydimethylsiloxane addition rate 0.05 mL/min. The scale bar indicates 500 µm.

To ensure a secure separation of the droplets from each other and to avoid sticking or agglomeration upon solvent extraction, the polymer-poor phase was considered to be the stabilizing phase during the transfer to the hardening bath. In there, the theoretical mean distance seems to be one major parameter besides the stirring efficiency during the injection into the hardening bath, because it helps reducing the collision frequency of the droplets (for details, see 1.3.1).

Considering the coacervate phase volumes as a function of the polydimethylsiloxane concentration (Figure 16), at 20 % polydimethylsiloxane the coacervate phase volume corresponds to a volume fraction of about 0.24 based on the total emulsion volume ($V_{tot} = 1\,mL$), while at 40 and 45 % polydimethylsiloxane the coacervate phase volume corresponds only to a volume fraction of about 0.09 and 0.05, respectively.

For simplification, a three-dimensional cluster of spherical, uniform, polymer-rich droplets distributed equidistantly within the polymer-poor phase and a given volume

fraction φ_1 of the polymer-rich phase in the total emulsion volume were assumed (Figure 21, left).

To calculate the theoretical mean distance between two adjacent droplets, a geometrical model can be used, where a single droplet in the cluster is taken as basis for the calculation. A single droplet, comprising the polymer-rich phase, is centered in an imaginary cube (corresponding to the total emulsion volume), which is three-dimensionally surrounded, face-to-face, by cubes comprising the adjacent droplets in the cluster (Figure 21, right, surrounding cubes are similar to the exemplary cube with dotted lines).
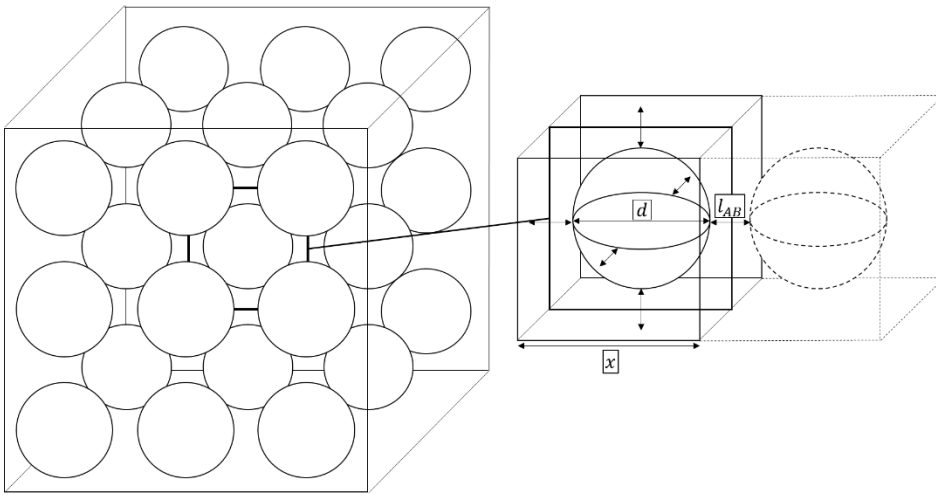
Figure 21 Schematic display of coacervate droplets of the polymer-rich phase of diameter d arranged equidistantly in the outer polymer-poor phase. The theoretical mean distance between the droplets, in all directions, is l_{AB}. The edges of the cubes in which single droplets are located are of the length x.

With this, the ratio of the volume of a single droplet with the diameter d to the volume of a theoretical surrounding cube with equidistant edges of the length x corresponds to the aforementioned volume fraction φ_1. By this follows

$$\frac{\pi d^3}{6x^3} = \varphi_1. \tag{11}$$

With

$$l_{AB} = x - d \tag{12}$$

an omnidirectional theoretical mean distance l_{AB} between two adjacent droplets A and B is then given by

$$l_{AB} = d\left[\left(\frac{\pi}{6\varphi_1}\right)^{\frac{1}{3}} - 1\right]. \tag{13}$$

By this can be concluded, that for constant droplet sizes the theoretical mean distance increases for decreasing volume fractions of the dispersed phase.

Assuming a droplet size of 50 µm, a polydimethylsiloxane concentration of 20 % shows a comparatively high volume fraction of the dispersed phase based on the total emulsion volume, causing a low theoretical mean distance between two droplets of 15 µm (Figure 16, Table 3). With increasing polydimethylsiloxane concentrations from 20 to 40 and 45 %, the volume of the coacervate phase decreased with a simultaneously increasing total emulsion volume, resulting in a significantly decreased coacervate phase volume fraction φ_1 from 0.24 to 0.09 and 0.05, respectively. Thereby, the theoretical minimum distance is increased from 15 to 39 and 60 µm, respectively, corresponding to a 2.6- and 4.0-fold increased theoretical minimum distance between the droplets.

These values were also reflected in the transmission data and the appearance obtained from the Crystalline® study (Figure 18, Figure 19). The mean distances between the droplets for 20, 40 and 45 % polydimethylsiloxane concentration were 11.4, 81.8 and 103.9 µm, respectively. With a mean droplet size of about 26, 91 and 94 µm, mean distances of 7.8, 70.9 and 111.7 µm were predicted, which were in congruence with the aforementioned measured mean distances (Table 3). The slight differences were most probably due to the calculation based on uniform droplet sizes, while the sample actually contained a broader droplet size range, leading to varying distances between the droplets. The mean distance determination in a three-dimensional system might as well increase the susceptibility to errors as the measurement was performed on two-dimensional pictures obtained from the Crystalline® study.

Table 3 Summary of the coacervate phase volume fractions and resulting theoretical mean distances between two droplets A and B in phase separated systems with different polydimethylsiloxane (PDMS) concentrations, 6 % w/w PLGA in methylene chloride and different particle diameters assumed.

PDMS concentration, %	Coacervate phase volume fraction φ_1	Theoretical minimum distance l_{AB}, µm			
		Exemplary particle size	50 µm	100 µm	150 µm
20	0.239		14.94	29.88	44.82
40	0.093		38.95	77.90	116.85
45	0.050		59.39	118.79	178.17

These results would now suggest a reduction of the coacervate fraction approaching a value of $\varphi_1 = 0$ to reduce the collision frequency, which is not feasible due to the coacervate's strong tendency to sticking at very high polydimethylsiloxane concentrations. This phenomenon was not considered in the theoretical approach. However, the approach proved that a process should be chosen inducing the coacervation at higher polydimethylsiloxane concentrations within the stability window range to minimize the likelihood of a contact between two adjacent droplets and to, ultimately, reduce the risk of agglomeration or broad particle size distributions upon injection to the hardening bath. The novel *in situ* method enabled a more precise determination of the stability window, and especially demonstrated the feasibility of preparation at higher polydimethylsiloxane concentrations, while the conventional method suggested a lower polydimethylsiloxane concentration.

To compare the results obtained from the conventional and the *in situ* stability determination method, placebo PLGA microparticles were prepared at two high polydimethylsiloxane levels. According to calculations on the theoretical mean distance, a lower risk of agglomeration upon addition to the hardening bath coupled with a lower risk of re-coalescence at comparatively higher polydimethylsiloxane concentrations was expected. The polydimethylsiloxane concentrations were chosen above the limit of the expected stability window following the conventional stability window determination results (upper limit at about 25 %) to challenge the results

obtained with the *in situ* visualization method, which showed instabilities starting from a higher polydimethylsiloxane concentration (upper limit at about 52 %). It was expected that the stability window determination in a process closer to the actual manufacturing process (higher stirring efficiency, closed set-up, temperature control) would show more precise results.
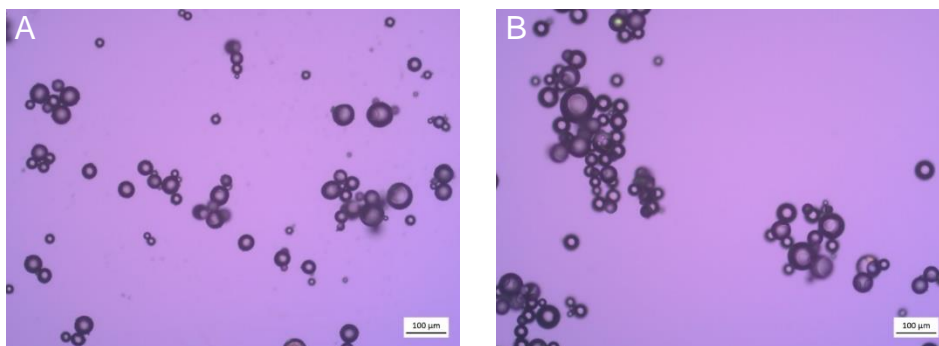
Figure 22 Microscopical appearance of microparticles formulated with 39 % (A) and 51 % (B) polydimethylsiloxane to induce coacervation.

Though the stability window per conventional method predicted an instable coacervate phase at polydimethylsiloxane concentrations higher than about 25 %, no agglomeration occurred in the hardening bath. Free-flowing microparticles were obtained after drying for both formulations and no agglomerates were observed microscopically (Figure 22). With increasing polydimethylsiloxane concentration, the mean particle size was slightly increased from 30 to 41 µm which was attributed to an increased coacervate phase viscosity. For the same reason, the size distribution width was slightly increased (D_{10}, D_{50} and D_{90} of 19, 30 and 49 µm and 20, 41 and 63 µm for 39 and 51 % polydimethylsiloxane concentration, respectively), which, however, was deemed acceptable for the preparation of microparticles.

This proved the suitability of the novel *in situ* method to determine more precisely the stability window of the phase separation process particularly at higher polydimethylsiloxane concentrations, which is important as coacervate stability correlated with polydimethylsiloxane concentrations due to higher theoretical mean distance between droplets.

3.1.1.3 Stability of the emulsion: polymer-rich phase in polymer-poor phase

The use of a stabilizer was avoided to minimize the number of excipients for the preparation of microparticles. Hence, a high risk of re-coalescence of the dispersed phase was likely. Besides the dilution effect at higher polydimethylsiloxane concentrations with increasing theoretical mean distances and thus decreasing collision frequency, the coalescence efficiency as well as the terminal velocity of the droplets are important for the emulsion stability (see also 1.3.1).

To assess the emulsion stability, phase-separation was induced by the addition of polydimethylsiloxane to a PLGA solution in methylene chloride (3 % or 6 %, w/w). An increasing stability of the coacervate emulsion was indicated with increasing time needed for complete separation of the polymer-rich and polymer-poor phase. A non-solvent concentration range within the stability window was chosen (polydimethylsiloxane concentrations of 36.4, 44.0 and 50.7 %).

All phase-separated PLGA solutions coalesced, resulting in two distinct phases separated by a discrete interface (Figure 23). In this study, emulsions fully separated within 9 to about 200 min, meaning a full coalescence of droplets and a clear interface. It must be marked that the actual emulsion instability occurs earlier, as the coalescence of single droplets is the starting point of the full phase separation and is critical for the final particle size distribution and the agglomeration risk upon hardening.
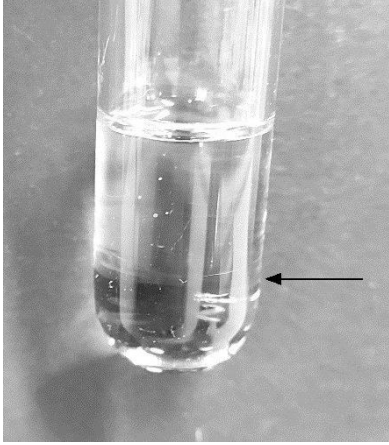
Figure 23 Appearance of a phase-separated system. The arrow points at interphase between lower polymer-rich and upper polymer-poor phase. 6 % w/w PLGA in methylene chloride, 42.9 % w/w polydimethylsiloxane.
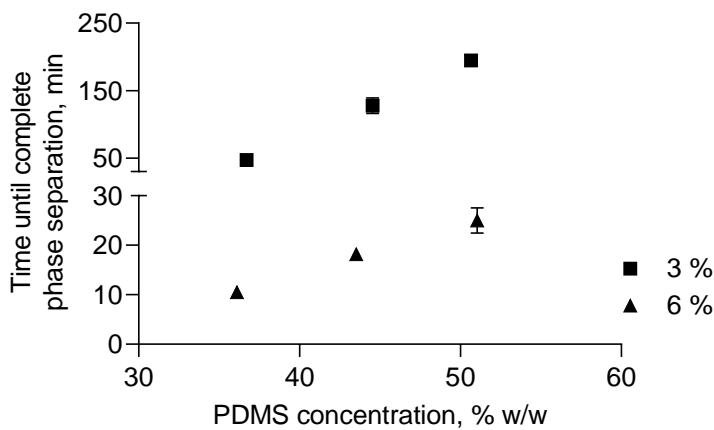
Figure 24 Effect of the polydimethylsiloxane (PDMS) concentration on the emulsion stability in mixtures with 3 % w/w and 6 % w/w PLGA in methylene chloride (n=3). Note the two segments of the y-axis with different scales.

For the 6 % PLGA solution, the time until full phase separation increased with increasing polydimethylsiloxane concentrations (Figure 24). This can be explained by various reasons.

First, the proceeding extraction of methylene chloride ($\rho = 1.318 \frac{g}{cm^3}$, [140]) from the polymer-rich phase to the dispersed phase leads to a decreasing density of the droplets. Additionally, the increasing concentration of polydimethylsiloxane ($\rho =$

$0.972 \frac{g}{cm^3}$, [141]) in the outer phase decreases its density. In accordance with Stoke's Law regarding the terminal velocity of a sphere falling in a fluid (Equation (5)), the sedimentation of the droplet is lowered for an equalization of the densities of the dispersed, polymer-rich, phase and the continuous, polymer-poor, phase. In combination with the increasing viscosity of the dispersed phase due to the proceeding dilution of methylene chloride ($\eta_{DCM} = 0.311\ cSt$, [140]) with polydimethylsiloxane ($\eta_{PDMS} = 350\ cSt$, [141]), the sedimentation velocity of the coacervate droplets was further decreased, resulting in longer times needed for full separation.

Second, the theoretical minimum distance between two adjacent droplets decreases with increasing non-solvent concentration, which leads to a lower collision frequency, and thus reduces the risk of coalescence (see 1.3.1). This is in congruence with simulated coalescence times of droplets in hexadecane/water emulsions, which decreased with increasing mean dispersed phase fractions [142]. Third, the proceeding polymer precipitation at the outer droplet layer due to the decreasing organic solvent content and thus increasing polymer concentration may result in a higher rigidity of the interfacial film and thereby an emulsion stabilization, which was already observed for asphaltene- and resin-stabilized emulsions [143]. The coalescence efficiency is thus decreased. The increasing viscosity of the continuous phase with increasing polydimethylsiloxane concentration may have additionally decreased the coalescence efficiency by impeding the film drainage.

Similar observations were made for the 3 % PLGA solution, where increasing polydimethylsiloxane concentrations led to higher coacervate stabilities. Reducing the polymer concentration led to an overall increased coacervate stability due to a reduced coacervate phase fraction in the mixture, additionally increasing the mean distance between the droplets, thereby further reducing the collision frequency and thus the risk of coalescence. The reduced viscosity of the polymer-rich phase most probably caused smaller droplet sizes, which, according to Stoke's law, further decreased the sedimentation velocity of the droplets, thus increasing the emulsion stability. The lower viscosity of the outer phase due to a higher dilution by methylene chloride seemed to be overweighed by the aforementioned effects.

3.1.1.4 Effect of formulation and process parameters on coacervate phase stability and risk of agglomeration by *in situ* visualization

Stability windows of ternary systems are commonly determined under conditions where a system equilibrium is allowed. The mixtures of a PLGA solution and different concentrations of the non-solvent are stirred for a comparatively long time and analyzed for the droplet appearance thereafter. The concentration needed for the induction of the phase separation can thus be precisely determined, as well as the non-solvent concentration from which onwards the coacervate phase tends to sticking and agglomeration.

However, the actual process of microparticle preparation is not a stepwise addition of the non-solvent, but a dynamic process where the non-solvent is added continuously. It was expected that addition rates above a critical threshold exist, where an equilibrium cannot be achieved and where a process control might be critical. Additionally, the polymer concentration was expected to be important, which could until now not be studied properly*, in situ*, in a dynamic system. The temperature might also influence the coacervate formation, as solubility and miscibility might be changed and influence the polymer desolvation.

The effect of formulation and process parameters on the coacervate phase was thus assessed by an *in situ* study of the droplet size distribution with Crystalline®.
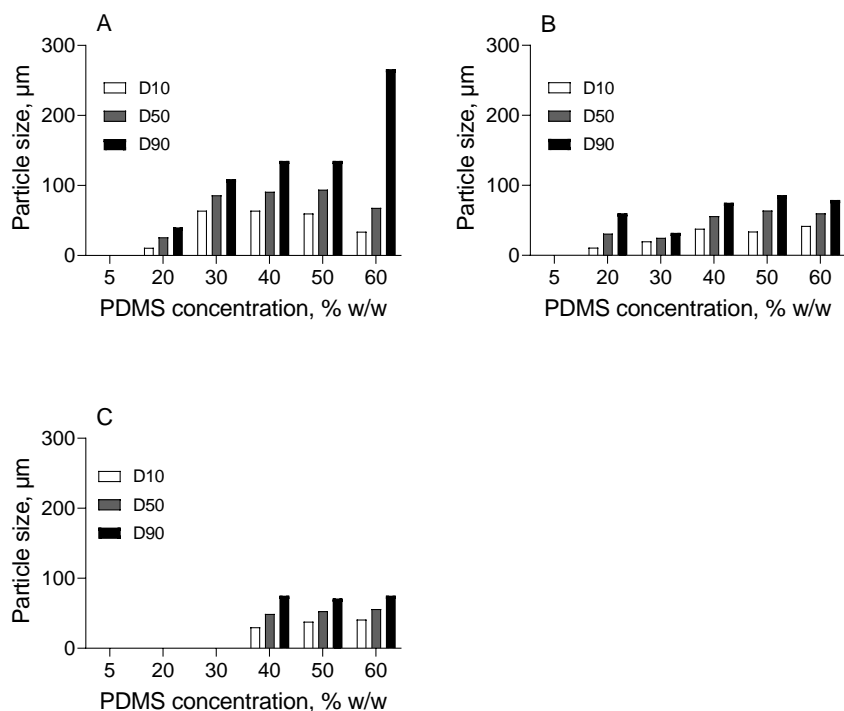
Figure 25 Effect of the polydimethylsiloxane (PDMS) addition rate on the *in situ* droplet size distribution of 6 % w/w PLGA in methylene chloride as a function of the polydimethylsiloxane concentration (A: 0.05 g/min, B: 0.22 g/min, C: 2.16 g/min). Temperature 20 °C.

With increasing polydimethylsiloxane concentrations, the droplets formed for all polydimethylsiloxane addition rates (Figure 25). According to the stability window, a critical concentration of 6.8 % polydimethylsiloxane in the ternary mixture was expected as minimum concentration to induce a liquid-liquid phase separation (Figure 17). For the comparatively fast polydimethylsiloxane addition rate of 2.16 g/min, droplets were only observed from 40 % polydimethylsiloxane onwards. This shift was most probably due to the time needed for a system equilibration as the nearly 1000-fold higher viscosity of polydimethylsiloxane compared to methylene chloride indicates [144]. This observation was in congruence with the droplet size distribution trend observed for different polydimethylsiloxane concentrations at different polydimethylsiloxane addition rates. For the slow addition rate of 0.05 g/min and at a polydimethylsiloxane concentration of 60 %, the sudden increase of the D_{90} value in the size distribution indicated an instability due to droplet coalescence or sticking. For higher addition rates, an increase in the droplet size was not observed. This might lead to the conclusion, that a higher addition rate would enlarge the stability window of the ternary mixture, however it is expected that an instability would occur as soon as a

phase equilibrium is reached. Considering the batch manufacturing process, the coacervate transfer to the hardening bath is a time-consuming step, which is why the increased addition rate only apparently enlarges the stability window. The phase separation depends on the polydimethylsiloxane concentration. However, the study underlined the importance of precise process control, as the addition rate may be faster than the phase separation process time.
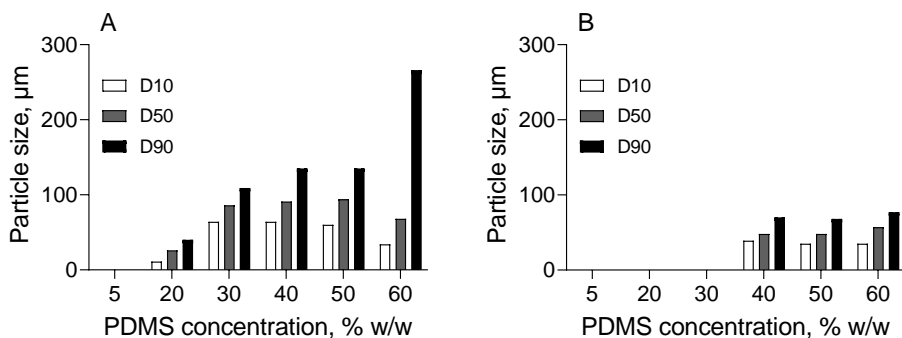
Figure 26 Effect of the PLGA concentration (A: 6 % w/w, B: 3 % w/w) on the *in situ* droplet size distribution as a function of the polydimethylsiloxane (PDMS) concentration. Temperature 20 °C, polydimethylsiloxane addition rate 0.05 g/min.

The polydimethylsiloxane concentration needed for droplet observation in the ternary system was inversely related to the polymer concentration (Figure 26). For 6 % PLGA in methylene chloride, droplets were observed at 20 % polydimethylsiloxane, while 40 % polydimethylsiloxane was needed for the mixture containing 3 % PLGA in methylene chloride. This was in congruence with decreasing PLA concentrations, where phase separation occurred later, because the critical total polymer concentration (polymer plus non-solvent) needed for phase separation is achieved only at higher non-solvent concentrations [120]. However, limitations in method sensitivity must also be considered. An increased polymer concentration allows for better recognizability of the droplets, as it shows a lower light transmissivity, which might lead to slightly shifted polydimethylsiloxane concentrations due to measuring inaccuracies for lower polymer concentrations. The shift can therefore be attributed to the polymer concentration, whereas the exact position might need further investigations.

Changes in temperature showed a strong effect on the start and progress of the phase separation of the ternary mixtures (Figure 27).
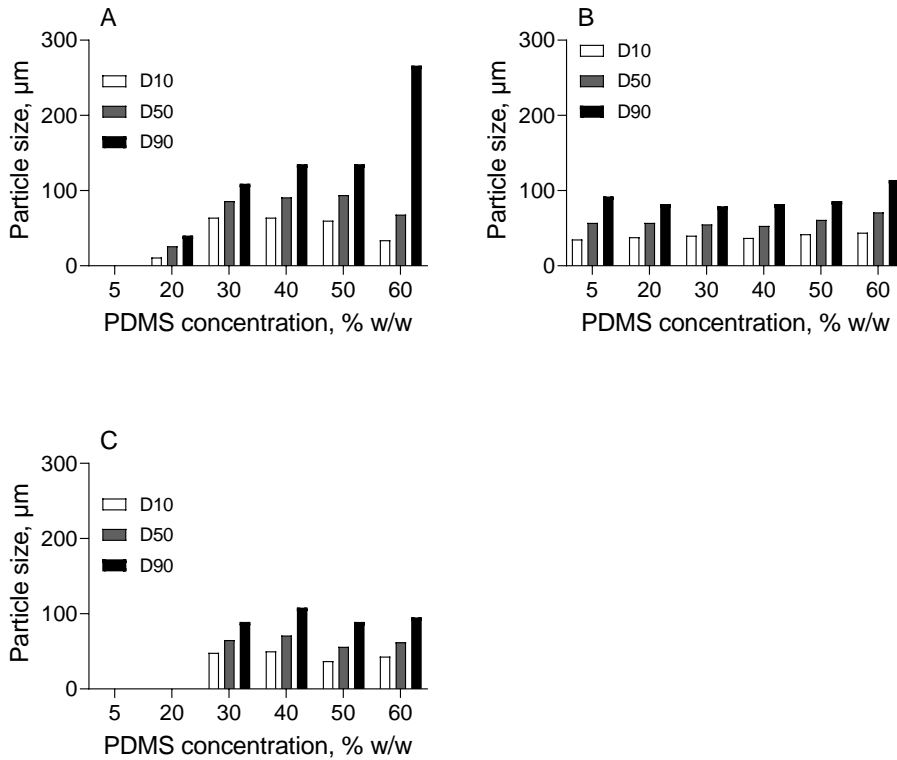
Figure 27 Effect of the system temperature on the *in situ* droplet size distribution as a function of the polydimethylsiloxane (PDMS) concentration (A: 20 °C, B: 10 °C, C: 0 °C). 6 % w/w PLGA in methylene chloride, polydimethylsiloxane addition rate 0.05 g/min.

Decreasing the temperature from 20 °C to 10 °C led to an onset of phase separation already at low polydimethylsiloxane concentrations. Also, droplets were more distinct, thus facilitating the measurement of droplet sizes at even low polydimethylsiloxane concentrations. A reason for this might be an improved miscibility at 10 °C of the polymer solution and the non-solvent polydimethylsiloxane.

With a further temperature decrease to 0 °C, the earlier onset was lost, and distinct droplets were only detected at higher polydimethylsiloxane concentrations, comparable to the droplet formation onset at 20 °C. This was most probably caused by the increasing viscosity of the mixture due to a lower polymer chain mobility (Table 4).

Despite the longer equilibration time needed, the inverse relationship between temperature und viscosity resulted in increased mixture stability compared to 20 °C. Increasing viscosity might also be a reason for the increased stability of the ternary mixture at lower temperatures. The droplet sizes of phase separated systems at 10

and 0 °C, did not change up to a polydimethylsiloxane concentration of 60 %, while the system at 20 °C showed an increased D90 at 60 % polydimethylsiloxane.

Table 4 Influence of the temperature on the viscosity of polydimethylsiloxane (mean ± SD).

Temperature, °C	Viscosity, mPas
20	389.14 ± 0.72
10	490.96 ± 0.72
0	551.17 ± 0.96
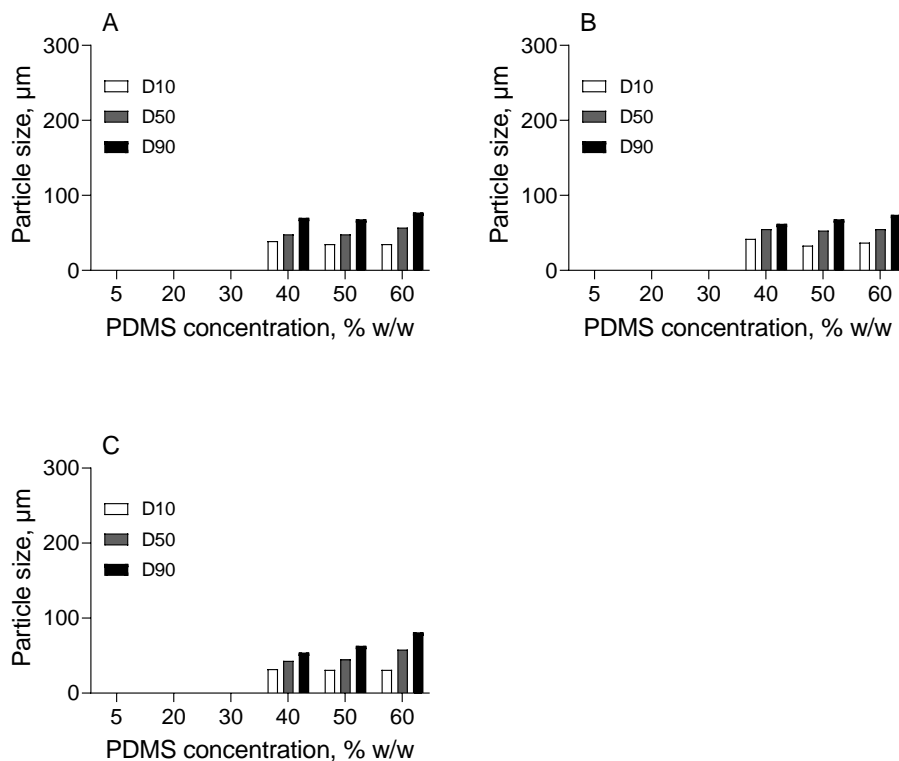
Figure 28 Effect of the system temperature (A: 20 °C, B: 10 °C, C: 0 °C) on the *in situ* droplet size distribution as a function of the polydimethylsiloxane (PDMS) concentration. 3 % w/w PLGA in methylene chloride, polydimethylsiloxane addition rate 0.05 g/min.

In contrast to the significant influence of the system temperature at 6 % PLGA, variations in the system temperature for a lower PLGA concentration (3 % PLGA in

methylene chloride) did not show an impact on the start of the phase separation and the droplet size distribution (Figure 28). Irrespective of the temperature, formation onset of distinct droplets started at about 40 % polydimethylsiloxane, while the droplet size distribution was comparable for temperatures from 0 to 20 °C and polydimethylsiloxane concentrations from 40 to about 60 %. The lower polymer concentration shifted the onset of the coacervate instability to higher polydimethylsiloxane concentrations. Due to the dilution effect, the inter-particular distance is increased, thus improving the coacervate stability at higher polydimethylsiloxane concentrations. Due to the low polymer concentration, more polydimethylsiloxane was needed to induce the coacervation, the effect of which was predominant compared to the temperature impact.

Overall, the droplet formation study by *in situ* visualization gave insights into the liquid-liquid phase separation dependency not only on the material characteristics of the non-solvent and its respective concentration, but also on various formulation and process parameters, more precisely the non-solvent addition rate, polymer concentration, and the system temperature, which had a critical influence on the coacervate stability and, ultimately, display critical parameters to be considered in process control to obtain a robust process for the preparation of polymer-based microparticles by organic phase separation.

3.1.2 Influence of the introduction of an inner aqueous phase on the coacervate stability

The introduction of an inner aqueous phase comprising a water-soluble drug may improve the drug distribution within the polymer matrix. The influence of an additional aqueous phase to the sensitive solvent system regarding the coacervate stability and the resulting risk of agglomeration upon addition to the hardening bath must be considered and critically evaluated to achieve a robust preparation process. Thus, key formulation and process parameters of the primary emulsion (W/O) were investigated in terms of droplet size distribution and its influence on the coacervate stability and characteristics of the microspheres.

3.1.2.1 Influence of the dispersion method on droplet size distribution of the primary emulsion and its influence on critical quality attributes of drug-loaded microparticles

To investigate the influence of the dispersion method on the coacervate stability and finally the critical quality attributes of the microparticles, aqueous drug solutions with a solid content of 10.5 % w/w were dispersed in a 6 % PLGA solution in methylene chloride with a rotor-stator-dispersing tool or with a sonication probe.

The obtained primary emulsions appeared homogeneous by visual examination irrespective of the preparation method. After drying, however, particles with the primary emulsion prepared by rotor-stator-dispersion were sticking, while a free-flowing powder was obtained for the primary emulsion prepared by ultrasonication. A high fraction of agglomerates was present in sticking microparticles, while particles in the free-flowing powder prepared with ultrasound were well-separated and homogeneous (Figure 29, Figure 30).

The primary emulsion prepared with the sonication probe resulted in smaller droplet sizes and a more uniform droplet size distribution (Figure 31). This increased the coacervate stability and hence concomitantly decreased agglomeration upon hardening. This indicates a superiority of the primary emulsion obtained by sonication compared to the primary emulsion obtained by rotor-stator dispersion and highlights the importance of the primary emulsion regarding coacervate stability and ultimately the appearance of the microparticles.
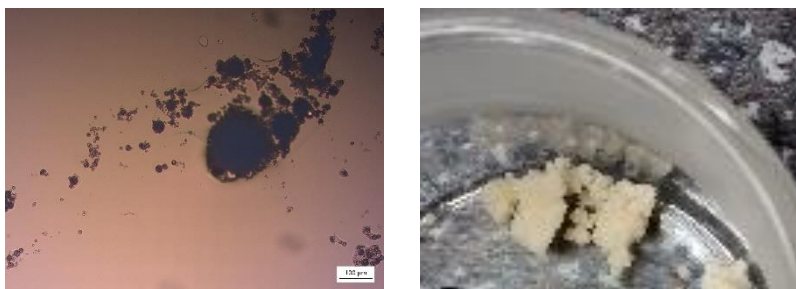
Figure 29 Microscopical (left, scale bar: 100 µm) and macroscopical (right) appearance of microparticles, the primary emulsion of which was prepared with a rotor-stator-mixer. Agglomerates could be separated after drying.

Figure 30 Microscopical (left, scale bar: 100 µm) and macroscopical (right) appearance of microparticles the primary emulsion of which was prepared by ultrasonication. Microparticles were free-flowing after drying and did not show agglomerates.

The primary emulsion stability regarding successful drug encapsulation into polymeric microparticles is important, as stabilizers in the primary emulsion affected the encapsulation efficiency, size and morphology of microparticles [145].

The primary emulsion obtained with the rotor-stator mixer showed a bimodal droplet size distribution with two non-separated peaks characterized by a D_{10}, D_{50} and D_{90} of 1.8, 4.3 and 18.3 µm, while the ultrasonicated emulsion showed a uniform droplet size distribution characterized by a d_{10}, d_{50} and d_{90} of 1.9, 3.5 and 6.6 µm, respectively (Figure 31). The superior homogeneity of the ultrasonicated emulsion was reflected by a span of 1.3 compared to a distinct higher value of 3.8 for the emulsion prepared with the rotor-stator mixer.
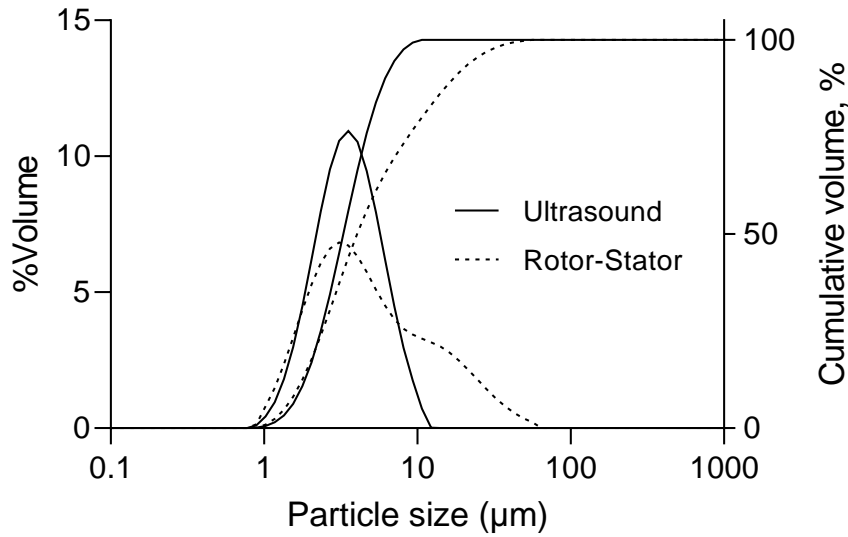
Figure 31 Droplet size distribution by LD and cumulative volume distribution of W/O-emulsions as a function of the preparation method (ultrasonication for 30 sec at 50 % amplitude compared to rotor-stator-dispersion for 3 min at 24,000 rpm). 10.5 % w/w solid content in aqueous phase, 6 % w/w PLGA in methylene chloride.
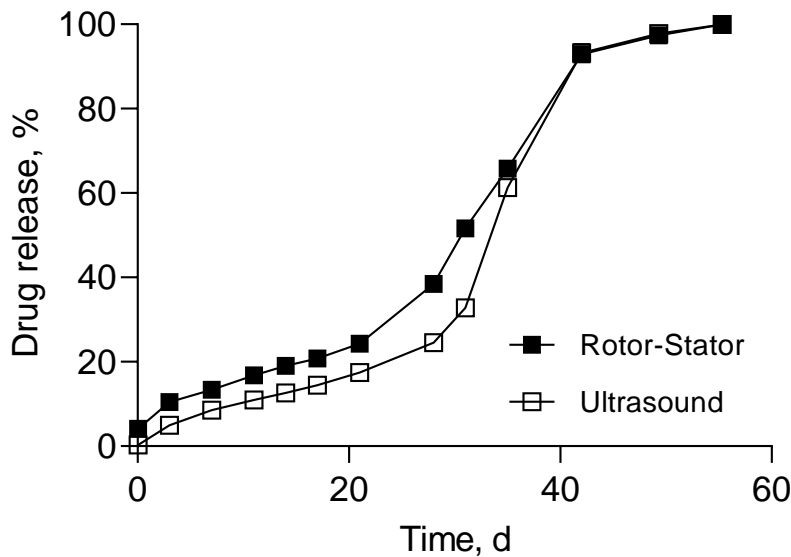
Figure 32 Influence of the primary emulsion dispersion method on drug release from PLGA microparticles (37 °C/80 rpm, n=3, mean ± SD, error bars shorter than the size of symbols not shown in graph).

Based on the differences observed regarding emulsion droplet size and microparticle size distribution, drug release from microparticles differing in primary emulsion preparation method was expected to be influenced as well. Primary emulsion droplet sizes impacted microparticle characteristics prepared by a double-emulsion solvent evaporation technique, where the emulsion stability regarding creaming, sedimentation, flocculation and coalescence was the driving factor for the final internal morphology of the microparticles [146].

Both formulations showed a comparable triphasic release profile. After the burst, the lag-phase for about 22 days was characterized by drug release by diffusion, followed by a fast release starting around day 23 (Figure 32).

However, the burst was influenced by the primary emulsion droplet size and preparation method. Using ultrasound led to decreasing droplet sizes and increasing droplet size distribution uniformity, and the initial release decreased from about 4.1 % to about 0.3 % compared to the rotor-stator method (Figure 32).

As microparticles showed comparable encapsulation efficiencies (~85%) and particle sizes (d_{50}~70-100 μm), the differences in initial release were attributed to the drug distribution within the polymeric matrix.

This can be explained by two phenomena. First, according to the hydrodynamics during the formation of the final microspheres, droplet size reduction is achieved if the shear exerted by micro-eddies on the droplet interfaces is higher than the existing cohesive forces. Latter depend on the internal droplet morphology. If an internal, immiscible phase is present in the phase to be dispersed, the cohesion forces may be altered due to the discontinuity of the phase. According to previous reports regarding W/O/W emulsions, these discontinuous regions may weaken the droplet and can therefore be located along the fragmentation routes, while the fragility increases with increasing droplet sizes [147]. The same seems to apply for W/O/O phase separation processes. With increasing primary emulsion droplet sizes, the coacervate droplet rupture is eased. Furthermore, the location of the large internal droplets comprising the water-soluble drug substance along the fragmentation route leads to an increased drug fraction exposed close to the particle surface after hardening, thus further increasing the initial drug release (Figure 33).
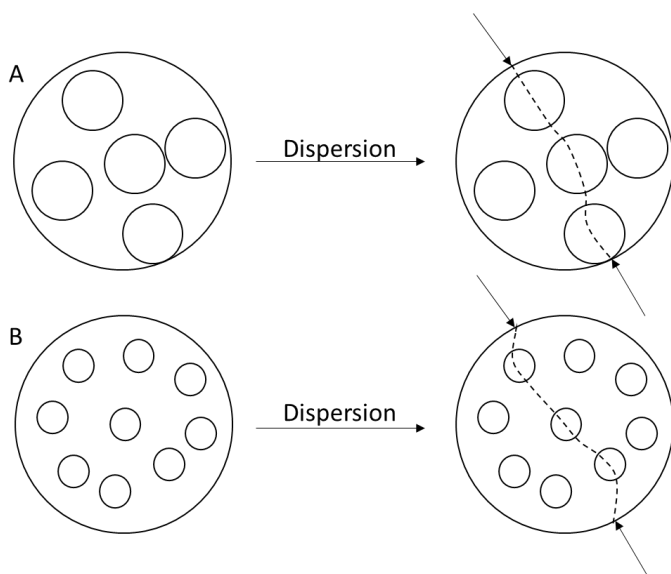
Figure 33 Schematic display of the fragmentation routes upon dispersion of droplets containing an inner aqueous phase characterized by large (A) or small (B) droplet sizes (adapted from [147]).

Second, with decreasing primary emulsion droplet sizes, the polymer layer thickness and, hence, the diffusion pathway for the water-soluble drug might be increased. By this, the drug amount available close to the microparticle surface is further decreased, leading to a reduced initial drug release as observed in the conducted study.

This observation is in accordance with numerous previous studies on PLGA microparticles prepared by W/O/W solvent evaporation methods. Increased primary emulsion droplet sizes led to collapsed particles due to reduced polymer layer thicknesses, which led to an increased initial drug release [119]. A destabilized BSA-containing primary emulsion also resulted in an increased burst, which was explained by an increased microparticle porosity [148]. An increasing burst was furthermore found for FITC-dextran loaded microparticles prepared from RG502H and RG503H PLGA grades with decreasing primary emulsion homogenization speeds, while particle size distribution and the second release phase was unaffected [149].

Overall, the importance of a precise control of the primary emulsion droplet size distribution for the preparation of drug-loaded PLGA microparticles by W/O/O phase separation method was revealed. Low primary emulsion droplet sizes and a uniform droplet size distribution support a stable coacervate phase and, finally, result in free-flowing microparticles. Additionally, the primary emulsion droplet size plays a critical role in the drug distribution within the polymeric matrix. This ultimately impacts the

burst of water-soluble drugs, which is of great importance for drug product development studies.

However, a minimum droplet size is not considered the optimum condition, as the lowest droplet size is limited by other critical formulation and process factors. The stability of the drug during the dispersion step might limit the size reduction step. This is, first, due to the increased energy input, which might facilitate the drug degradation progress [150]. Second, with special regard to sensitive drugs like peptides and proteins, due to the increasing interfacial surface area between aqueous and organic phase, which may lead to increased drug-polymer or drug-solvent-interactions, facilitating possible drug instability and raising the need for further stabilization approaches [151, 152]. Last, the dispersion energy input should evidently be limited to a minimum for ecological and economic reasons, which should already be considered at small-scale manufacturing process development stages.

3.1.2.2 Influence of the dispersing mode

With regard to a subsequent scale-up, the application of a dispersing unit is despite the discussed drawbacks the preferred option in comparison to the application of a sonication probe, as dispersion units are available for the preparation of large emulsion volumes, possibly including a recirculation unit [153]. Transitioning from batch to continuous rotor-stator mixing is demanding, but feasible [89]. Passing the emulsion repeatedly along the dispersion unit, improves the formation of a homogeneous emulsion characterized by a narrow droplet size distribution [153]. It was hence the objective to optimize the dispersion step with regard to time and modus to obtain droplet sizes leading to a stable coacervate thus reducing the risk of coalescence and agglomeration during coacervation and hardening.

Figure 34 Droplet size distribution by LD and cumulative volume distribution of W/O-emulsions as a function of the dispersion time (rotor-stator-dispersion for 3, 4 and 5 min at 24,000 rpm). 10.5 % w/w solid content in aqueous phase, 6 % w/w PLGA in methylene chloride.

The dispersion time had a strong influence on the droplet size distribution (Figure 34). With increasing dispersion time from 3 to 4 and 5 min, the D90 decreased from 18 to 10 and 8 µm, respectively. This was in congruence with decreasing droplet sizes at increasing stirring times of PMMA-solutions in methylene chloride emulsified in PVA solutions [85].

Increasing the dispersion time did not affect the D10 (1.8, 1.8 and 1.7 µm, respectively), indicating the presence of a lower droplet size threshold for the applied stirring time, type and emulsion composition. This was in congruence with an existing threshold in stirring speed, above which droplet sizes changed only slightly [94].

Furthermore, the inclusion of fluctuations in stirring speed is known to improve the comminution efficiency [94].
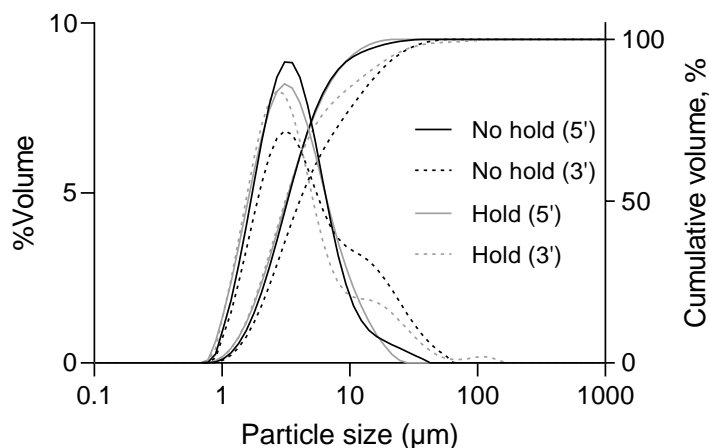
Figure 35 Droplet size distribution by LD and cumulative volume distribution of W/O-emulsions as a function of the dispersion modus (dispersion for 3 and 5 min, with or without 1-minute-holds every minute). Stirring speed 24,000 rpm, 10.5 % w/w solid content in aqueous phase, 6 % w/w PLGA in methylene chloride.

In the present study, the addition of hold-times was not able to decrease the droplet size (Figure 35). This was most probably due to the high density of the organic phase consisting mainly of methylene chloride ($\rho = 1.318 \ \frac{g}{cm^3}$, [140]), while the density of the aqueous inner phase was close to $\rho = 1 \ \frac{g}{cm^3}$. The deposition and accumulation of the inner phase during the hold times was thus characterized by floating of the inner phase, which could hence not improve the comminution by the dispersion unit. For both continuous and step-wise dispersion, a minimum dispersion time of 5 min was needed to achieve unimodal droplet size distributions with a D90 smaller than 10 µm (D90 after 3, 4 and 5 min: 15, 12 and 9 µm versus 18, 10 and 8 µm for dispersions prepared with and without one-minute hold steps, respectively). The smaller droplets were practically not impacted by an increased stirring time as reflected by the D10 trend after 3, 4 and 5 min (1.5, 1.6 and 1.5 µm versus 1.8, 1.8 and 1.7 µm for dispersions prepared with and without one-minute hold steps, respectively).

Due to the negligible effect of the inclusion of hold-times, a continuous dispersion was regarded to be the most appropriate dispersion mode for the formulation and process at hand. A temperature increase and hence risk of accelerated drug degradation was excluded by cooling of the emulsion during the dispersion step.

3.1.2.3 Influence of the solid content in the aqueous and organic phase on the droplet size distribution of the primary emulsion

The solid contents of the aqueous and organic phase were expected to impact the droplet size distribution due to the direct correlation with the viscosities of the dispersed and continuous phase of the primary emulsion. As the theoretical drug loading was aimed to be kept constant, a change in solid content was compensated by a change in the aqueous to organic phase volume ratio. With decreasing the aqueous phase solid content, the aqueous phase volume was increased, resulting in higher W:O ratios.
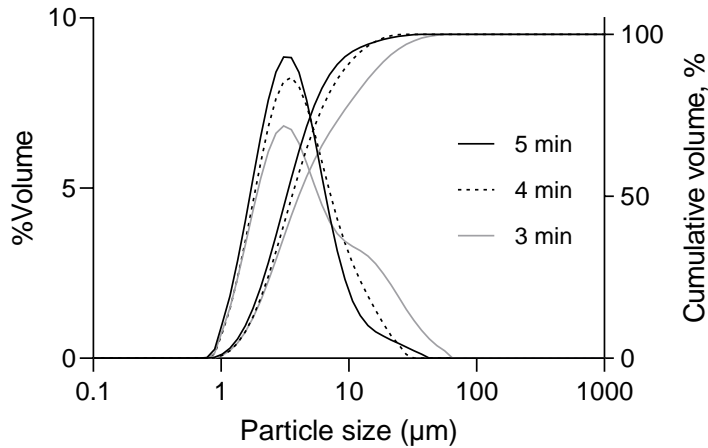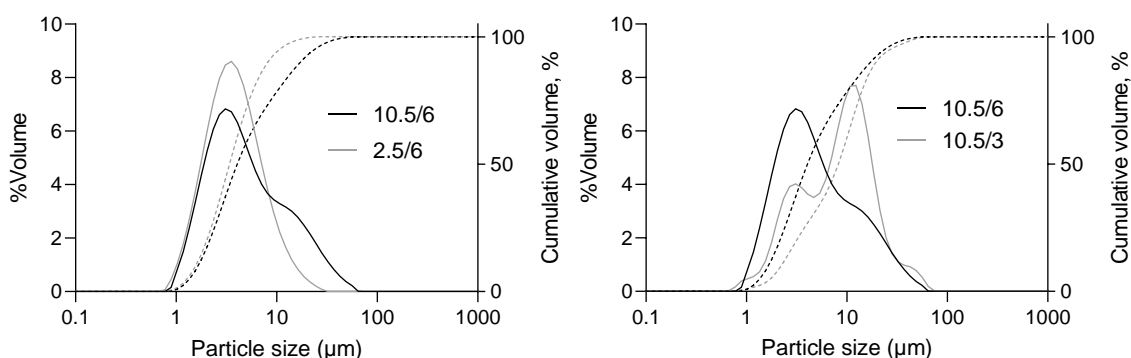

Figure 36 Droplet size distribution by LD and cumulative volume distribution of W/O-emulsions as a function of the aqueous phase solid concentrations (2.5 and 10.5 % w/w, left) and PLGA concentrations in methylene chloride (3 and 6 % w/w, right).

Decreasing the inner aqueous phase solid content from 10.5 % to 2.5 % w/w dispersed in a 6 % w/w PLGA solution in methylene chloride led from a bimodal droplet size distribution to a unimodal droplet size distribution characterized by D10, D50 and D90 values of 2, 4 and 18 µm and 2, 4 and 9 µm, respectively (Figure 36). This was most probably due to two reasons. First, the viscosity of the inner phase was decreased by decreasing the solid content by factor 4.2 and therefore decreasing the energy needed to disrupt the droplets. This was in congruence with decreasing mean droplet sizes in O/W-emulsions with decreasing viscosities of the dispersed phase produced by homogenization [93, 154]. Second, the increased aqueous phase volume leads to an increased total viscosity of W/O-emulsions [155]. This may have additionally improved the energy transfer during dispersion and hence resulted in smaller droplet sizes. The

increased viscosity most probably additionally stabilized the droplets and thus led to a narrower droplet size distribution.

Decreasing the outer organic phase solid content from 6 to 3 % resulted in a trimodal droplet size distribution characterized by a D10, D50 and D90 of 2, 4 and 18 µm and 2, 9 and 21 µm (Figure 36). Due to the lower viscosity of the organic phase, the energy transfer was possibly decreased, leading to a negative impact with regard to the droplet size reduction of the dispersed phase.

It was thus concluded that the solid concentrations in the inner and outer phase had a critical impact on the primary emulsion droplet size, which ultimately determined the coacervate stability.

3.1.3 Influence of the hardening step

After the preparation of a stable coacervate, the nascent microparticles are transferred to a hardening bath. The hardening agent is characterized by an increased capacity to extract the polymer solvent from the coacervate droplets compared to the coacervation agent, thus able to induce polymer precipitation for the solidification of the microparticles. Several parameters in terms of hardening bath composition and condition need thus to be considered when optimizing the process step of hardening. The effect of hardening time, composition and temperature of the hardening bath were tested for their suitability to harden coacervate droplets in an acceptable time while assuring stabilizing conditions resulting in free-flowing microparticles without agglomerates. Additionally, the dispersion of the coacervate emulsion in the hardening bath is expected to significantly influence the risk of agglomeration upon injection. Thus, the effect of the coacervate transfer rate, but also of the stirring rate was investigated regarding the influence on particle agglomeration.

3.1.3.1 Effect of the hardening time, hardening agent composition and temperature of the hardening bath

Physicochemical material properties determine the mutual affinity between solvent and hardening agent, and thus the hardening time to fully extract the polymer solvent.

The particle size distribution only slightly changed during hardening in octamethylcyclotetrasiloxane (Figure 37). At a polydimethylsiloxane concentration of 43.0 % w/w which was used for the induction of the phase separation, only a comparatively low organic solvent fraction of 5.8 % is left in the coacervate phase, while the majority of the methylene chloride (94.2 %) is already extracted to the polymer-poor phase. This leads to comparatively low shrinking rates of the particles during the hardening step compared to size reduction factors of 1.5 to 4 known for the solvent evaporation process [156]. The emulsification during coacervation is thus assumed to be the predominating size tuning step.
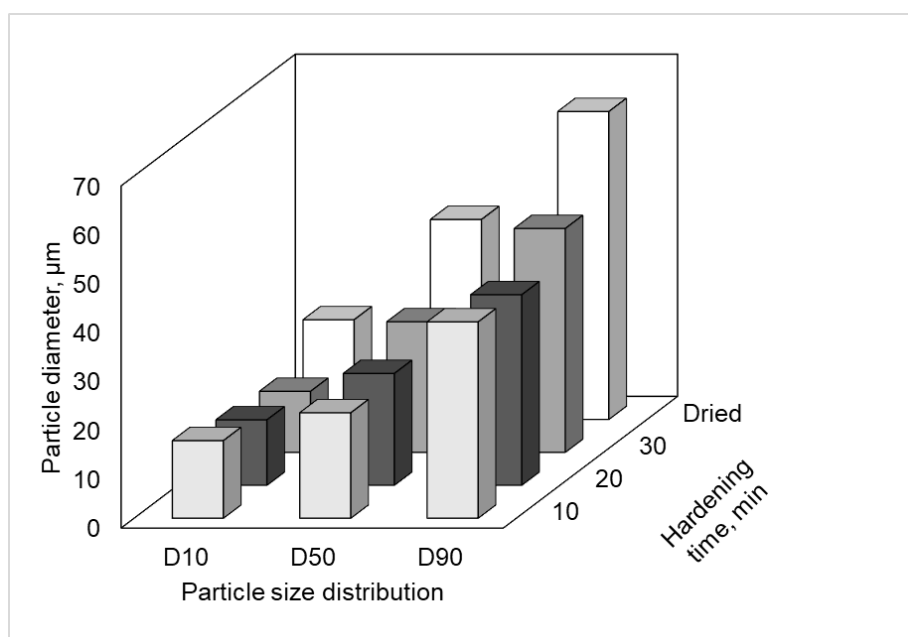
Figure 37 Effect of the hardening time on the particle size distribution. 6 % w/w PLGA in methylene chloride, polydimethylsiloxane to methylene chloride ratio 0.8:1.0 w/w, methylene chloride to octamethylcyclotetrasiloxane ratio 1:25 w/w.

A too fast extraction of the PLGA solvent from the nascent microparticles by the hardening agent was expected to be critical due to the time needed for dispersion in the hardening bath. The distance between the particles needs to be maximized as the droplets cross a "sticky state" before polymer precipitation is completed.

For a better control of the extraction velocity of methylene chloride from the nascent microdroplets, alternative hardening agents, additives as well as the influence of the temperature were investigated, which were expected to control the mutual affinity between hardening bath and methylene chloride.

Octamethylcyclotetrasiloxane and alkanes (e.g. heptane) are common hardening agents [122]. In opposite to other mineral oils, the octamethylcyclotetrasiloxane volatility shall facilitate a removal by drying without the need of an additional washing step. However, the boiling point of octamethylcyclotetrasiloxane is significantly higher than for e.g. heptane (176 and 98 °C, respectively). An advantage displays the higher viscosity of the silicon oil (3.824 mPas) compared to the one of heptane (0.389 mPas), improving the stabilization of the coacervate droplets in the hardening bath. To compare the mutual affinity between methylene chloride and heptane and octamethylcyclotetrasiloxane, respectively, the static methylene chloride diffusion was investigated from a 6 % PLGA solution (Figure 38) towards the hardening agents and possible additive. The diffusion plot of methylene chloride to heptane was characterized by a sigmoidal shape. Up to 20 min, the solvent diffusion was comparatively slow, while it increased thereafter. After reaching 10 % of the total volume, the diffusion rate decreased and plateaued.

The diffusion of methylene chloride to octamethylcyclotetrasiloxane was slower, indicating a slower extraction of the organic solvent from the coacervate phase upon hardening.
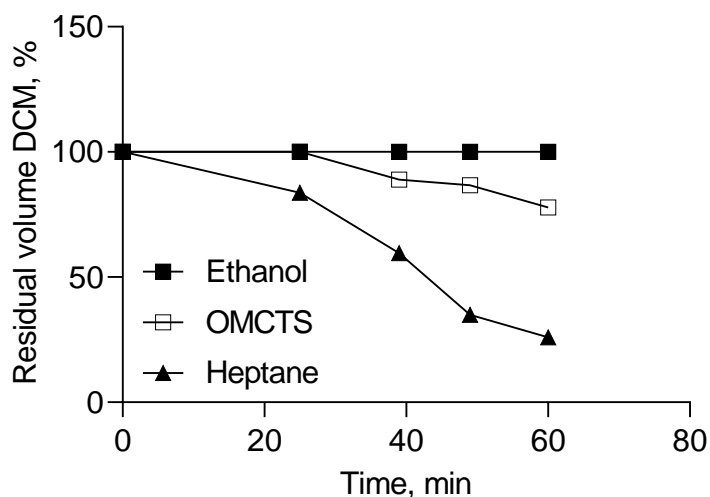
Figure 38 Diffusion of methylene chloride (DCM) from a 6 % w/w PLGA solution in methylene chloride to heptane, ethanol and octamethylcyclotetrasiloxane during 60 min as a function of time under static conditions.

Table 5 Physicochemical properties of octamethylcyclotetrasiloxane (OMCTS) and heptane from the classes of volatile silicon oils and alkanes, used as hardening agents for the preparation of PLGA microparticles by organic phase separation. Polydimethylsiloxane (PDMS), methylene chloride (DCM).

Parameter	Unit	OMCTS	Heptane
Viscosity (25°C)	mPas	3.824	0.389
Density (25 °C)	g/cm³	0.956	0.680
Miscibility with PDMS	-	Fully miscible	
DCM diffusion (static)	µL/mincm²	2.947	7.289

To compare the two hardening agents octamethylcyclotetrasiloxane and heptane, placebo batches were prepared at the "lower" end of the stability window (polydimethylsiloxane concentration of 36.1 %), as the influence of the hardening agent was expected to be more pronounced at higher methylene chloride concentrations in the coacervate droplets.

For both hardening agents, free-flowing microparticles with comparable mean particle sizes were obtained. However, for heptane, the particle size distribution (span 2.38) was broader than for octamethylcyclotetrasiloxane (span 0.99), which was attributed to a better stabilization of the coacervate droplets after the addition to the hardening bath, thus a lower risk of coalescence or agglomeration. The higher viscosity and density of octamethylcyclotetrasiloxane helped to stabilize the coacervate droplets, and the methylene chloride diffusion rate was slower, leading to an increased time gap between complete solvent extraction and the full dilution and thus increased distance between the droplets in the hardening agent.

Then, additives and process parameters were investigated to reduce the methylene chloride extraction velocity to reduce the sticking at the injection site.

Table 6 Appearance of microparticles and required hardening time as a function of the composition and temperature of the hardening bath. Range from "no agglomeration" (-) to "pronounced agglomeration" (+++). Hardening was assumed to be finished when microparticles appeared non-transparent under optical microscope. Ethanol (EtOH), polydimethylsiloxane (PDMS).

Hardening bath composition	Temperature, °C	Agglomeration	Hardening time, min
Heptane	15	-	25
Heptane: EtOH, 95:5 w/w	15	+	30
Heptane: EtOH, 80:20 w/w	15	+	40
Heptane: EtOH, 50:50 w/w	15	+++	60
Heptane: EtOH gradient	15	+	30
Heptane: PDMS 90:10	15	++	30
Heptane	2	+++	60

The addition of ethanol, which is miscible with heptane and immiscible with polydimethylsiloxane, increased the hardening time due to a lower mutual affinity of methylene chloride to the hardening bath (Figure 38), and thus a slower diffusion of methylene chloride from the coacervate droplets to the hardening bath. An ethanol concentration from 0 to 5 and 20 % w/w increased the hardening time from 25 to 30 and 40 min, still being an acceptable duration for a microparticle preparation. A further increase of ethanol to 50 % w/w resulted in a hardening time of 60 min and pronounced agglomeration starting after 15 min. This indicated that a too slow methylene chloride extraction promotes agglomeration, suggesting a medium solvent extraction velocity to be the optimum for a minimum agglomeration risk.

The alternative use of a heptane gradient, starting with a heptane to ethanol weight ratio of 90:10 and resulting in a ratio of 94:6, did not influence the hardening time compared to hardening in a mixture with a heptane to ethanol weight ratio of 95:5. Besides, agglomeration was observed with optical microscopy starting from 10 min hardening time, which might be due to a too slow solvent extraction and the lower volume at the beginning of hardening (methylene chloride: hardening bath ratio from 1:16 to 1:26).

The addition of polydimethylsiloxane to heptane at a concentration of 10 % w/w did not influence the hardening time but increased the agglomeration risk. Moreover, microparticles were not spherical, but deformed. This was most probably due to a slower methylene chloride extraction, hindering the polymer precipitation at the outer shell and thus reducing the stability of the nascent microparticles. Additionally, the increased viscosity of the outer phase may have influenced the stirring geometries, thus causing differences in the microparticle shape.

Decreasing the heptane temperature from 15 °C to 2 °C increased the hardening time from 25 min to 60 min, which was due to a restricted diffusion of methylene chloride to the hardening bath. This led to strong sticking and pronounced agglomeration.

In conclusion, the affinity of the polymer solvent to the hardening agent plays a critical role in the extraction process. With increasing affinity, the solvent extraction becomes faster, while hardening bath additives with low affinity to methylene chloride, i.e. ethanol, can decrease the methylene chloride extraction speed and thus increase hardening times. The temperature also influences the hardening time, as a decrease lowers the affinity of the polymer solvent to the outer phase and decreases molecular diffusion, thus increasing the hardening time of microparticles. A slight decrease in affinity of the hardening bath is feasible with hardening baths based on heptane, but too long hardening times increase the risk of agglomeration, as the risk of particle collision in the sticky state is increased.

3.1.3.2 Effect of the stirring rate during the coacervate addition and the coacervate addition rate

The addition of the coacervate emulsion to the hardening bath is another critical step in the preparation process. Coacervate droplets are expected to show less agglomeration with increasing mean distance between droplets during the methylene chloride extraction. Thus, the dilution, stirring rate and emulsion addition rate should be optimized to reduce the risk of contact and agglomeration.

Table 7 Influence of the stirring rate, coacervate addition rate and the methylene chloride (DCM) to heptane ratio on the agglomeration extent of placebo microparticles. Range from "no agglomeration" (-) to "pronounced agglomeration" (+++).

Tip speed, ms^{-1}	Addition rate, gmin^{-1}	DCM:heptane ratio, w/w, 1:x	Agglomeration
69.12	1.7	26	-
51.84	1.7	26	++
34.56	1.7	26	+++
69.12	3.3	26	-
69.12	50	26	-
69.12	1.7	16	-

The stirring rate during hardening had a strong influence on agglomeration of the microparticles. Reducing the tip speed from 69 to 52 and 35 ms^{-1} resulted in increasing agglomeration, thus a certain tip speed (in this geometry 69 ms^{-1}) is needed to prevent nascent droplets and resulting microparticles from agglomeration.

Increasing the coacervate addition rate from 1.7 to 3.3 and 50 g/min did not impact particle agglomeration and resulted in homogeneous, free-flowing microparticle without agglomerates.

Decreasing the volume of the hardening bath (increase of methylene chloride: heptane ratio from 1:26 to 1:16) increased the concentration of coacervate droplets, causing a higher probability of agglomeration. A tip speed of 69 ms^{-1} could sufficiently prevent agglomeration and the amount of heptane was still sufficient to extract the organic solvent from the coacervate droplets.

The stirring efficiency was thus the limiting parameter in microparticle hardening, as a sufficient movement of the coacervate phase prevents strong microparticle agglomeration. If sufficient movement of the particles is guaranteed, parameters such as the volume of the hardening bath and the addition rate are negligible in influence.

3.1.4 Development of a continuous manufacturing approach for a liquid-liquid phase separation method with static mixer

The scale-up of discontinuous production processes that include stirring steps is generally considered critical. Due to the mixing-rate heterogeneity at different scales, particle size distributions are often hard to control [109]. This applies especially to processes comprising time-dependent steps which can often not be directly transferred to large scales. Maa et al. applied a dimensional analysis of a continuously stirred tank reactor for a scale-up from 1 L to 100 L for the preparation of microparticles by solvent extraction, resulting in predictable microsphere sizes [108]. However, a stringent geometric scale-up lacks flexibility regarding batch sizes meeting industrial needs. Additionally, challenges regarding time-dependent parameters as for organic phase separation processes cannot be solved by this approach.

For small scales, the transfer of the phase-separated emulsion to the hardening bath is very fast and usually performed manually in a discontinuous manner [157-159]. This approach is not applicable for large scales. During the transfer, significant emulsion amounts are in an unstirred state. Time is important regarding coalescence and, hence, droplet size distribution and agglomeration (see 3.1.1.3). Additionally, the remaining emulsion volume in the phase-separation vessel decreases upon gradual transfer, thereby constantly changing the geometry of stirring. This clearly leads to mixing differences within one batch over the manufacturing time profile. Inconsistencies of droplet sizes due to mixing inhomogeneity within one batch are reflected by broad particle size distributions and are especially expected for larger scales. This may lead to unacceptable high variabilities of critical quality attributes (CQAs) within one batch, the risk of which increases with increasing batch sizes.

Static mixers allow a time-independent manufacturing process compared to batch processes by continuous manufacturing approaches. Independent of the amount of emulsion transferred, it faces similar stirring conditions throughout the complete manufacturing process.

Continuous manufacturing methods are attracting more attention due to their higher agility, flexibility, cost, and robustness compared to batch processes [160]. Though a setup with static (micro-)mixers for the preparation of microparticles was applied successfully for the solvent evaporation/ extraction method [109, 113, 161], the phase

separation process by static mixing is rarely discussed in the scientific literature [162, 163].

Results from emulsion-based investigations usually deliver precise and transferable models for other applications [109], as viscosities can be considered constant, and the dispersed and continuous phase are usually immiscible to form stable droplets [56, 109].

Liquid-liquid phase separation processes show comparatively high viscosities in contrast to commonly processed emulsions for microencapsulation [147], leading to high device demands. Additionally, the composition of the two phases dynamically changes upon the solvent partitioning, as PLGA solvent and anti-solvent are fully miscible with each other [7]. This results in dynamic phase composition changes during the mixing ultimately determining substantial phase characteristics like viscosity and Reynolds number. These define the droplet deformation mechanism and, finally, the particle size distribution, which is one of the most important critical quality parameters of microparticles intended for parenteral administration.

To assess the applicability of a static mixer set-up for a phase separation process, placebo and drug-loaded PLGA microparticles were prepared using a continuous manufacturing set up. The effect of formulation and process parameters, as well as a scale-up was analyzed in terms of particle size distribution, span, yield and encapsulation efficiency.

3.1.4.1 Effect of the polymer concentration

The influence of the polymer concentration, known to determine the PLGA solution viscosity, the coacervate phase stability and the stability window, was investigated.

Table 8 Influence of the PLGA concentration in methylene chloride (DCM) on particle size distribution, span, residual solvents and yield of placebo microparticles prepared with a static mixer. Methylene chloride to polydimethylsiloxane (PDMS) ratio 1:0.7 w/w, total flow rate 150 mL/min, hardening agent octamethylcyclotetrasiloxane (OMCTS).

PLGA concentration, % w/w	PSD, μm (D10/50/90)	Span	Mean residual solvent level, % w/w			Yield, %
			DCM	PDMS	OMCTS	
1.5	7/11/17	0.884	1.38	4.61	2.91	91.7
3.0	5/14/27	1.636	2.81	6.74	2.44	93.4
6.0	8/19/57	2.520	3.92	9.41	1.79	95.9

Decreasing the polymer concentration in methylene chloride from 6.0 to 3.0 and 1.5 % narrowed the microparticle size distribution, indicated by a decreasing span from 2.5 to 1.6 and 0.9 (Table 8). This was most probably caused by the decreasing PLGA solution viscosity causing smaller droplets during dispersion, which was also observed for polymer solutions emulsified in aqueous solutions [109], and the lower risk of coalescence due to the higher dilution as indicated by decreasing D90 values from 57 to 27 and 17 μm for 6.0, 3.0 and 1.5 % PLGA in methylene chloride.

The appearance with scanning electron microscopy showed an increasing number of very small particles sticking to the particle surface with decreasing polymer concentration. This was most probably due to the higher number of very small droplets, which were stabilized during the preparation of microparticles (Figure 39). This was in congruence with the stabilization of very small droplets at very high stabilizer concentrations in the preparation of microparticles by solvent evaporation with a static mixer [109].

The residual solvent levels were affected by the polymer concentration. A direct correlation between residual polydimethylsiloxane and polymer concentration existed (Table 8). With decreasing polymer concentrations from 6.0 to 3.0 and 1.5 %, polydimethylsiloxane decreased from 9.4 to 2.8 and 1.4 %. This was attributed to a more efficient removal of the non-solvent upon hardening due to the decreasing mean particle size at lower polymer concentrations. Additionally, the agglomeration of particles, as indicated by increasing D90 values for increasing polymer concentrations,

might have led to an inclusion of silicon oil into the particle, the extraction of which is hindered by the polymer matrix.

Methylene chloride decreased with decreasing polymer concentrations from 3.9 to 2.8 and 1.4 %. The smaller droplet size and thus higher surface area led to a more efficient solvent extraction upon hardening and solvent evaporation during drying.

Octamethylcyclotetrasiloxane residuals were not influenced by changes in the polymer concentration.

With decreasing polymer concentration, the yield decreased slightly from 96 to 92 % (Table 8). As the processing time was kept constant, the batch size decreased with decreasing polymer concentration, which led to a higher influence of relative loss by material sticking to equipment.

The polymer concentration thus was a key factor controlling the particle size distribution for emulsions prepared with static mixers. With decreasing polymer concentrations, the viscosity of the inner phase and outer phase were decreased, and the higher dilution of the polymer-rich droplets in the outer, polymer-poor phase improved the emulsion stabilization.
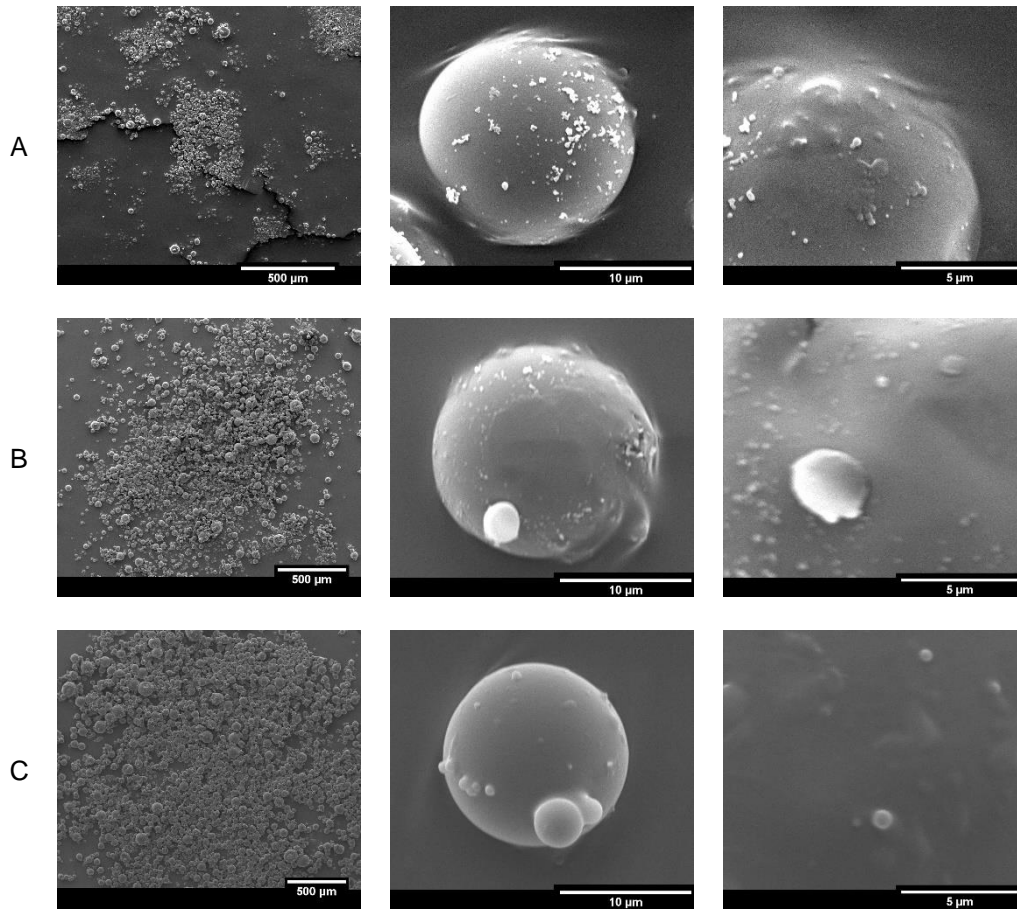
Figure 39 Influence of the PLGA concentration in methylene chloride on the appearance of the powder (left), single microsphere (middle) and surface (right) by scanning electron microscopy (A: 1.5 %, B: 3.0 %, C: 6.0 % PLGA in methylene chloride).

3.1.4.2 Effect of the total flow rate

The total flow rate has a major influence on the stretching and folding of the phases during the passage through the static mixer. Thus, the effect of the total flow rate on blank PLGA-microparticles was investigated in terms of mean particle sizes, particle size distribution, yield and residual solvent levels.

Table 9 Influence of the total flow rate on particle size distribution, span, residual solvents and yield of placebo microparticles prepared with a static mixer. Methylene chloride (DCM) to polydimethylsiloxane (PDMS) ratio 1:0.7 w/w, 6 % w/w PLGA in methylene chloride. Hardening agent octamethylcyclotetrasiloxane (OMCTS).

Total flow rate, mL/min	PSD, µm (D10/50/90)	Span	Mean residual solvent level, % w/w			Yield, %
			DCM	PDMS	OMCTS	
100	12/30/65	1.785	4.63	7.34	1.53	71.5
150	8/19/57	2.520	3.92	9.41	1.79	95.9
200	6/12/46	3.317	4.31	6.89	2.22	98.6

By increasing the total flow rate from 100 to 150 and 200 mL/min, the span increased from 1.8 to 2.5 and 3.3. However, agglomeration occurred in the case of 100 mL/min, which was not reflected in the particle size distribution values, resulting in a false-low span. The effect of the total flow rate on the span is thus not as pronounced than first assumed.

Mean particle sizes were decreased from 30 to 19 and 12 µm, which was in congruence with decreasing droplet sizes of O/W emulsions from 250 to 100 µm with increasing flow rates from 70 to 340 mL/min prepared with a static mixer [109]. The difference in droplet sizes is not only due to the different geometry and flow regime but also due to the viscosity differences, which have a critical influence on the Reynolds number and thus the droplet diminution. Furthermore, the dynamic phase composition change of the phase separation process within the static mixer may lead to different observations, compared to common static conditions in emulsions of non-miscible phases [113].

The surface morphology determined with SEM was independent of the total flow rate (Figure 40).

The residual solvent levels were unaffected by the change in total flow rates from 100 to 200 mL/min (Table 9). This indicated a similar mixing efficiency, leading to comparable solvent distribution profiles and residual solvent levels.

The yield for 200 and 150 mL/min was comparable (98.6 and 95.6 %, respectively), but a further decrease in the total flow rate to 100 mL/min resulted in a significantly

decreased yield of 72 %, which was due to agglomeration of particles in the hardening bath. The lowest flow rate was not sufficient to produce a homogeneous emulsion, resulting in bigger droplets which agglomerated upon injection to the hardening bath. A dependency of the droplet sizes on the total flow rate and the existence of a minimum total flow rate thus exists.

Figure 40 Influence of the total flow rate on the appearance of the powder (left), single microsphere (middle) and surface (right) by scanning electron microscopy (A: 100 mL/min, B: 150 mL/min, C: 200 mL/min).

3.1.4.3 Effect of the polydimethylsiloxane concentration

The polydimethylsiloxane concentration in the phase-separated ternary mixture has a strong influence on the solvent distribution between the polymer-rich and polymer-poor phase. With increasing polydimethylsiloxane concentrations, the emulsion stability of the polymer-rich phase in the polymer-poor phase increased until the end of the

stability window was reached. Furthermore, the coacervate viscosity increased with increasing polydimethylsiloxane concentrations. Different polydimethylsiloxane concentrations within the stability window (32.1 %, 39.8 % and 48.5 %) were thus investigated for the preparation of PLGA microparticles with a static mixer.

Table 10 Influence of polydimethylsiloxane (PDMS) concentration in the coacervate emulsion on particle size distribution, span, residual solvents and yield of placebo microparticles prepared with a static mixer. Total flow rate 150 mL/min, 6 % w/w PLGA in methylene chloride (DCM), hardening agent octamethylcyclotetrasiloxane (OMCTS).

PDMS concentration, % w/w	PSD, µm (D10/50/90)	Span	Mean residual solvent level, % w/w			Yield, %
			DCM	PDMS	OMCTS	
32.1	6/13/38	2.543	4.10	6.58	2.91	65.3
39.8	8/19/57	2.520	3.92	9.41	1.79	95.9
48.5	6/13/28	1.724	4.26	8.57	1.34	98.5

For increasing polydimethylsiloxane concentrations from 32.1 to 39.8 and 48.5 %, the span decreased from 2.5 to 2.5 and 1.7. The lowest polydimethylsiloxane concentration led to a significantly lower yield of 65 % due to agglomeration in the hardening bath. Lost particles are not reflected in the particle size measurement and span, thus the true D90 and span value of the lowest polydimethylsiloxane concentration are actually higher.

Despite the increasing viscosity of the polymer-rich phase with increasing polydimethylsiloxane concentrations, the mean particle size was unaffected, indicating an efficient dispersion of the coacervate phase in the continuous phase, and a sufficient stabilization of the dispersed droplets in the continuous phase. According to the theory on coalescence efficiency, the film drainage is hindered by increasing viscosity of the continuous phase. To determine the effect of the increased polydimethylsiloxane concentration, the viscosities of different mixtures were measured.

Upon solvent distribution, the dilution of polydimethylsiloxane with methylene chloride may decrease the outer phase viscosity from 390 to 22 mPas (100 %

polydimethylsiloxane versus 33 % polydimethylsiloxane in methylene chloride, w/w, Table 11), while the viscosity of the dispersed phase increased from 25 cSt to 2070 cSt [121]. The pronounced effect of the dilution on the viscosity (18-fold lower viscosity for a solution of 33 % polydimethylsiloxane in methylene chloride, Table 11) did not follow a linear correlation and indicated a strong interaction between methylene chloride and silicon oil molecules. However, even the minor effect of increase in viscosity by increasing polydimethylsiloxane concentration from 32 to 40 and 49 % helped stabilizing the emulsion and preventing coalescence.

Table 11 Viscosities of different solvents and compositions occurring during liquid-liquid phase separation (mean ± SD, n=100). Polydimethylsiloxane (PDMS), methylene chloride (DCM).

Composition	Viscosity (±SD), mPas
PDMS (100 %)	389.14 (± 0.72)
33 % PDMS in DCM	21.82 (± 1.34)
DCM (100 %)	0.41 [140]

The surface morphology was not influenced by the polydimethylsiloxane concentration. For all formulations, some smaller particles were observed sticking to the particle surface.

The residual solvent concentrations were independent of the polydimethylsiloxane concentration (Table 10), which showed an efficient solvent dilution/extraction in the hardening bath.

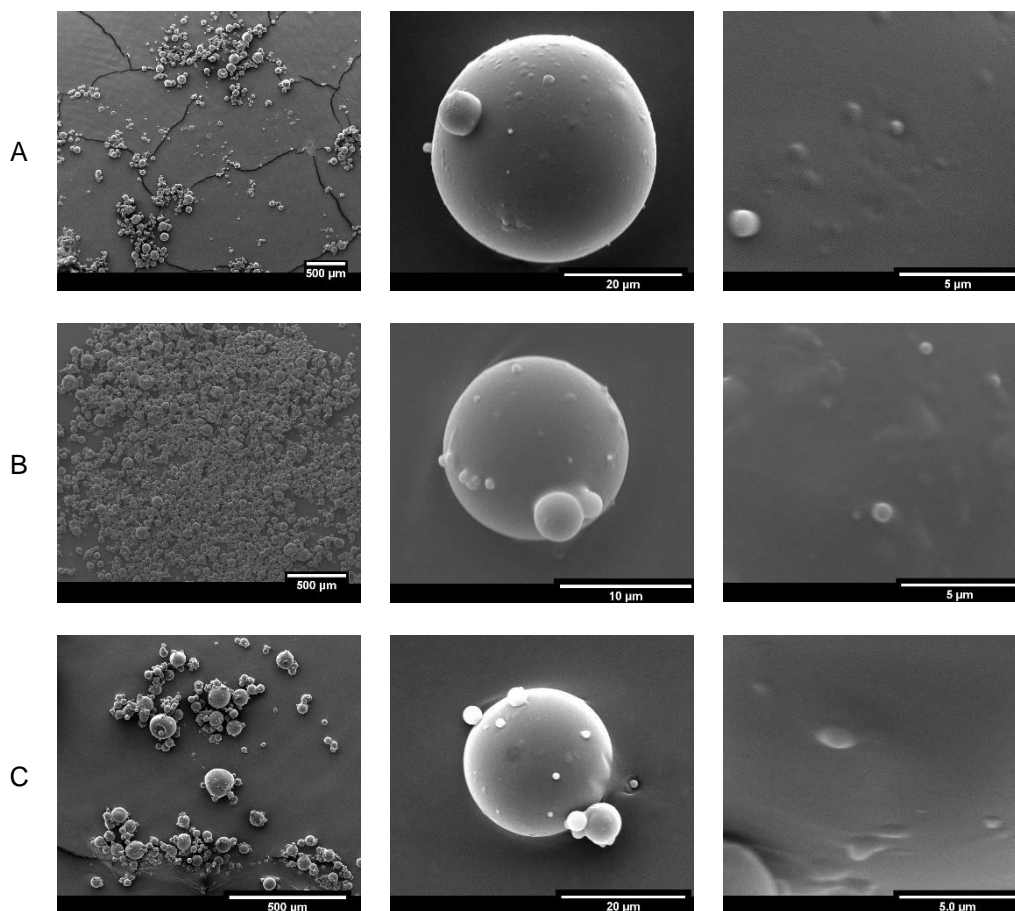**Figure 41** Influence of polydimethylsiloxane concentration on the appearance of the powder (left), single microsphere (middle) and surface (right) by scanning electron microscopy (polydimethylsiloxane concentrations of 32.1 (A), 39.8 (B) and 48.5 (C) % w/w).

3.1.4.4 Effect of drug loading

A further compound introduced to the system may have a critical influence on the emulsion stability and the solvent distribution during coacervation. The effect of dispersing a micronized, hydrophilic drug into the PLGA solution prior to the coacervation with a static mixer was investigated.

The span (1.6 and 1.7) and the mean particle sizes (D50 14 and 14 µm) were unaffected by the drug loading.

The encapsulation efficiency was very high (97.9 %), showing the suitability of the microparticle preparation with a static mixer.

Table 12 Influence of the drug loading on particle size distribution, span, encapsulation efficiency, residual solvents and yield of microparticles prepared with a static mixer. Total flow rate 150 mL/min, polydimethylsiloxane (PDMS) concentration 39.8 % w/w, 3 % w/w PLGA in methylene chloride (DCM). Hardening agent octamethylcyclotetrasiloxane (OMCTS).

Drug loading, % w/w	PSD, µm (D10/50/90)	Span	%EE	Mean residual solvent level, % w/w			Yield, %
				DCM	PDMS	OMCTS	
0	5/14/27	1.636	-	2.81	6.74	2.44	93.4
10	6/14/31	1.749	97.9	2.55	7.17	1.86	91.8

The appearance by scanning electron microscopy (Figure 42) showed small particles on the surface of the microparticles for placebo and drug-loaded formulations, which might be due to the presence of very small droplets or, for the drug-loaded formulation, drug crystals on the microparticle surface.

The residual solvent levels were unaffected by the drug loading (Table 12) for the formulations prepared with a static mixer, as well as the yield with 93.4 % and 91.8 % for blank and drug-loaded microparticles.

The continuous preparation of the phase-separated emulsion with a static mixer is thus suitable to successfully prepare drug-loaded PLGA microparticles by organic phase separation.

Figure 42 Influence of drug loading on the appearance of the powder (left), single microsphere (middle) and surface (right) by scanning electron microscopy (drug loading of 0 (A) and 10 (B) % w/w).

3.1.4.5 Effect of scale-up

Microparticles were produced by solvent evaporation/extraction with static mixers, and scale-up was feasible by dimensional analysis allowed for correlation of different mixer sizes [113]. "Numbering up" from development to production scale simplified the preparation of microparticles using static mixers [164]. For this approach, mixers identical in geometry are installed in parallel, thus significantly accelerating the preparation of larger batches and increasing batch size flexibility.

The use of static mixers for a liquid-liquid phase separation process and the respective scale-up has been, to date, rarely discussed in the scientific literature. One of the most critical steps regarding agglomeration is the coacervate transfer to the hardening bath, as it is a time-dependent step. Thus, the influence of increasing the total material amount passed through the static mixer on microparticle characteristics was investigated and used as a surrogate parameter for a potential scale-up.

Table 13 Influence of the scale factor on particle size distribution, span, encapsulation efficiency, residual solvents and yield of microparticles prepared with a static mixer. Total flow rate 150 mL/min, methylene chloride (DCM) to polydimethylsiloxane (PDMS) ratio 1:0.7 w/w, 3 % w/w PLGA in methylene chloride, drug loading 10 %. Hardening agent octamethylcyclotetrasiloxane (OMCTS).

Scale factor	PSD, µm (D10/50/90)	Span	%EE	Mean residual solvent level, % w/w			Yield, %
				DCM	PDMS	OMCTS	
1	6/14/31	1.749	97.9	2.55	7.17	1.86	91.8
10	8/16/32	1.548	95.4	2.91	7.82	2.05	103.1

The span (1.7 and 1.5) as well as the mean particle size (D50 of 14 and 16) were unaffected by the 10-fold scale-up (Table 13), which showed the suitability of the application of a static mixer for the time-dependent coacervate manufacturing process. The appearance and surface morphology were also independent of the scale-up (Figure 43). For both formulations, small particles were present on the surface, which might be due to unencapsulated drug crystals, and, as also observed for the placebo batch, due to the presence of very small microparticles (Figure 42).

The residual solvent levels were also not affected, while the yield increased from 92 % to 103 %, which was due to the lower relative loss on the equipment used for particle production.

These results proved the suitability of the application of static mixers for the organic phase separation process, resulting in an independence of the emulsion quality on the batch size. With increasing batch sizes, the transfer time of the coacervate phase to the hardening bath increases for discontinuous batch processes. The stirring geometry changes during the transfer step by decreasing coacervate volume. Thus, inconsistencies are expected in terms of the coacervate quality as a function of the transfer time point. An optimized, continuous preparation process was developed, leading to a coacervate characterized by a consistent quality throughout the manufacturing process. A significantly improved batch quality is expected especially for larger scale-up factors.
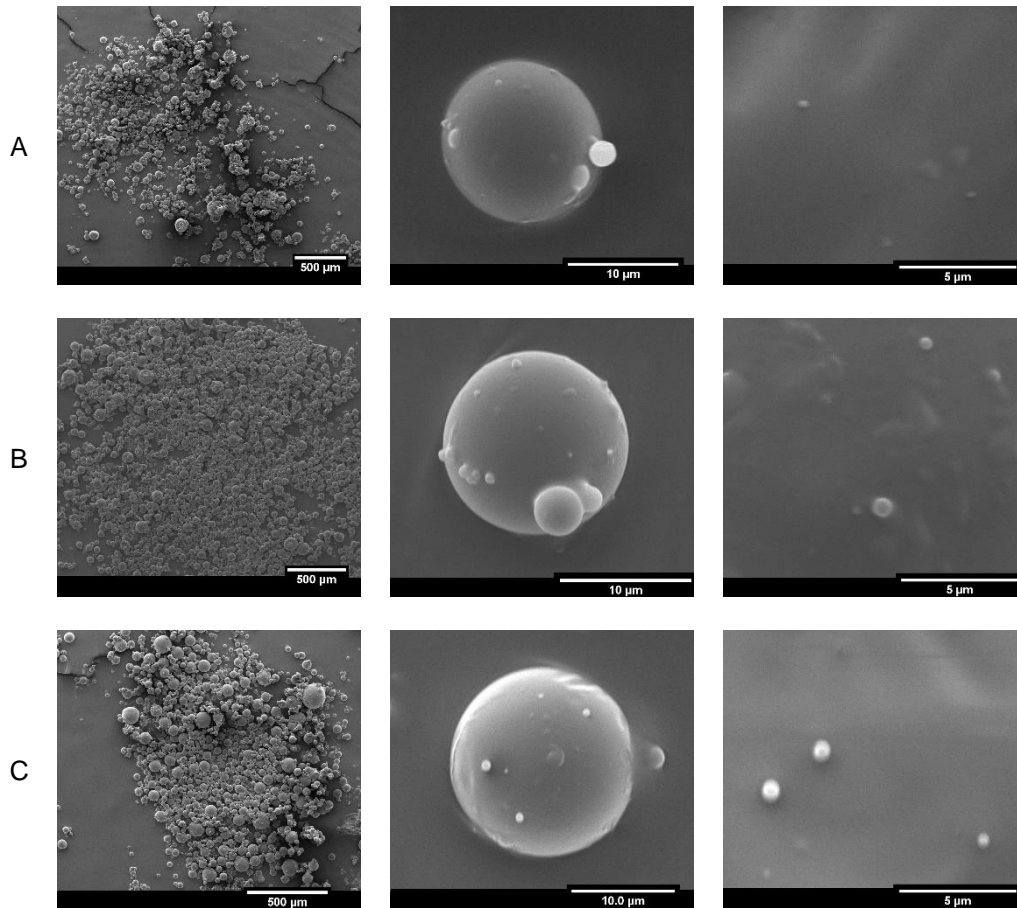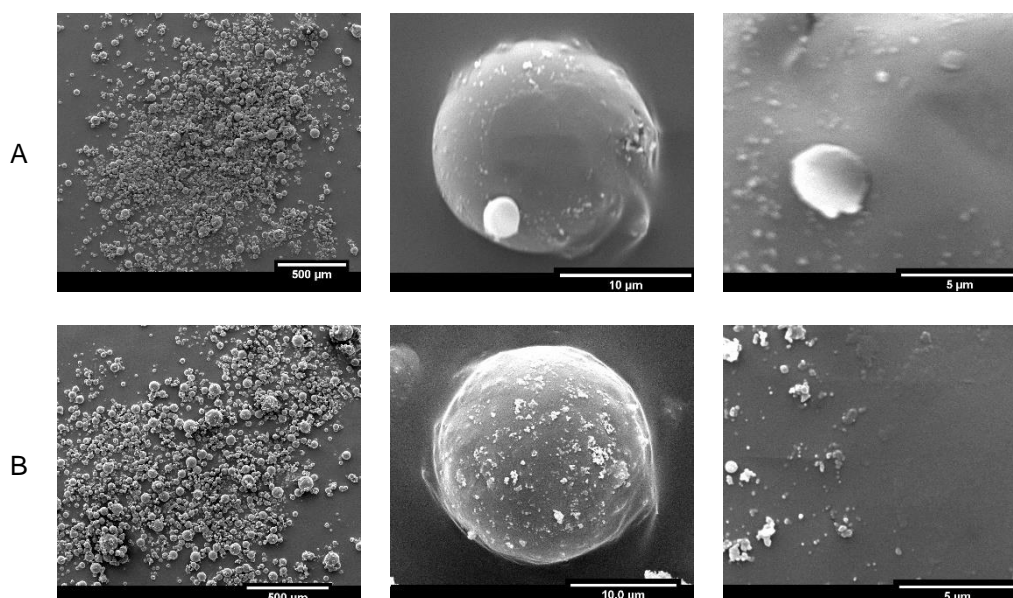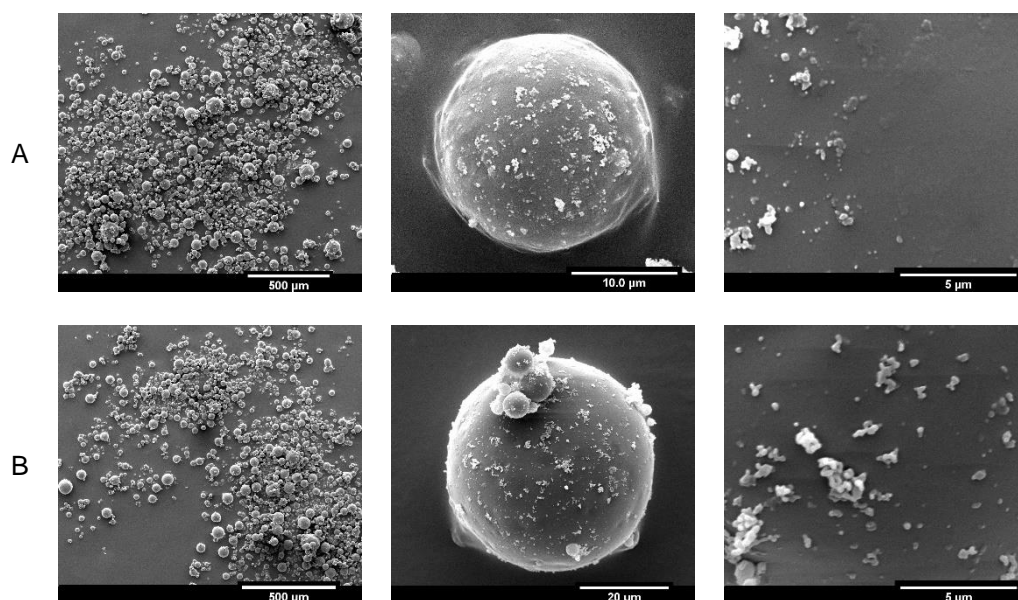
Figure 43 Influence of scale factor on the appearance of the powder (left), single microsphere (middle) and surface (right) by scanning electron microscopy (scale factor of 1 (A) and 10 (B)).

3.2 Simultaneous quantification of three volatile and non-volatile residual solvents in PLGA microparticles with an H-NMR method

Only few methods are available to prepare PLGA drug delivery forms without the use of solvents, i.e. melting or extrusion, which require high processing temperatures causing restricted suitability for thermosensitive drugs [165]. The solvents used for preparation are often critical in residual content, especially, when the microparticles are intended for parenteral use as they may have severe consequences for the patient like allergic reactions or liver, kidney and central nervous system (CNS) toxicity.

A common preparation method for PLGA microparticles is the organic phase separation, which has proven its suitability in the preparation of microparticles especially in the case of water-soluble drugs due to the non-aqueous preparation method, but also for water-sensitive drugs. Besides an organic polymer solvent, a non-solvent to induce the coacervation process and a hardening agent to solidify the coacervate droplets resulting in microspheres are needed. Regularly, methylene chloride is used to dissolve the biodegradable matrix polymer. Further common processing aids represent non-volatile (polydimethylsiloxane, anti-solvent) and volatile (octamethylcyclotetrasiloxane, hardening agent) silicon oils [7, 159].

Residual solvent monitoring is essential during product development and quality control at the production stage due to their inherent toxicity for the patient, as well as the possible influence on critical quality attributes of the product. Methylene chloride is classified by International Conference on Harmonization's guideline for residual solvents (ICH Q3C) as a "class 2" solvent [123]. As per definition, their solvent content should be limited as they are suspected of having significant, but reversible toxicities. According to ICH Q3C, methylene chloride's permitted daily exposition in pharmaceutical products should be no more than 6 mg/day or 600 ppm. Although polydimethylsiloxane and octamethylcyclotetrasiloxane are not limited according to the guideline, residual processing aids need generally to be reduced and monitored during manufacturing processes.

Common quantification methods like gas chromatography require extensive sample preparation if samples consist of volatile and non-volatile excipients in parallel, while extraction of residuals might be incomplete from insoluble matrices [166]. Additionally,

only the volatile compounds can be detected by head-space gas chromatography, and more than one analytical method is required, increasing the analytical effort in terms of time and costs. Additionally, to the problem of difference in volatility, a further challenge has to be circumvented, as the two silicon oils differ only slightly in their molecular structure. Octamethylcyclotetrasiloxane is a cyclic silicon oil, while polydimethylsiloxane is a linear silicon oil. Thus, polydimethylsiloxane shows a terminal methyl-group, which was assumed to be detectable by H-NMR. Quantitative H-NMR has been successfully applied for the analysis of purity of active pharmaceutical ingredients [167-169], the determination of assay [170, 171], combined quantitative and qualitative analysis (i.e. polymers) [172] and determination of impurities [173]. H-NMR was used for the quantification of the non-volatile anti-solvent polydimethylsiloxane [122]. However, polydimethylsiloxane was not quantified when octamethylcyclotetrasiloxane was used as the hardening agent because interferences were expected. Thus, polydimethylsiloxane was only estimated in a batch where hardening was conducted in hexane instead of octamethylcyclotetrasiloxane. Additionally, the method was not validated and both octamethylcyclotetrasiloxane and methylene chloride were determined by other analytical methods.

It was thus the intension of the present study to assess the suitability of quantitative H-NMR to simultaneously determine the volatile organic solvent methylene chloride and the two volatile and non-volatile silicon oils octamethylcyclotetrasiloxane and polydimethylsiloxane appearing as residual solvents in drug-loaded PLGA microparticles prepared by a common organic phase separation method. To prove the suitability of the analytical method for the intended purpose, the method was formally validated according to the current ICH guideline on validation [174].

3.2.1 Suitability of FTIR for the quantification of non-volatile silicon oil in presence of octamethylcyclotetrasiloxane in drug-loaded PLGA microparticles

The most common analytical method to determine residual solvents in pharmaceutical products is the headspace gas chromatography, as it represents the recommended compendial method being validated and proven for the intended use. However, it is not possible to quantify the non-volatile silicon oil polydimethylsiloxane by gas chromatography, which requires the residual solvents in a gaseous state.

Quantification of the non-volatile silicon oil polydimethylsiloxane in PLGA drug-delivery systems was performed by FT-IR, following the correlation according to Beer's law [122]. Thomasin et. al followed a twostep method, starting with the precipitation of poly(lactide-*co*-glycolide) (PLGA), followed by the evaluation of the polydimethylsiloxane characteristic peak at 1300-1230 cm^{-1}, corresponding to the symmetric Si-CH$_3$ stretching vibration of polydimethylsiloxane. Polydimethylsiloxane residuals above a limit of 5000 ppm could be detected with this method. However, the method was restricted to samples comprising only one silicon oil with a sensitivity of 5,000 ppm.

Due to the selected manufacturing process conditions, two residual silicon oils were present in the microparticles (octamethylcyclotetrasiloxane and polydimethylsiloxane), which cannot be easily separated in sample preparation due to very likely chemical structures.

The characteristic peaks observed in FT-IR spectra at 790 cm^{-1} (Si-C stretching and CH$_3$-rocking of Si-CH$_3$-functions) and at 2950 cm^{-1} (Si-CH$_3$ stretching) occur for both silicon oils (Figure 44, Table 14, [122] [175]).

Despite a different peak shape at 950-1150 cm^{-1} (Si-O-Si stretching, [175]) for polydimethylsiloxane (doublet) and octamethylcyclotetrasiloxane (singlet) which is due to the different molecular structures (linear *versus* ring structure, [176]), a differentiation between the two silicon oils was not feasible due to the strong interference of both substances at similar wavenumbers, also due to PLGA showing a peak at a wavenumber of 1084-1270 cm^{-1}, which was the reason for the twostep method applied by Thomasin et. al. It was thus not possible to use FT-IR to simultaneously quantify different silicon oils occurring as residual solvents in PLGA matrices.
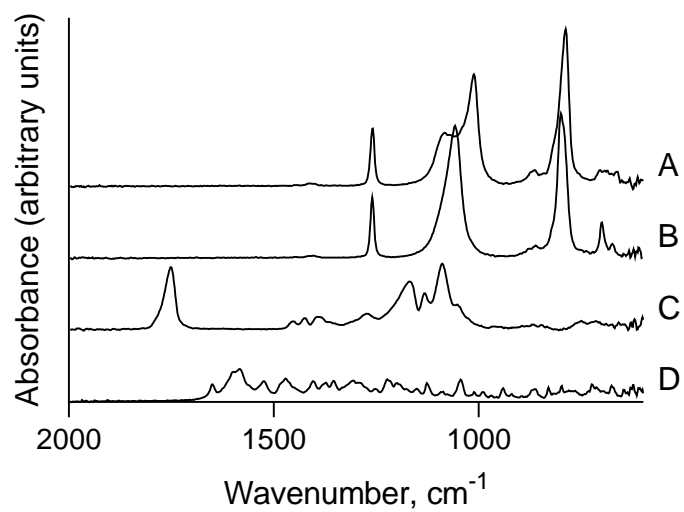
Figure 44 FT-IR spectra of polydimethylsiloxane (A), octamethylcyclotetrasiloxane (B), PLGA (C) and Minocycline HCl (D).

Table 14 Peak assignment for FT-IR analysis of the non-volatile silicon oil polydimethylsiloxane (PDMS), volatile octamethylcyclotetrasiloxane (OMCTS) and PLGA used for the preparation of microparticles by an organic phase separation method.

Compound	Wavenumber (cm^{-1})	Chemical structure and vibration mode assignment	Reference
PDMS	789-796	-CH$_3$ rocking and Si-C stretching	[175]
	1020-1074 950-1160 [122]	Si-O-Si stretching (doublet)	
	1260-1259	CH$_3$ deformation in Si-CH$_3$	
	2950-2960	Asymmetric CH$_3$ stretching in Si-CH$_3$	
OMCTS	789-796	-CH$_3$ rocking and Si-C stretching	[122]
	1020-1074 950-1160	Si-O-Si stretching (singulet: ring structure)	
	1260-1259	CH$_3$ deformation in Si-CH$_3$	
	2950-2960	Asymmetric CH$_3$ stretching in Si-CH$_3$	
PLGA	1084-1270	C-O stretch	[177]
	1384-1451	-CH-	
	1745	C=O stretch	

3.2.2 Development and validation of a novel analytical method to simultaneously quantify non-volatile and volatile solvents in PLGA microparticles by H-NMR

According to USP 38, a validated method needs to meet the requirements for specificity, linearity, accuracy, precision and robustness. The non-volatile silicon oil polydimethylsiloxane (non-solvent), volatile silicon oil octamethylcyclotetrasiloxane (hardening agent) and the volatile methylene chloride (polymer solvent) were analyzed for their respective chemical shifts separately and when in the presence of the other residual solvents and PLGA. For each residual solvent, one peak was chosen for quantification (Figure 45).

Table 15 Chemical shifts in H-NMR spectra for quantification of the solvents polydimethylsiloxane (PDMS), octamethylcyclotetrasiloxane (OMCTS), toluene and methylene chloride (DCM).

Solvent	Chemical shift, ppm	Assigned structural function
PDMS	0.094	Methyl-group (singlet-signal)
OMCTS	0.102	Methyl-group (singlet-signal)
Toluene	2.38	CH_3-group (singlet-signal)
DCM	5.30	CH_2-group (singlet-signal)

Polydimethylsiloxane showed the lowest chemical shift (0.094 ppm), as the nuclei are well shielded by electrons, followed by the cyclic silicon oil octamethylcyclotetrasiloxane (0.102 ppm) which is not methyl terminated and therefore slightly less shielded than the linear silicon oil. Toluene's methyl group showed a peak at 2.38 ppm due to the electronegativity of the phenyl group. Methylene chloride exhibited the strongest chemical shift (5.32 ppm) due to the two chloride atoms leading to a low electron density in the nucleus.
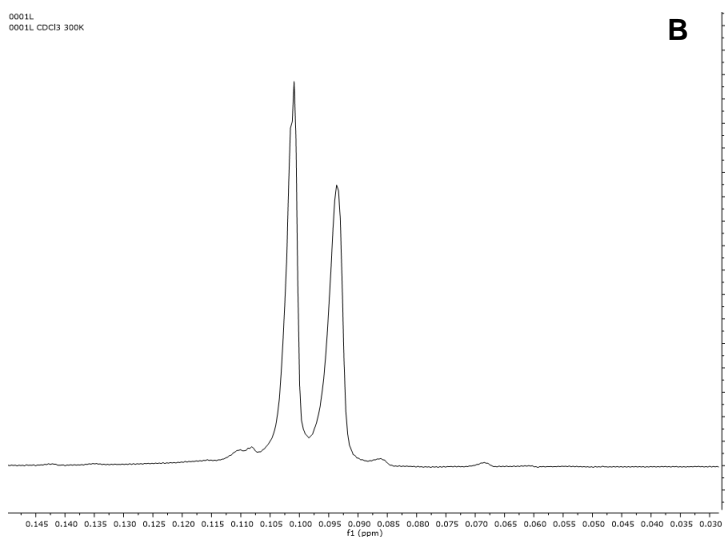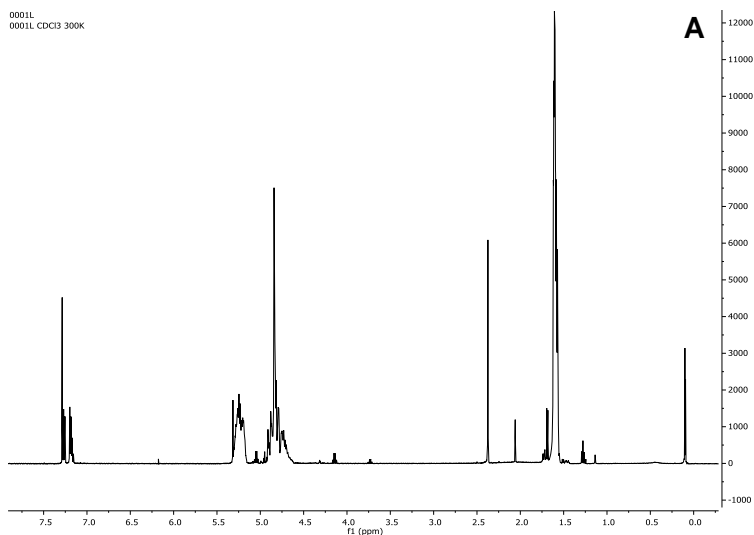
Figure 45 H-NMR spectra of a sample (A: overview, B: zoom at about 0.1 ppm) with methylene chloride (5.30 ppm), octamethylcyclotetrasiloxane (0.11 ppm) and polydimethylsiloxane (0.09 ppm), toluene (2.38 ppm) and PLGA (5.20 ppm, 4.75 ppm and 1.75 ppm) in deuterated chloroform.
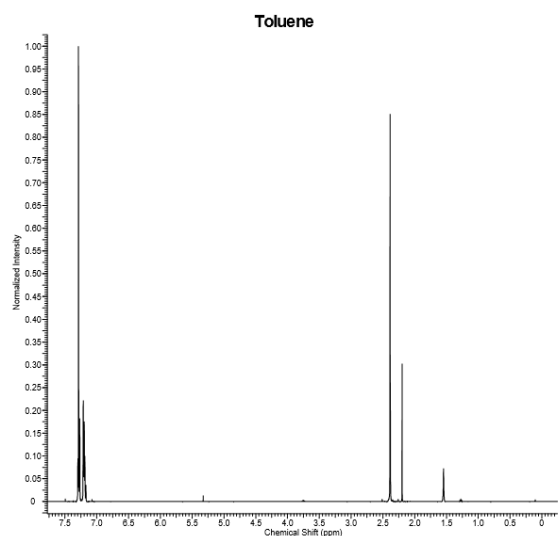
Figure 46 H-NMR spectrum of toluene in deuterated chloroform (toluene-methyl group at 2.4 ppm, toluene-benzene ring at 7.2 ppm and deuterated chloroform at 7.3 ppm).
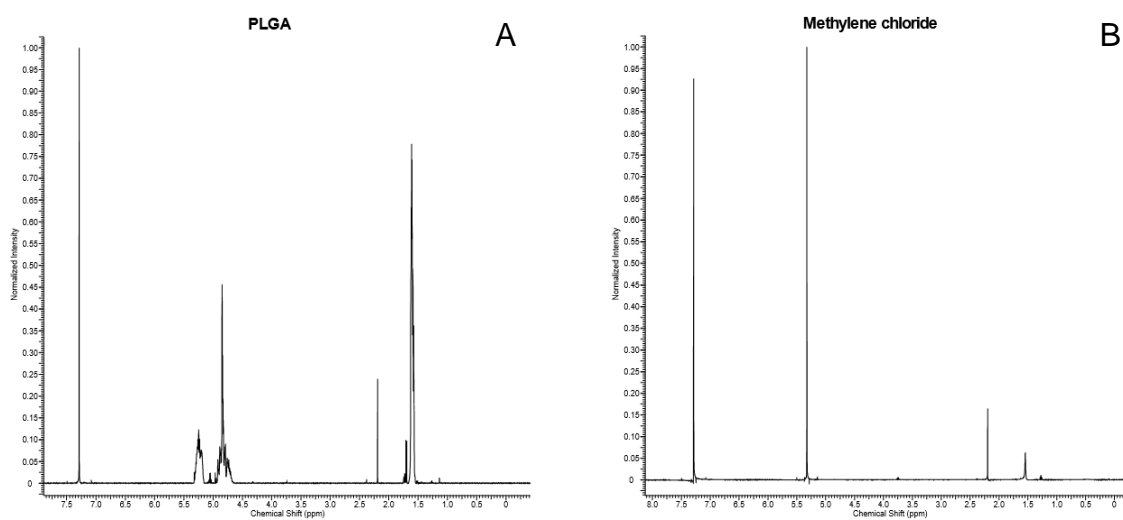
Figure 47 Spectra from H-NMR analysis for PLGA (A) and methylene chloride (B) in $CDCl_3$ comprising 0.2 % toluene as internal standard.
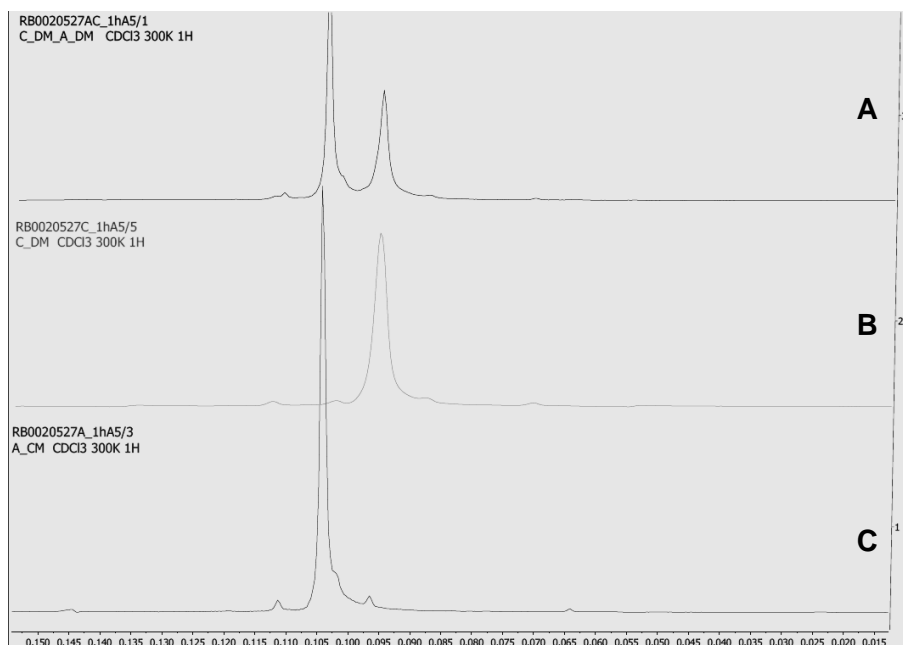
Figure 48 H-NMR spectra of a mixture of both polydimethylsiloxane and octamethylcyclotetrasiloxane (A) and the single substances polydimethylsiloxane (B) and octamethylcyclotetrasiloxane (C) in deuterated chloroform.

The specificity was proven by visual analysis the spectra of the single substances, and non-interfering peaks were chosen for the solvent quantification (Figure 46). Two impurities were present in deuterated chloroform: One was related to water (2.19 ppm), the other impurity was unknown (1.54 ppm).

A concentration of 1 mg/mL was selected as the upper limit for residual solvent linearity. Assuming a total amount of 20 to 40 mg of microparticles dissolved per milliliter, the upper limit of the investigated range of residual solvents corresponds to a residual level of 5.0 % w/w. The lower limit for linearity was chosen close to the quantitation limit. Normalization of the peaks was conducted to compensate for the differences in toluene contents in the sample.
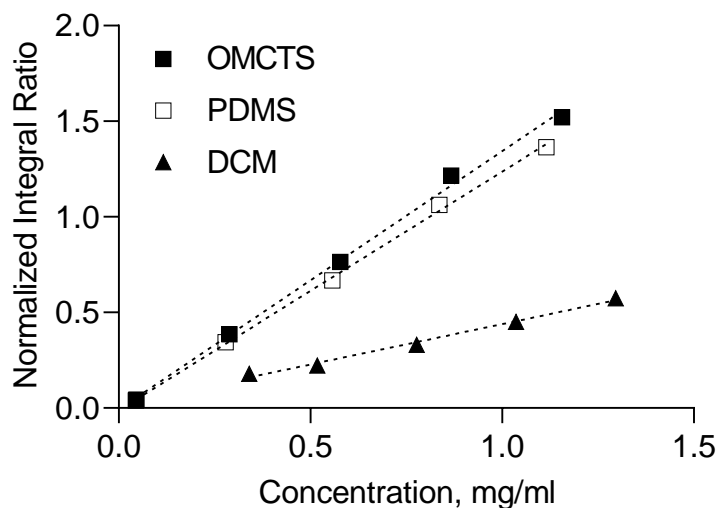
Figure 49 Normalized integral ratio by H-NMR as a function of the concentration of octamethylcyclotetrasiloxane (OMCTS, R² 0.9972), polydimethylsiloxane (PDMS, R² 0.9987) and methylene chloride (DCM, R² 0.9918).
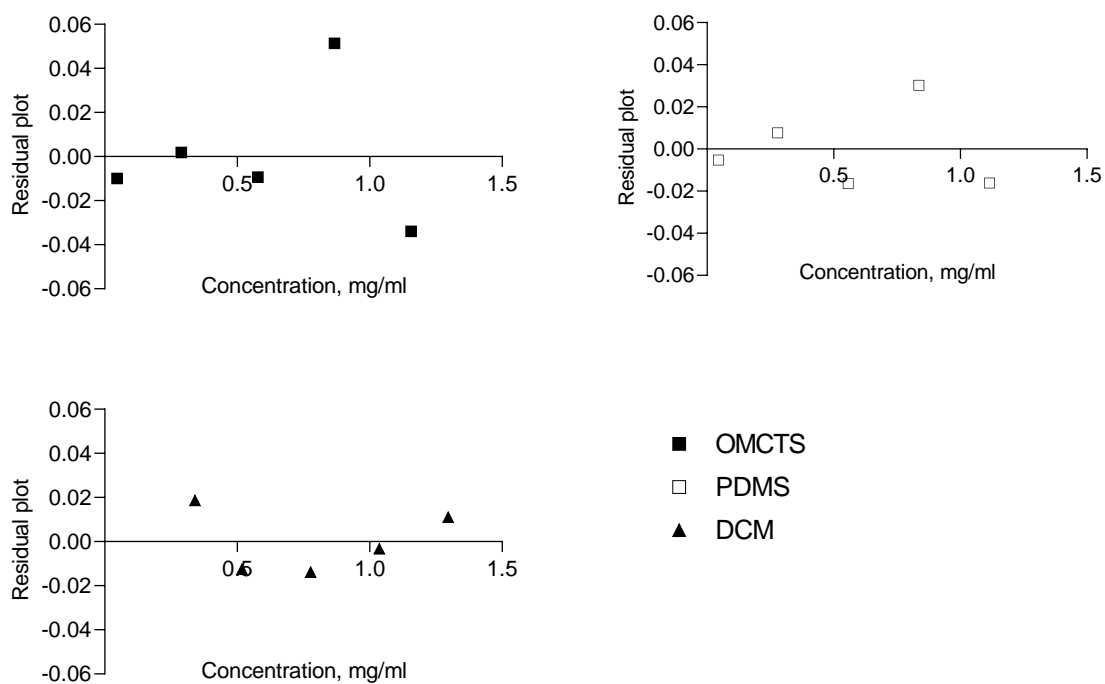
Figure 50 Residual plots of octamethylcyclotetrasiloxane (OMCTS), polydimethylsiloxane (PDMS) and methylene chloride (DCM) of the corresponding linearity study.

The acceptance criteria for Category II quantitative tests (according to USP 38) are correlation coefficients of NLT 0.99, which was well achieved for all solvents (Table 16). Linearity plots occurred linear by visual examination (Figure 49), and residual plots did not show any trends (Figure 50), indicating the suitability of the method to quantify residual solvents by H-NMR.

LOD values of 1025 and 175 ppm were found for methylene chloride and octamethylcyclotetrasiloxane, which were suitable for the detection of residual solvents in microparticles (Table 16). For polydimethylsiloxane, a detection limit of less than 100 ppm by H-NMR [122] was comparable to our result (275 ppm).

The accuracy was assessed using 9 determinations over 3 concentration levels covering a range from about the limit of quantitation to 1 mg/ml (Table 16).

According to USP 38, for Category II assays a recovery between 80.0 %-120.0 % should be met throughout the intended range. For all residual solvents at low, medium and high concentration level (methylene chloride: 0.3, 0.6 and 1.1 mg/ml, polydimethylsiloxane and octamethylcyclotetrasiloxane: 0.05, 0.5 and 1.0 mg/ml), the %total mean recovery was between 80.0 %-120.0 %.

The repeatability was investigated by preparing samples at three different concentration levels at three measurements per samples (Table 16). For quantitative impurity analysis, a relative standard deviation of NMT 20.0 % is required according to USP 38. Polydimethylsiloxane, octamethylcyclotetrasiloxane and methylene chloride met the validation criteria at all concentration levels.

To evaluate the intermediate precision, three different concentrations were prepared on three days and compared with each other to account for intra-day differences. Influencing effects were not studied individually. To meet the Category II validation criteria for intermediate precision according to USP 38, the relative standard deviation must be NMT 25.0 %. Polydimethylsiloxane, octamethylcyclotetrasiloxane and methylene chloride satisfied the validation criterion throughout the concentration range.

The range was chosen to cover residual amounts from approximately the quantitation limit to 5 % w/w residual solvent content. The validation criterion is therefore deemed to be fulfilled. Precision, accuracy and linearity were suitable in these intervals for the quantification of residual solvents in biodegradable PLGA microspheres (Table 16).

To assure the process robustness, an internal reference standard co-dissolved in the matrix test solution was used to account for any occurring differences due to adsorption during sample filtration and, especially, instrumental performance.

All criteria were met according to the requirements of USP 38. The method is thus suitable for the simultaneous quantification of volatile and non-volatile residual solvents in PLGA-based microparticles, even for two silicon oils similar in their molecular structure (Table 16).

Table 16 Validation results of H-NMR Method: Accuracy by Recovery of polydimethylsiloxane (PDMS), octamethylcyclotetrasiloxane (OMCTS) and methylene chloride (DCM) in PLGA matrix from samples with known concentration (n=3). Repeatability of different solvents in PLGA matrix at different concentration levels (n=3, α=0.05). Intermediate precision of different residual solvents in PLGA matrix prepared and measured on different days (n=3, α=0.05) with toluene normalization due to individual sample preparation on different days. Linearity based on 5 concentration levels covering respective concentration range. Detection and quantitation limits for different solvents in PLGA matrix based on signal-to-noise ratio. LOD (ppm) is based on 20 mg/mL polymer concentration in sample solution.

Residual solvent	Conc. level	Accuracy		Repeatability		Intermediate Precision		Linearity		LOD, mg/mL	LOQ, mg/mL	LOD, ppm
		Recovery, %	RSD, %	RSD, %	CI, ±	RSD, %	CI, ±	Concentration range, mg/mL	R^2			
PDMS	Low	87.65	6.45	1.00	0.00	7.79	0.33					
	Medium	101.03	0.46	2.70	0.04	1.55	0.09	0.045 - 1.115	0.9987	0.011	0.019	550
	High	98.12	2.64	2.79	0.07	1.17	0.07					
OMCTS	Low	86.29	12.89	0.52	0.00	15.70	0.79					
	Medium	106.05	5.81	0.96	0.01	5.79	0.41	0.046 - 1.156	0.9972	0.007	0.011	350
	High	105.68	1.38	2.62	0.07	3.09	0.21					
DCM	Low	92.99	0.29	2.47	0.01	13.31	0.41					
	Medium	97.47	0.61	1.22	0.01	7.46	0.15	0.340 - 1.296	0.9918	0.041	0.321	2050
	High	104.25	2.64	3.35	0.03	8.78	0.18					

3.2.3 Residual solvents by compendial static headspace gas chromatography

The H-NMR method was compared to the compendial headspace gas chromatography, which should be applied for the quantification of Class 1 or Class 2 residual solvents [178].

Based on the fundamentals of an equilibrium existing between dissolved and gaseous state of volatile compounds, the headspace gas chromatography measures the amount of volatile gases in the headspace of the vial under test. An aliquot of the gaseous mixture is injected and passes the column under application of a temperature program, leading to a separation of the volatile compounds on the column and the final detection by flame ionization detector.

The GC solvent should dissolve the analytes and the PLGA matrix to circumvent complex extraction steps prior the analysis. Dimethylformamide dissolved both residual solvents (methylene chloride and octamethylcyclotetrasiloxane) as well as the polymeric matrix (PLGA). As the boiling points of the components greatly differed (40, 153 and 175 °C for methylene chloride, dimethylformamide and octamethylcyclotetrasiloxane, respectively), a broad temperature gradient from 40 to 230 °C was essential for the solvent quantification under maintenance of accuracy by prevention of carry-over effects. The peak assignment was performed by analyzing chromatograms of single substances, mixtures and simulated samples dissolved in dimethylformamide (Figure 51). The peaks of the volatile residual solvents methylene chloride (R_t 5.4 min) and octamethylcyclotetrasiloxane (R_t 28.5 min) and of the sample solvent dimethylformamide (R_t 25.1 min) did not overlap. No additional peaks were observed in a simulated sample of PLGA, minocycline hydrochloride, polydimethylsiloxane, octamethylcyclotetrasiloxane and methylene chloride (dissolved in dimethylformamide), which proved a sufficient specificity of the method (Figure 52). Repeatability at the upper concentration range investigated (0.5 mg/mL) showed higher relative standard deviations for the GC method for methylene chloride (5.69 % for GC and 1.22 % for H-NMR) and for octamethylcyclotetrasiloxane (4.18 % for GC and 0.96 % for H-NMR), which was most probably due to the more extensive sample preparation for GC and thus a higher risk of errors and variation.

The linearity of GC was proven visually from 0.01 to 0.5 mg/mL for methylene chloride and octamethylcyclotetrasiloxane, with correlation coefficients R^2 of 0.9935 and 0.9925, and no trend was observed for the residual plot (Figure 53, Figure 54). Thus, the quantitation of both methylene chloride and octamethylcyclotetrasiloxane by gas

chromatography is feasible (NLT 0.99). The robustness of the measurement was assured by using the method of standard additions to exclude potential matrix effects. For methylene chloride, the limit of detection for GC was lower than for H-NMR (817 ppm versus 2050 ppm, respectively, Table 17). As methylene chloride concentrations of 50 ppm were quantified by GC earlier, a lower LOD was expected for GC [122]. The difference between the reported value and the LOD of the present method was most probably due to the reported sample preparation: Methylene chloride shows a high affinity to PLGA. By removing PLGA by precipitation prior to analysis, the volatility of methylene chloride was increased, causing a higher response factor and thus a 16-fold lower LOD compared to the present method, which analyzes methylene chloride in the presence of PLGA. However, headspace GC (without polymer precipitation) and H-NMR were able to quantify residual methylene chloride in microparticles down to 0.2 % (GC) and 1.6 % (H-NMR), which was sufficient for the quantification of residual methylene chloride in microparticles intended for parenteral use.

For octamethylcyclotetrasiloxane, the limit of detection was 4-fold lower when measured by H-NMR compared to the headspace GC results (350 ppm versus 1255 ppm, Table 17). This was attributed to the high boiling point (175 °C), causing a comparatively low response factor in GC, ultimately increasing the limit of detection.

Sample preparation for the analysis by H-NMR was simpler than for GC. The analysis time of H-NMR (internal standard) was about 10 min compared to 300 min for GC including the standard addition samples and the material consumption in terms of analyte and solvents was also lower.
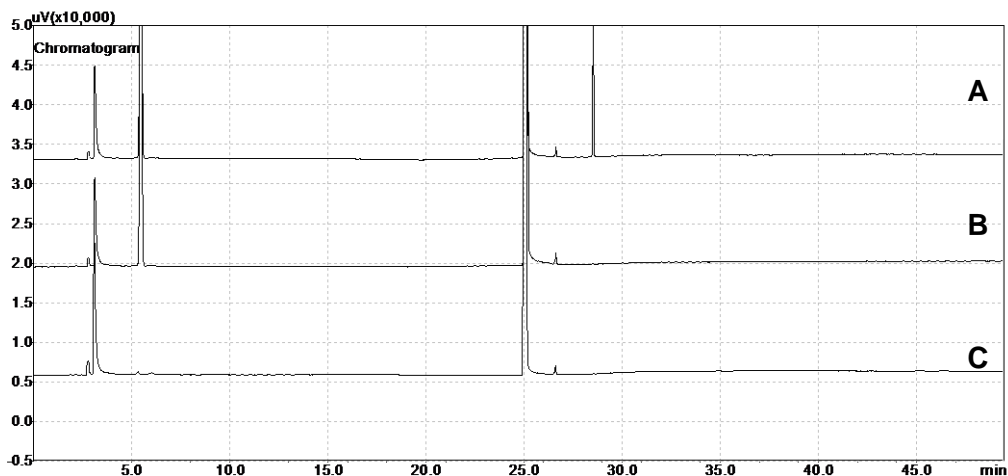
Figure 51 Stack of gas chromatograms of methylene chloride and octamethylcyclotetrasiloxane in dimethylformamide (A), methylene chloride in dimethylformamide (B), and dimethylformamide (C).
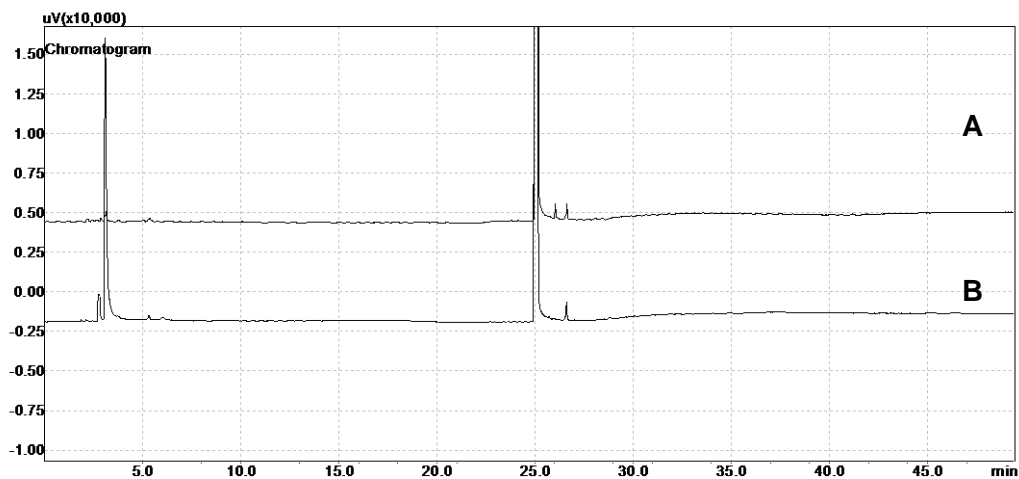
Figure 52 Stack of gas chromatograms of minocycline hydrochloride with polydimethylsiloxane in dimethylformamide (A) and dimethylformamide (B).
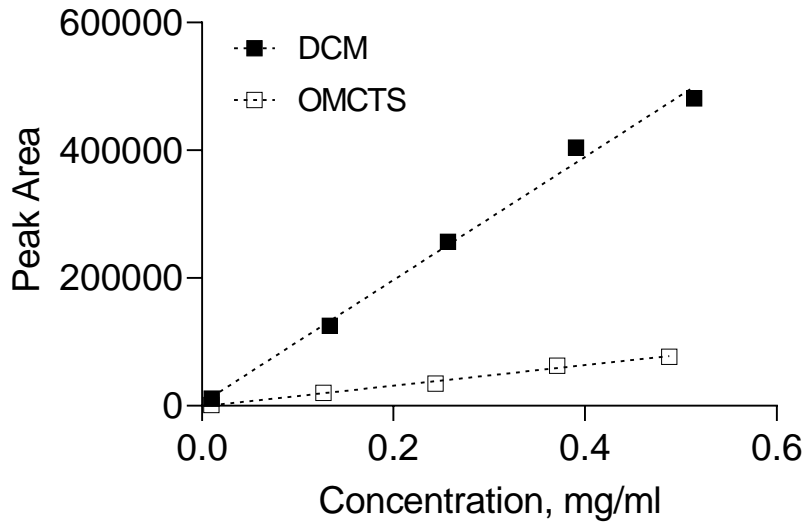
Figure 53 Peak area by headspace GC-FID as a function of the concentration of methylene chloride (DCM, R² 0.9935) and octamethylcyclotetrasiloxane (OMCTS, R² 0.9925).
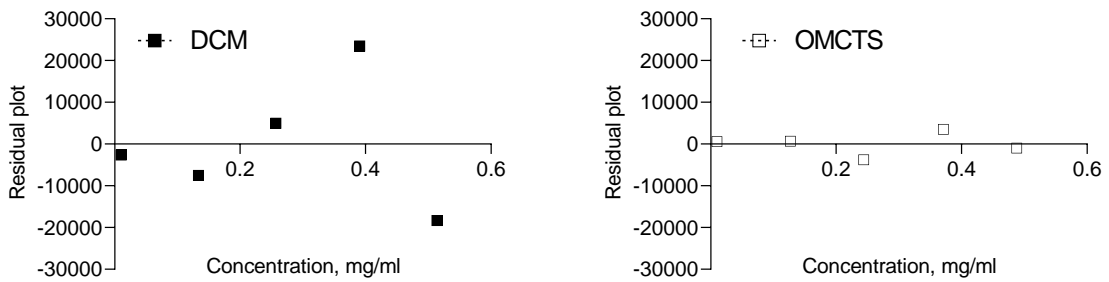
Figure 54 Residual plots of methylene chloride (DCM) and octamethylcyclotetrasiloxane (OMCTS) for linearity study by headspace GC.

Table 17 Comparison of analytical methods for the quantification of volatile (methylene chloride (DCM), octamethylcyclotetrasiloxane (OMCTS)) and non-volatile (polydimethylsiloxane (PDMS)) residual solvents in PLGA matrices.

Attribute	Analytical method	
	H-NMR	Headspace gas chromatography (USP)
Quantifiable solvents		
Volatile	Y	Y
Non-volatile	Y	N
Sample and standard preparation	Fast	Tedious
Calculation basis	Weight-based	Volume-based
Analysis time (including standards), min	10	300
Material consumption	40 mg	250 mg
Possible interferences	Volatile and non-volatile $CDCl_3$-soluble substances	Volatile dimethylformamide-soluble substances
LOD DCM (ppm)	2050	817
LOD OMCTS (ppm)	350	1255
LOD PDMS (ppm)	550	-

3.3 Reduction of residual solvent levels in PLGA microparticles prepared by phase separation method

The common preparation process of PLGA microparticles by phase separation method includes the use of volatile organic solvents (i.e. methylene chloride), non-volatile coacervation agents (i.e. dimethicone) and volatile hardening agents (i.e. cyclomethicone or heptane). Processing aids should not appear in the product and therefore should be removed upon manufacturing, keeping the residual level at minimum. In official guidelines limits are stated that must be considered during development of drug delivery systems, where solvents are used during the manufacturing process [123]. For volatile excipients, the removal effort correlates with the volatility of the excipient to be removed at a particular concentration from the respective matrix. By drying optimization, levels of common volatile solvents are expected to be controllable in the polymer-based systems. On the other hand, non-volatile processing aids have to be controlled by other formulation and process conditions, which appears to be very critical.

Residual levels of solvents have a critical influence on the safety and quality of the drug delivery systems. As residual solvents are not only harmful to the patient, which requires a *minimization* of the solvents due to the implied toxicity according to the respective official guidelines, they also pose a risk of affecting critical quality attributes, which shows that besides a solvent minimization a strict *control* of the residuals is required. First, residual solvents are small molecules acting as plasticizers in the polymeric matrix, thus reducing the T_g [124] and hence eventually affecting the drug release or raising stability issues during the shelf-life. Second, high residual solvent levels lower the assay of the microparticles, leading to higher microparticle amounts needed for the delivery of a particulate dose to the patient, thus potentially decreasing the patient compliance due to higher volumes needed during injection.

There is only limited information on residual solvents in microparticles prepared by phase separation, and most of the studies of residual solvents in microparticles focus on the residual organic solvent content which can be reduced effectively by applying optimized drying conditions at elevated temperatures close to the T_g of the PLGA [122, 128, 165, 179-181], and only few studies discussed the residual solvent contents of

silicon oils serving as non-solvent and hardening agents and alkanes serving as hardening agents [120, 122, 163, 182-184].

Detailed knowledge on the influence of formulation and process parameters is expected to support the development of a robust preparation process for drug-loaded microparticles intended for controlled parenteral drug delivery. Thus, relevant formulation and process parameters were investigated in terms of influence on the residual solvents, microsphere appearance and particle size distribution. The drug release was not tested, as the differentiation between influence of the formulation and process parameters or the respective residual solvents was beyond the scope of this study. The focus of the study was to evaluate the general influence of formulation and process parameters on the residual solvents in microparticles prepared by an organic phase separation process. Thus, the influence of various formulation and process parameters such as drug loading and coacervation, hardening and drying parameters on residual solvent levels in the PLGA microparticles were investigated.

3.3.1 Effect of the incorporation of a hydrophilic model drug

The introduction of a further component, i.e. a drug, adds complexity to the system, with more interfaces available for interactions to occur between the PLGA, the PLGA solvent methylene chloride, non-solvent polydimethylsiloxane, and hardening agent octamethylcyclotetrasiloxane. This might lead to changes in the solvent distribution upon phase separation and solvent extraction. Thus, the impact of incorporation of a water-soluble drug on residual solvents was investigated at different drug loadings.

Table 18 Influence of the drug loading on residual solvent levels (n=3), particle size distribution (n=100) and encapsulation efficiency (EE) of microparticles prepared by organic phase separation. 6 % w/w PLGA in methylene chloride (DCM), polydimethylsiloxane (PDMS) addition rate 4.6 g/min, methylene chloride to octamethylcyclotetrasiloxane (OMCTS) ratio 1:15 w/w.

Drug loading, %	Mean residual solvent level, % w/w			Particle size distribution, µm				%EE
	DCM	PDMS	OMCTS	D10	D50	D90	Span	
0	2.73	5.12	0.88	22	33	65	1.308	-
5	3.56	8.77	0.53	20	37	78	1.564	96.1
10	3.83	9.51	0.35	20	38	69	1.280	92.5

Increasing the drug loading from 0 to 5.0 to 10 % increased polydimethylsiloxane from 5.1 to 8.8 and 9.5 % and methylene chloride levels from 2.7 to 3.6 and 3.8 %. This might have been due to an increased affinity to the drug-polymer-matrix causing a higher polydimethylsiloxane entrapment. Simultaneously, octamethylcyclotetrasiloxane decreased from 0.9 to 0.5 and 0.4 % (Table 18), which might be explained by repulsion forces between octamethylcyclotetrasiloxane and the drug. This was in congruence with increasing octamethylcyclotetrasiloxane residuals after incorporation of bovine serum albumin in PLGA microparticles, which was explained by repulsion forces between the drug and octamethylcyclotetrasiloxane [122].

A particle size effect regarding the solvent residuals was excluded, as the particle size distributions were comparable for the different drug loadings with mean particle sizes ranging between 33 and 38 µm. Increasing the drug loading did not affect the encapsulation efficiency (96.1 and 92.5 %).

3.3.2 Effect of the coacervation process

To induce phase-separation, the non-solvent polydimethylsiloxane is added to the PLGA solution in methylene chloride. By this, a polymer-rich and a polymer-poor phase is formed.

The polymer concentration determines viscosities of the phase-separated phases, and the solvent distribution between the polymer-poor and polymer-rich phase is expected to differ. To achieve a low overall excipient consumption, a high polymer concentration is aimed to produce microparticles by phase separation. An upper concentration limit exists, which is influenced by the polymer molecular weight and the chemical composition of the polymer influencing the viscosity of the organic solution. With increasing polymer concentration, the "stability window" became narrower. The low dilution of the coacervate droplets and leads to an increased probability of collision of coacervate droplets and hence facilitates coalescence and agglomeration of microparticles in the hardening bath. Common preparation processes therefore use, depending on the molecular weight, PLGA concentrations in methylene chloride between 2 and 10 % w/w [46, 120, 157]. Thus, polymer concentrations within this range (3 and 6 % w/w) were chosen for the preparation of PLGA microparticles and compared for their influence on the final solvent residuals in the obtained microparticles (Table 19).

Table 19 Influence of drug loading (DL) and PLGA concentration (PC) on the residual solvent levels (n=3), particle size distribution (n=100) and encapsulation efficiency (EE) of microparticles prepared by organic phase separation. Polydimethylsiloxane (PDMS) addition rate 4.6 g/min, methylene chloride (DCM) to octamethylcyclotetrasiloxane (OMCTS) ratio 1:15 w/w.

DL, % w/w	PC, % w/w	Mean residual solvent level, % w/w			Particle size distribution, μm				%EE
		DCM	PDMS	OMCTS	D10	D50	D90	Span	
0	6	2.73	5.10	0.88	22	33	65	1.308	-
0	3	2.24	1.64	0.58	19	29	43	0.845	-
10	6	3.83	9.51	0.35	20	38	69	1.280	92.5
10	3	1.90	1.17	0.98	25	32	40	0.481	89.2

For blank microparticles, decreasing the polymer concentration from 6.0 to 3.0 % w/w reduced the polydimethylsiloxane residuals from 5.1 % w/w to 1.6 % w/w (Table 19). Due to a higher dilution of the polymer-rich phase in the polymer-poor phase, a lower

risk of re-coalescence or agglomeration in the hardening bath occurred, thus facilitating a more efficient polydimethylsiloxane removal during the hardening step.

For drug-loaded microparticles, the effect was even more pronounced resulting in a polydimethylsiloxane level reduction from 9.5 % to 1.2 %. With reduced polymer concentration in the organic phase and a constant drug loading of 10 %, the amount of drug decreased in the organic phase, while the methylene chloride amount was higher. The interaction between drug and polydimethylsiloxane was lower than between methylene chloride and polydimethylsiloxane, causing a more efficient removal of the non-solvent during the hardening step.

For blank microparticles, methylene chloride residuals were not influenced by reducing the polymer concentration in the organic phase. For the drug-loaded formulations, methylene chloride residuals were reduced from 3.8 % to 1.9 %, which was most probably related to the lower drug amount available for interactions with methylene chloride in combination with a lower viscosity of the polymer-rich phase and hence an eased and more efficient methylene chloride extraction during the hardening step.

For blank microparticles, octamethylcyclotetrasiloxane residuals were not influenced by reducing the polymer concentration in the organic phase, while for drug-loaded formulations, octamethylcyclotetrasiloxane residuals were increased with decreasing polymer concentration (0.35 % versus 0.98 %). The slower polymer precipitation may have caused an eased distribution of the hardening agent into the coacervate droplets, leading to a slightly increased entrapment. Additionally, the higher drug amount in the organic phase of higher polymer concentration might have caused a higher repulsive effect, thus resulting in lower octamethylcyclotetrasiloxane residuals of higher polymer concentration.

Particle sizes were expected to be influenced by the polymer concentration, as the viscosity of the PLGA solution increases with increasing polymer concentration. However, mean particle sizes of the four formulations were comparable (between 29 to 38 µm), which was most probably due to comparable coacervate viscosities independent of the polymer concentration. However, the particle size distribution of the lower polymer concentration was more uniform, possibly due to the lower coacervate phase volume.

The reduction of the polymer concentration seems to be a suitable method for a pronounced methylene chloride and polydimethylsiloxane reduction in PLGA microparticles prepared by organic phase separation, as octamethylcyclotetrasiloxane

residuals of less than 1 % were achieved for all polymer concentrations and drug loadings.

The polymer concentration did not influence the encapsulation efficiency.

Generally, a higher amount of polydimethylsiloxane reduces agglomeration upon the addition of the coacervate phase into the hardening bath. The higher dilution factor of the coacervate droplets decreases the risk of droplet collision and thus coalescence. However, the amount of coacervation agent is limited due to increased sticking of the coacervate droplets at high polydimethylsiloxane concentrations. The influence of polydimethylsiloxane concentrations in the center (41 %) and close to the upper limit (52 %) of the stability window on residual solvent levels and particle size distribution was investigated (Table 20).

For blank microparticles, the highest polydimethylsiloxane concentration (52.4 %) led to a partial agglomeration in the hardening bath, showing a slight instability of the coacervate phase at the upper limit of the stability window. This falsely narrowed the distribution as it did not reflect the agglomerates. For the lower polydimethylsiloxane concentrations (37.5 % and 41.2 %), free-flowing microparticles without agglomerates were obtained, showing comparable particle size distributions with mean sizes of 30 µm and 41 µm. Increasing the polydimethylsiloxane concentration from 37.5 % to 41.2 % and 52.4 % did not affect the residual polydimethylsiloxane level, which was unexpected, as the affinity of the silicon oil to the coacervate phase increased at high polydimethylsiloxane concentrations (3.1.1.1). The extraction seemed to overweigh the distribution of the polydimethylsiloxane between coacervate phase and hardening bath, leading to independent polydimethylsiloxane residuals. Also, the methylene chloride concentration was only slightly increased from 1.41 % to 2.57 % by increasing the polydimethylsiloxane concentrations used for coacervation induction, which was most probably due to an increased viscosity of the coacervate phase, hindering the extraction of methylene chloride from the nascent microdroplets to the hardening agent. This observation was in accordance with earlier results: For PLA microparticles prepared with increasing polydimethylsiloxane concentrations of 60, 73 and 80 %, increasing methylene chloride residuals were found of 0.2, 0.3 and 0.4 %. This was explained with an increasing viscous polymer network at increasing polydimethylsiloxane concentrations, counteracting the methylene chloride diffusion and exchange of the components [120]. On the other hand, the octamethylcyclotetrasiloxane concentration decreased from 1.36 % to 0.74 % and

0.32 % w/w with increasing polydimethylsiloxane concentrations in the coacervate phase. The increasing polymer concentration due to the organic solvent extraction from the coacervate to the outer phase and decreasing methylene chloride concentration in the coacervate phase might have lowered the octamethylcyclotetrasiloxane affinity to the coacervate phase and most probably hindered octamethylcyclotetrasiloxane diffusion into deeper layers of the nascent microdroplets, and thus prevented the hardening agent from entrapment within the polymer matrix. The hardening agent could thus possibly be better removed upon drying. Similar observations were also made with PLA microparticles. With increasing polydimethylsiloxane concentration from 60 to 73 and 80 %, octamethylcyclotetrasiloxane decreased considerably from 1.9 to 0.4 and 0.05 % [120]. Furthermore, similar observations were made for polymeric microparticles, where lower heptane residuals were found with increasing polydimethylsiloxane concentration [184].

As the effect of polydimethylsiloxane concentration particularly on the polydimethylsiloxane residuals was less pronounced than expected, the volume of the hardening agent was reduced for the preparation of drug-loaded microparticles to increase the method sensitivity. Free-flowing microparticles without agglomerates were obtained for both PMDS concentrations. The mean particle size increased 2-fold with increasing polydimethylsiloxane concentration due to the higher viscosity of the coacervate phase. The lower particle size of the blank microparticles prepared at the same polydimethylsiloxane concentration was due to the agglomerates of the blank microparticle formulation not reflected in the particle size measurement, which falsely shifted the particle size distribution to smaller particles.

Despite the "forced instability" of the coacervate phase, the polydimethylsiloxane residuals were only slightly influenced by increasing the polydimethylsiloxane concentration during coacervation, which were decreased from 9.51 % to 8.25 %. This was most probably due to the proceeding polymer desolvation during the phase separation step, decreasing the silicon oil entrapment upon hardening of the nascent microdroplets. The methylene chloride residuals were not influenced by the amount of coacervation agent. In contradiction to the blank microparticles, the octamethylcyclotetrasiloxane residuals were also not influenced by an increased polydimethylsiloxane concentration in the coacervate phase. This can be explained by the lower amount of hardening agent used for the preparation of the drug-loaded

microparticles. Due to less octamethylcyclotetrasiloxane available for interaction with the coacervate droplets upon hardening, the risk of entrapment was lower.

Increasing the polydimethylsiloxane concentration from 41 to 52 % decreased the encapsulation efficiency from 92.5 to 82.5 %. The decrease might be due to a change in the interfacial energy interplay between the polymer-rich phase, polymer-poor phase and the drug, determining the wettability and thus the entrapment of the drug [38, 39].

Table 20 Influence of polydimethylsiloxane concentration during the coacervation step and the drug loading on the residual solvent levels (n=3), particle size distribution (n=100) and encapsulation efficiency (EE) of microparticles prepared by organic phase separation. Polydimethylsiloxane (PDMS) addition rate 4.6 g/min, methylene chloride (DCM) to octamethylcyclotetrasiloxane (OMCTS) ratio 1:25 w/w (0 % dl) and 1:15 w/w (10 % w/w dl), 6 % w/w PLGA in methylene chloride.

DL, % w/w	PDMS, % w/w	Mean residual solvent level, % w/w			Particle size distribution, µm				%EE
		DCM	PDMS	OMCTS	D10	D50	D90	Span	
0	37.5	1.41	3.51	1.36	19	30	49	0.991	-
0	41.2	2.16	3.25	0.74	20	41	63	1.042	-
0	52.4	2.57	3.24	0.32	11	18	30	1.049	-
10	41.2	3.83	9.51	0.35	20	38	69	1.280	92.5
10	52.4	3.40	8.25	0.39	33	79	116	1.053	82.5

As the polydimethylsiloxane addition rate was expected to influence the formation velocity of the coacervate phase, the polymer desolvation rate and thus the solvent distribution of methylene chloride and polydimethylsiloxane between the polymer-rich and polymer-poor phase, the effect of a lower polydimethylsiloxane addition rate was investigated.

Table 21 Influence of polydimethylsiloxane addition rate on the residual solvent levels (n=3), particle size distribution (n=100) and encapsulation efficiency (EE) of microparticles prepared by organic phase separation. Polydimethylsiloxane (PDMS) addition rate 4.6 g/min, methylene chloride (DCM) to octamethylcyclotetrasiloxane (OMCTS) ratio 1:15 w/w, 6 % w/w PLGA in methylene chloride, 10 % w/w drug loading.

PDMS addition rate, g/min	Mean residual solvent level, % w/w			Particle size distribution, µm				%EE
	DCM	PDMS	OMCTS	D10	D50	D90	Span	
4.6	3.83	9.51	0.35	20	38	69	1.280	92.5
1.8	3.12	2.42	0.32	29	43	70	0.964	90.9

Decreasing the addition rate from 4.6 to 1.8 g/min reduced the polydimethylsiloxane residuals from 9.51 % to 2.42 % (Table 21). The slower phase separation led most probably to a more controlled distribution of the silicon oil towards the outer, polymer-poor phase and hence a lower risk of silicon oil entrapment in the polymer matrix. For the same reason, the methylene chloride residuals were reduced from 3.8 to 3.1 %. The octamethylcyclotetrasiloxane residuals were practically unaffected by the polydimethylsiloxane addition rate, because the coacervate phase exhibited similar polydimethylsiloxane concentrations when added to the hardening agent, thus not influencing the octamethylcyclotetrasiloxane entrapment. The encapsulation efficiency was also not affected by changing the polydimethylsiloxane addition rate.

As the temperature influenced the coacervate droplet formation and stability, the influence of the coacervation temperature on the residual solvents was investigated.

Table 22 Influence of coacervation temperature on the residual solvent levels (n=3) and particle size distribution (n=100) of microparticles prepared by organic phase separation. 0 % w/w drug loading, polydimethylsiloxane (PDMS) addition rate 4.6 g/min, methylene chloride (DCM) to octamethylcyclotetrasiloxane (OMCTS) ratio 1:15 w/w, 6 % w/w PLGA in methylene chloride.

Temperature, °C	Residual solvent level, % w/w (SD)			Particle size distribution, µm			
	DCM	PDMS	OMCTS	D10	D50	D90	Span
10	2.73 (0.08)	5.10 (0.22)	0.88 (0.05)	22	33	65	1.308
0	2.40 (0.17)	4.63 (0.15)	0.95 (0.03)	19	28	49	1.074

Decreasing the temperature from 10 °C to 0 °C did not influence the residual concentrations of polydimethylsiloxane, octamethylcyclotetrasiloxane and methylene chloride (Table 22). Though the solvent distribution during phase separation might be changed due to temperature influences, the extraction effect overweighed and led to an efficient extraction of the silicon oil and the organic solvent from the microparticles. The particle size distribution was also not affected by the reduced temperature with comparable mean particle sizes of 33 µm (10 °C) and 28 µm (0 °C).

3.3.3 Effect of the hardening process

In the phase-separated mixture, the polymer-rich droplets are emulsified in the polymer-poor phase. This emulsion is then transferred to a hardening bath, which extracts the PLGA solvent and thus solidifies the microparticles.

The affinity of the organic solvent and the non-solvent to the hardening agent is essential regarding an efficient extraction and removal associated with low residual solvent contents in the microparticles.

Table 23 Influence of the hardening agent and drug loading (DL) on the residual solvent levels (n=3), particle size distribution (n=100) and encapsulation efficiency (EE) of microparticles prepared by organic phase separation. Polydimethylsiloxane (PDMS) addition rate 4.6 g/min, methylene chloride (DCM) to hardening agent ratio 1:25 (0 % DL) and 1:15 (10 % DL), 6 % w/w PLGA in methylene chloride. Hardening agent octamethylcyclotetrasiloxane (OMCTS).

DL, % w/w	Hardening agent	Mean residual solvent level, % w/w			Particle size distribution, µm				%EE
		DCM	PDMS	OMCTS	D10	D50	D90	Span	
0	OMCTS	1.41	3.51	1.36	19	30	49	0.991	-
0	Heptane	2.12	5.16	4.30	16	30	87	2.384	-
10	OMCTS	3.83	9.51	0.35	20	38	69	1.280	92.5
10	Heptane	2.61	10.91	2.26	22	38	59	0.996	76.8

For blank microparticles, the use of octamethylcyclotetrasiloxane led to lower polydimethylsiloxane residuals (3.5 %) than the use of heptane (5.2 %). Two reasons might explain these observations: First, the molecular structure of the two silicon oils is very similar, leading to a higher affinity of polydimethylsiloxane to octamethylcyclotetrasiloxane than to heptane. Second, the methylene chloride extraction in octamethylcyclotetrasiloxane is slower than for heptane (Figure 38, Table 5). This might have led to a slower polymer precipitation and hence a more efficient removal of the non-solvent polydimethylsiloxane entrapped in the coacervate droplets. The use of octamethylcyclotetrasiloxane and heptane led to comparable methylene chloride residuals of 1.4 % and 2.1 %, despite a higher affinity of methylene chloride to hexane compared to octamethylcyclotetrasiloxane [122].

Octamethylcyclotetrasiloxane (176 °C) was more efficiently removed during the drying step despite the lower boiling point of heptane (98 °C) (1.4 % versus 4.3 %, respectively). Lower residual concentration levels of octamethylcyclotetrasiloxane (0.5-3.0 %) than of hexane (3.8 %) and heptane (5-15 %) in PLGA microparticles were reported before [122, 182, 185]. The lower content despite a lower vapor pressure in combination with strong drying conditions (ramp to 40 °C, prolonged drying time) was most probably due to a higher affinity of alkanes to the polymer matrix compared to octamethylcyclotetrasiloxane, leading to a less efficient hardening agent removal

during the drying. Additionally, the 1.5-fold higher polydimethylsiloxane level in the microparticles prepared with heptane may have "bound" parts of the heptane, ultimately increasing the heptane residuals compared to octamethylcyclotetrasiloxane levels.

For drug-loaded microparticles, a lower amount of the hardening agent was used to further challenge the process. For blank microparticles, the use of octamethylcyclotetrasiloxane led to comparable polydimethylsiloxane residuals (9.5 %) compared to the use of heptane (10.9 %). The affinity of polydimethylsiloxane to octamethylcyclotetrasiloxane is higher than to heptane, but with introduction of the hydrophilic model drug a competing interaction between polydimethylsiloxane, drug/polymer and the hardening agent occurred. Due to the higher polydimethylsiloxane-to-drug affinity compared to its affinity difference between the two hardening agents, the remaining amount of polydimethylsiloxane in the microparticles becomes unaffected by the hardening agent choice, leading to a less pronounced difference of polydimethylsiloxane residuals in octamethylcyclotetrasiloxane- and heptane-hardened microparticles compared to blank PLGA microparticles.

The heptane residuals (2.26 %) were higher than octamethylcyclotetrasiloxane residuals (0.35 %), which was in congruence with the results from blank microparticles. Despite the lower boiling point of heptane (98 °C) compared to octamethylcyclotetrasiloxane (176 °C), the affinity of heptane to the drug-polymer matrix seems to be predominant, leading to a less efficient solvent removal upon drying.

For drug-loaded microparticles, the methylene chloride residuals were reduced when hardened in heptane, which was due to the higher affinity of methylene chloride to heptane, which was in compliance with eased removal for other alkanes [122]. In opposite to blank microparticles, this effect could be shown for the drug-loaded microparticles, as the methylene chloride to hardening agent was chosen higher (1:15 for 10 % drug loading versus 1:25 for 0 % drug loading), thus increasing the test sensitivity for the influence of the hardening agent on the methylene chloride extraction efficiency.

The encapsulation efficiency was lower for heptane than for octamethylcyclotetrasiloxane (77 % versus 93 %).

The solvent extraction upon hardening is determined not only by the affinity, but also the extraction capacity of the hardening agent towards the extractable. Increasing the amount of hardening agent is expected to lead to a faster and more efficient solvent removal, also fastening the polymer precipitation upon injection. The total amount of solvents used for the phase separation process should be considered from an economical as well as an ecological perspective.

Table 24 Influence of the drug loading and the methylene chloride (DCM) to octamethylcyclotetrasiloxane (OMCTS) ratio on residual solvent levels (n=3), particle size distribution (n=100) and encapsulation efficiency (EE) of microparticles prepared by organic phase separation. Polydimethylsiloxane (PDMS) addition rate 4.6 g/min, 6 % w/w PLGA in methylene chloride.

DL, % w/w	DCM: OMCTS ratio, 1:x	Mean residual solvent level, % w/w			Particle size distribution, µm				%EE
		DCM	PDMS	OMCTS	D10	D50	D90	Span	
0	15	2.73	5.10	0.88	22	33	65	1.308	-
0	25	2.16	3.25	0.74	20	41	63	1.042	-
10	15	3.83	9.51	0.35	20	38	69	1.280	92.5
10	25	2.72	3.49	0.61	19	32	49	0.920	83.1

For blank microparticles, decreasing the methylene chloride to octamethylcyclotetrasiloxane ratio from 1:15 to 1:25 reduced the polydimethylsiloxane residuals from 5.1 to 3.3 % (Table 24). This was most probably due to a higher concentration gradient, leading to a more efficient polydimethylsiloxane dilution towards the outer phase.

Methylene chloride residuals were slightly reduced from 2.7 % to 2.2 %. Due to the higher amount of the hardening agent, the extraction upon hardening was more efficient. However, due to the drying step, the difference was not as pronounced as for the non-volatile compound polydimethylsiloxane, underlining the importance of the drying step for volatile compounds, but simultaneously the importance of formulation and process control for non-volatile residuals like polydimethylsiloxane.

Octamethylcyclotetrasiloxane residuals were comparable with decreasing the methylene chloride to octamethylcyclotetrasiloxane ratio (0.9 % and 0.7 %).

For drug-loaded microparticles, decreasing the methylene chloride to octamethylcyclotetrasiloxane ratio from 1:15 to 1:25 decreased the polydimethylsiloxane residual concentration 2.7-fold from 9.5 % to 3.5 %, and methylene chloride decreased from 3.8 % to 2.7 Increasing the amount of hardening agent increases the concentration gradient, resulting in a more efficient solvent removal. Concomitantly, octamethylcyclotetrasiloxane increased from 0.4 to 0.6 % most probably due to a higher risk of incorporation.

The effect was more pronounced as for the blank microparticles. This was most probably due to the interaction between the drug and the ternary mixture. Generally, the risk of incorporation of the hardening agent exists, and higher octamethylcyclotetrasiloxane residuals were found in blank microparticles than in drug-loaded microparticles. However, when the outer phase volume is increased for drug-loaded microparticles, the repulsive effect seems to be overweighed, leading to increased octamethylcyclotetrasiloxane residuals.

Similar observations were made for varying the hardening time: By increasing the hardening time from 30 to 60 min, polydimethylsiloxane decreased from 9.5 to 4.6 %, and methylene chloride decreased from 3.8 to 2.0 % (Table 25). By increasing the hardening time from 30 to 60 min, octamethylcyclotetrasiloxane increased 1.9-fold from 0.4 to 0.7 %, which was most probably due to a penetration of the hardening agent in the microparticles. A further increase in stirring time to 120 min did not impact solvent residuals, indicating an equilibrium after an extraction time of 60 min.

Increasing the hardening agent volume decreased the encapsulation efficiency from 92.5 to 83.1 %. A similar effect was observed for increasing the hardening time from 30 to 60 and 120 min, where the encapsulation efficiency decreased from 92.5 to 83.7 and 78.3 %. This was most probably due to the drug-octamethylcyclotetrasiloxane interaction: With increased interaction time or a higher concentration gradient, less drug was encapsulated.

Table 25 Influence of the hardening time on residual solvent levels (n=3), particle size distribution (n=100) and encapsulation efficiency (EE) of microparticles prepared by organic phase separation. 10 % w/w drug loading, polydimethylsiloxane (PDMS) addition rate 4.6 g/min, methylene chloride (DCM) to octamethylcyclotetrasiloxane (OMCTS) ratio 1:25, 6 % w/w PLGA in methylene chloride.

Hardening time, min	Mean residual solvent level, % w/w			Particle size distribution, µm				%EE
	DCM	PDMS	OMCTS	D10	D50	D90	Span	
30	3.83	9.51	0.35	20	38	69	1.280	92.5
60	1.97	4.63	0.66	23	38	54	0.818	83.7
120	2.19	4.84	0.63	28	39	63	0.869	78.3

3.3.4 Effect of changes in the drying process on volatile residuals

The major fraction of the volatile PLGA solvent methylene chloride should be already extracted during the coacervation and hardening process. However, a final drying process of the filtered microparticles determines the final levels of the volatile solvents in the microparticles and is necessary to achieve acceptable residual solvent levels. The application of a temperature ramp to temperatures close to the glass transition temperature T_g of the polymer reduced volatile residuals [122]. Microparticles exhibit lower T_g's prior to drying compared to pure PLGA (46-50°C), as residual solvents act as plasticizers. Exceeding the T_g of the polymeric matrix could alter critical quality attributes, i.e. loss of particle integrity or irreversible agglomeration/sticking. The application of a temperature ramp represents a suitable alternative to avoid sticking, as the shelf temperature follows a T_g increase due to continuous reduction in residual solvent content.
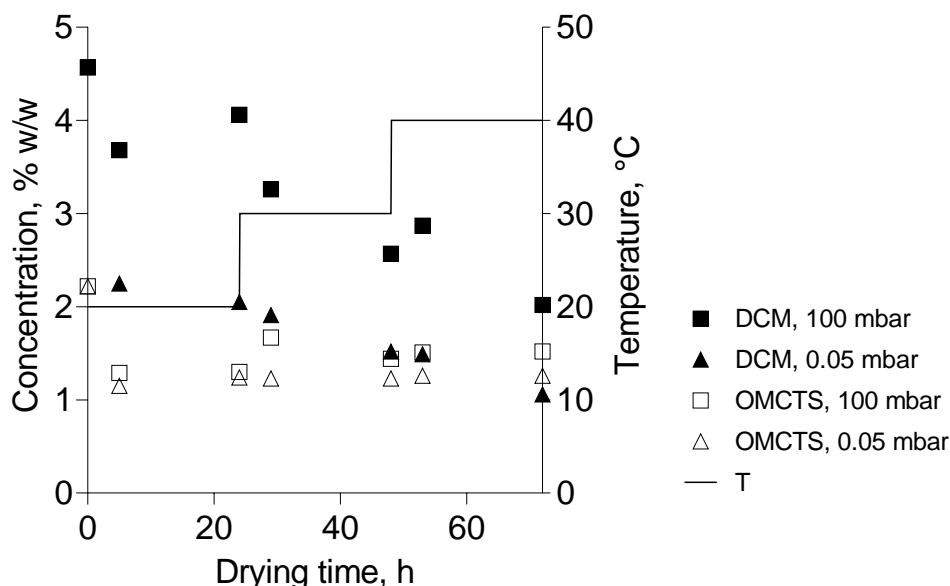
Figure 55 Effect of drying time, temperature (T) and pressure on the residual levels of the volatile methylene chloride and octamethylcyclotetrasiloxane in drug-loaded PLGA microparticles. 30 % w/w drug loading, methylene chloride (DCM) to octamethylcyclotetrasiloxane (OMCTS) ratio 1:15 w/w, 3 % w/w PLGA in methylene chloride.

With increasing temperatures, the methylene chloride content decreased from 4.6 % to 2.0 % at 100 mbar (Figure 55). The solvent reduction rate increased with increasing temperature. Despite earlier reports on hindered methylene chloride diffusion upon vacuum drying of PLGA microparticles at ambient temperature, methylene chloride decreased slightly already for the drying at 20 °C [122]. The reason for this was most probably the initial residual solvent content, which decreased the T_g, leading to an increased methylene chloride diffusivity through the polymer matrix. With decreasing solvent content, the glass transition temperature is constantly increased, leading to a decreasing diffusivity for the solvent, which is supported by the achievement of a solvent plateau at the end of the temperature steps.

The application of a stronger vacuum of 0.05 mbar led to a change in the solvent removal pattern. For the first 20 h, methylene chloride decreased at a high rate, followed by a plateauing up to 50 h upon temperature raise to 40 °C. Thereafter, the methylene chloride content started to decrease again, clearly indicating a dependency of the drying rate to temperature. With a stronger vacuum, the final content could be decreased from 4.6 to less than 1.6 %. The methylene chloride residuals were in

accordance with earlier reports, where drying of PLGA-microparticles resulted in methylene chloride residuals of about 4.3 to 0.7 % after drying at ambient (25°C, 5 mbar, 24 h) and increased (40°C, 0.05 mbar, 48 h) temperatures [122]. The lower solvent content after drying might be due to the lower polymer weight used in the study (50:50 acid-terminated PLGA, intrinsic viscosity of 0.2 dL/g), causing a lower polymer-solvent affinity and thus an improved removal upon drying.

Despite the volatility of octamethylcyclotetrasiloxane, a reduction of the hardening agent residuals in microparticles could neither be observed at 100 mbar nor at 0.05 mbar (1.3 and 1.5 %, respectively). The boiling point of octamethylcyclotetrasiloxane was estimated to be 100 and 39.9°C at pressures of 100 and 0.05 mbar, respectively [186]. As the pressure reduction and accordingly drying above the estimated boiling point (0.05 mbar) did not affect octamethylcyclotetrasiloxane residuals, it is most likely that octamethylcyclotetrasiloxane was incorporated in the microparticles and the surrounding PLGA prevented its diffusion and therefore evaporation. This is in accordance with previous studies, where application of vacuum and increased temperature could not improve the reduction of octamethylcyclotetrasiloxane in microparticles [122], though other reports stated that octamethylcyclotetrasiloxane was not entrapped in polymeric microparticles [182]. After drying, the PLGA microparticles were free-flowing and particle size or shape did not change, indicating that the T_g was not crossed during drying (Figure 56). The surface morphology was also not impacted upon drying at elevated temperatures and drying times. The absence of pores indicated a sufficiently slow methylene chloride removal without disrupting the microparticle surface.

The volatile organic solvent methylene chloride can thus be effectively reduced by the application of a temperature ramp in combination with low pressures. The suitability has, however, to be tested for the specific drug substance to be incorporated with special focus to physico-chemical stability at elevated temperatures. Additionally, octamethylcyclotetrasiloxane cannot be reduced upon drying despite its volatility. Thus, a strict control of the hardening agent by formulation and process parameters is essential for drug development.
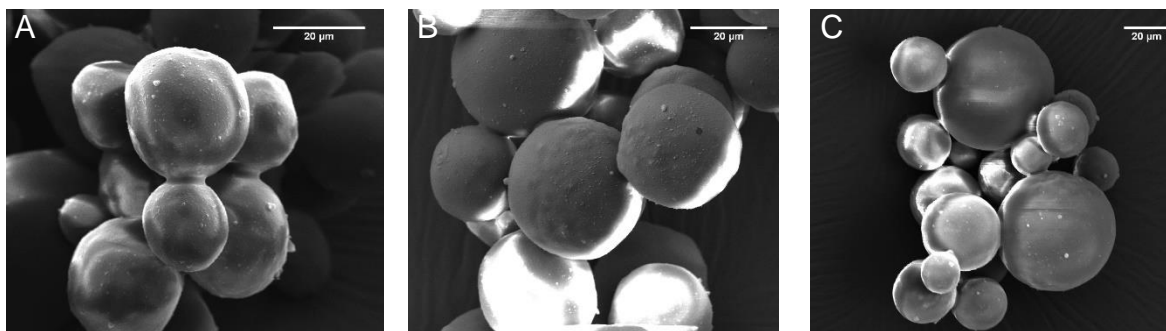
Figure 56 Appearance surface morphology by scanning electron microscopy of microparticles dried for 24 hrs at 20 °C (A), 24 hrs at 20 °C plus 24 hrs at 30 °C (B) and 24 hrs at 20 °C, 24 hrs at 30 °C plus 24 hrs at 40 °C (C). Scale bar: 20 µm.

3.3.5 Summary of effect of formulation and process parameters on residual solvents

The effects of formulation and process parameters on the residual solvents in blank and drug-loaded PLGA microparticles are summarized in heat maps (Figure 57, Figure 58), which shall provide a guide on how to reduce residual solvents. Together with the legend of changed parameters (Table 26, Table 27), it can be clearly seen that the reduction of the polymer concentration is the most effective parameter leading to reduced residual solvent contents (polydimethylsiloxane, hardening agent and methylene chloride) for both placebo microparticles and microparticles loaded with a hydrophilic model substance. Additionally, reducing the polydimethylsiloxane addition rate and increasing the hardening agent volume had a pronounced effect.
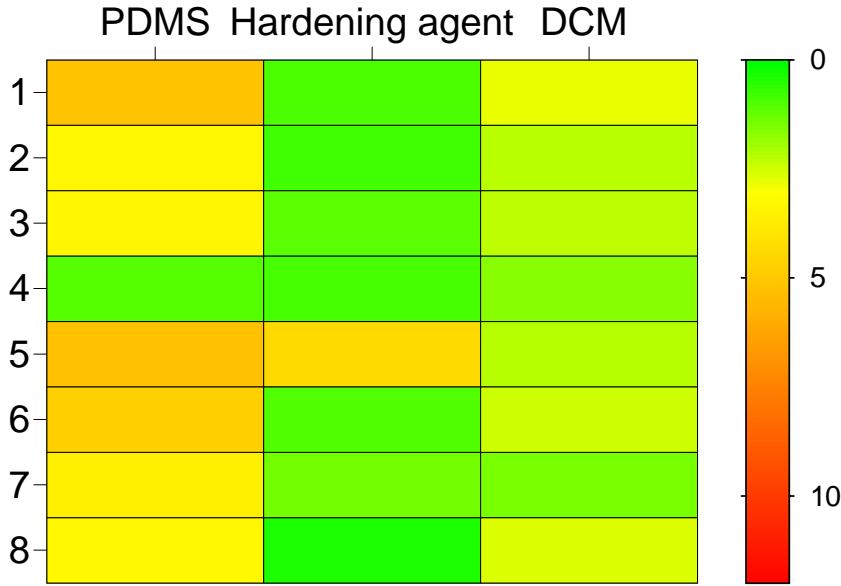
Figure 57 Heat map of effect of formulation and process parameters on residual polydimethylsiloxane (PDMS), hardening agent and methylene chloride (DCM) content in placebo microparticles after drying. Colormap represents the mean (n=3) solvent levels in the different formulations from green (0 %) over yellow (3 %) to red (12 %). Formulation and process parameters: see table.

Table 26 Formulation legend for the preparation of the heat-map for placebo microparticles. Solvent methylene chloride (DCM), hardening agent octamethylcyclotetrasiloxane (OMCTS), non-solvent polydimethylsiloxane (PDMS).

#	Changed parameter	Direction of change
1	Standard placebo formulation	-
2	DCM to OMCTS ratio	↓
3	PDMS addition rate	↓
4	PLGA concentration	↓
5	Heptane as hardening agent	-
6	Coacervation temperature	↓
7	DCM to PDMS ratio	↑
8	DCM to PDMS ratio	↓
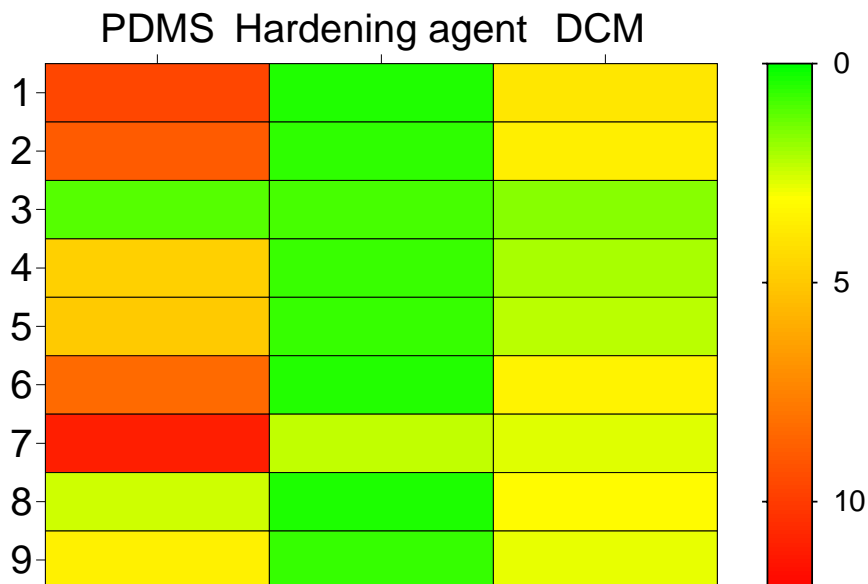
Figure 58 Heat map of effect of formulation and process parameters on residual polydimethylsiloxane (PDMS), hardening agent and methylene chloride (DCM) content in drug-loaded microparticles after drying. Colormap represents the mean (n=3) solvent levels in the different formulations from green (0 %) over yellow (3 %) to red (12 %). Formulation and process parameters: see table.

Table 27 Formulation legend for the preparation of the heat-map for drug-loaded microparticles. Solvent methylene chloride (DCM), hardening agent octamethylcyclotetrasiloxane (OMCTS), non-solvent polydimethylsiloxane (PDMS).

#	Changed parameter	Direction of change
1	Standard drug-loaded formulation	-
2	Drug loading	↓
3	PLGA concentration	↓
4	Hardening time	↑
5	Hardening time	↑↑
6	DCM to PDMS ratio	↓
7	Heptane	-
8	PDMS addition rate	↓
9	DCM to OMCTS ratio	↓

3.4 Influence of the aqueous phase temperature on the solvent removal during the preparation of PLGA microparticles by solvent evaporation

A common technique for the preparation of drug-loaded PLGA microparticles is the solvent evaporation technique. Therein, the drug is either dispersed, emulsified or dissolved in a PLGA solution, which is then emulsified in an aqueous phase containing a stabilizer and stirred to evaporate the solvent. Solidified microparticles are collected and dried.

The solvent removal rate is critical for the encapsulation of water-soluble drugs, which diffuse to the aqueous phase until the polymer precipitation hinders diffusion. Thus, it predetermines the encapsulation efficiency and the process time [56]. A common approach for the accelerated methylene chloride removal is an increased methylene chloride extractability by decreasing the O:W ratio [135, 187, 188]. However, approaches of increasing the outer phase volume face the drawback of high volumes and thus lower batch sizes.

The removal of the solvent from the organic phase depends not only on the solubility in the outer phase, but also on the evaporation rate from the aqueous phase by evaporation, which itself is dependent on the outer phase temperature [189]. To increase the removal rate of the organic solvent, process temperatures were increased close to or slightly above the boiling point of methylene chloride (39.6 °C). The process times were comparatively long, and no foaming or boiling occurred despite process temperatures of up to 42 °C [59, 60, 190-192].

In a novel "Advanced Evaporative Precipitation into Aqueous Solution process" for the preparation of nanocrystals, which is an amended anti-solvent induced nanoprecipitation process, process temperatures were distinctly above the solvent's boiling point. The increased evaporation rates due to higher aqueous phase temperature caused high supersaturation levels, leading to faster drug precipitation. For this, itraconazole solutions in methylene chloride were sprayed in hot aqueous phases at temperatures of about 80 °C [193], being 40 °C above the boiling point of methylene chloride.

As increased processing temperatures have the potential of shortening the process time while maintaining low total volumes and thus large batch sizes, the objective of the study was to characterize the boiling of methylene chloride in the polymer solution when emulsified in an aqueous phase comprising a stabilizer. Moreover, the impact of microparticle preparation at different temperatures was investigated in terms of droplet and particle size distribution, appearance, encapsulation efficiency, residual solvents and drug release.

3.4.1 Influence of the preparation temperature on the solvent removal profile and process time

The influence of the increasing temperature from 25 °C to 75 °C on the methylene chloride removal from an emulsion of methylene chloride in a 1 % poly (vinyl alcohol) (PVA) solution was investigated with a weight loss study.

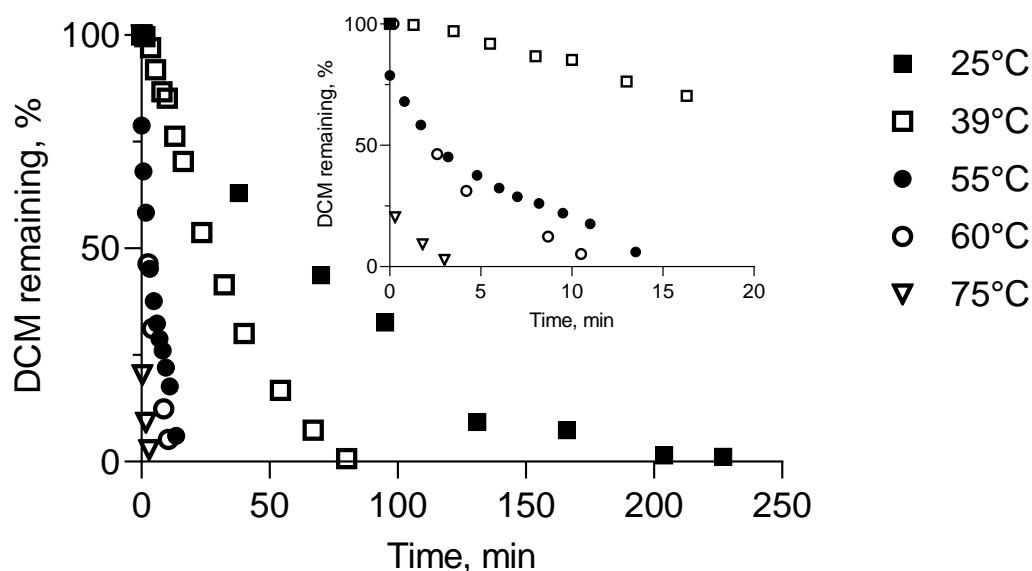**Figure 59** Remaining methylene chloride (DCM) in weight % as a function time, emulsified in 1 % w/v polyvinyl alcohol solutions as a function of time and different temperatures (n=1).

With increasing temperatures from 25 °C to 75 °C, the solvent removal rate increased, which was due to a shift of the equilibrium between liquid and gaseous methylene chloride to the right (Figure 59). At 55 °C, the aqueous phase temperature was above

the boiling point of the solvent (39.6 °C) and instant removal was expected. However, only about 20 % of methylene chloride were removed directly upon injection, while the removal of the remaining 80 % took another 15 min. Despite up to 1.9-fold higher temperatures than the methylene chloride boiling point were investigated, no boiling or the formation of bubbles occurred, indicating a super-heated state of the dispersed phase.

This complied with the boiling behavior of water emulsified in hexadecane, which showed a 2-fold increased boiling point compared to pure water, indicating a superheated state in the emulsion [194].

For the boiling of a dispersed liquid, nucleation sites are needed. At temperatures above the true boiling point, the droplets are in a meta-stable state, and the liquid starts to boil as soon as it is in contact with a liquid-vapor interface or it experiences a disturbance that initiates boiling. Atmospheric gases trapped in impurities in form of floccules in the liquid, coming out of solution and forming nuclei for vapor bubbles, initiate a chain reaction [195]. Vapor bubbles expand upon vaporization, and a shockwave breaks up floccules in adjacent droplets causing the boiling of the other droplets. This sudden boiling of a dispersed phase is known as microexplosion and occurs when a certain temperature, specific for this emulsion, is reached, i.e. the limit of superheat. Microexplosions are of particular interest in the field of combustion improvement since many years [196], and attempts have been made to predict the limit of superheat. It has been found, that emulsion composition, droplet sizes and additives like surfactants may impact the microexplosion behavior [194].

Based on this concept, the objective was to determine the temperature which is needed to achieve an instant methylene chloride removal when being emulsified in a PVA solution.
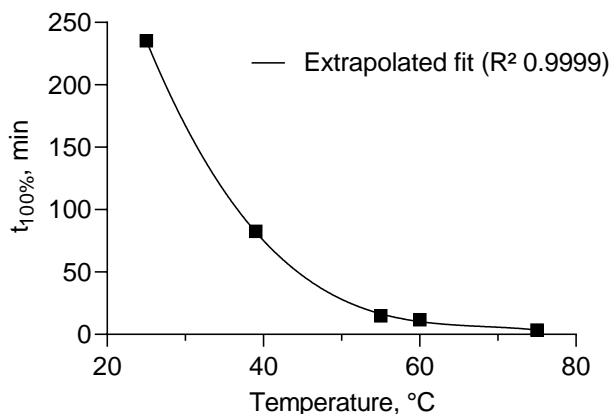
Figure 60 Time needed to fully remove methylene chloride ($t_{100\%}$) emulsified in a 1 % w/v polyvinyl alcohol solution as a function of temperature. Curve fitting was performed with third degree polynomial.

The theoretical time to instantly remove methylene chloride was calculated using the extrapolated times needed at 25, 39, 55, 60 and 75 °C (Figure 60). The non-linear pattern showed the increasing energy needed to remove the solvent completely (third-degree polynomial, R^2 = 0.9999). The solution to the obtained equation gave a temperature of 79.42 °C, which was assumed to be the numerical approximation of the limit of superheat for this emulsion.

In order to confirm these results, an aliquot of an emulsion of methylene chloride in 1 % w/v PVA solution was observed with a hot-stage-microscope (Figure 61).

| 25 °C | 40 °C | 70 °C | 74 °C |

Figure 61 Appearance of methylene chloride emulsified in a 1% w/v polyvinyl alcohol solution as a function of temperature, observed with a hot-stage-microscope.

Around the boiling point of pure methylene chloride (39.6 °C) droplets showed a high mobility. However, the droplet integrity was maintained, indicating a stabilization of the droplets in the emulsified state also at increasing temperatures. Around 70 °C, droplet sizes increased, which was due to a methylene chloride expansion. At 74 °C, the

droplets were explosively disrupted due to a sudden methylene chloride vaporization. This temperature was considered as an experimental approximation of the limit of superheat of this emulsion.

The difference of the value by hot-stage-microscopy (74 °C) to the predicted value by weight loss study (79 °C) can be explained by differences in the experimental set-up. In the weight loss study, the emulsion was stirred, and the solvent was not in direct contact with the heating element, thus requiring a higher temperature to remove methylene chloride. Additionally, the weight loss study detected the total methylene chloride removal, while with the hot-stage-microscopy only the rupture of the droplet. Hence, evaporation might have not been completed at this stage. Finally, the weight loss study was performed at a constant temperature, whereas a heating ramp was applied for the determination by hot-stage microscopy. This ramp allowed an emulsion equilibration and an earlier methylene chloride removal.

In order to determine the impact of a polymer in the organic phase, thus simulating the preparation of microparticles by solvent evaporation method, a poly(lactide-*co*-glycolide) (PLGA) solution in methylene chloride was emulsified in a 1 % w/v PVA solution and observed under the hot-stage microscope.

| 25 °C | 40 °C | 80 °C | 84 °C | 85 °C |

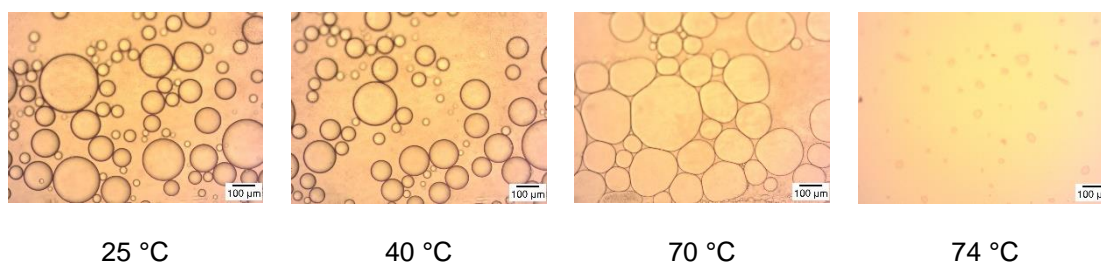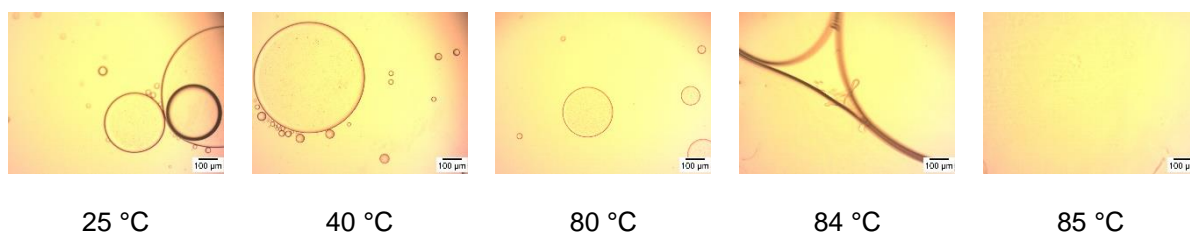**Figure 62** Appearance of a 10 % w/w PLGA solution in methylene chloride emulsified in 1 % w/v polyvinyl alcohol solution as a function of temperature, observed with a hot-stage-microscope.

The introduction of PLGA to the organic phase (10 % w/w) led to a comparable observation as for the pure solvent emulsified in the aqueous phase (Figure 61, Figure 62). Around the boiling point of methylene chloride, droplets were highly mobile, while the droplet integrity was maintained. At 83.7 °C, the droplet structure ruptured, which was due to an explosive solvent evaporation, leading to a disintegration of the shell consisting of precipitated polymer (Figure 62, 84 °C). The temperature of microparticle-rupture was higher than the previously determined limit of superheat for pure

methylene chloride in an aqueous PVA solution (between 74-79 °C). This was most probably due to a higher rigidity of the particles, as the proceeding polymer precipitation stabilizes the microparticular structure. Thus, the explosive rupture is delayed to higher temperatures compared to the actual limit of superheat of the emulsion. Additionally, according to colligative properties, the polymer might increase the boiling point of the organic phase.

3.4.2 Stabilization of heated emulsions

To test the polyvinyl alcohol surfactant activity at elevated temperatures, PLGA solutions were injected into a heated aqueous solution and the appearance of the particles was observed at different polyvinyl alcohol concentrations.

For 0 % PVA, a lump was formed after the injection of a PLGA solution into the aqueous phase (Figure 63). With increasing polyvinyl alcohol concentration, the extend of sticking of particles to each other decreased, indicating a surfactant activity of polyvinyl alcohol at elevated temperatures (Figure 63, Figure 64). Additionally, it was concluded that a minimum of 1 % polyvinyl alcohol was needed to sufficiently decrease the surface energy and prevent particles from sticking (Figure 64).
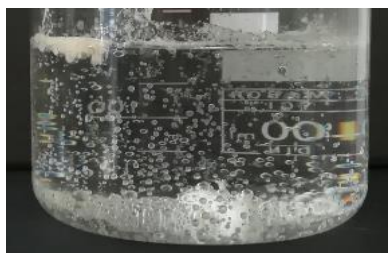
Figure 63 Macroscopical appearance after injection of a PLGA solution in heated water under stirring.
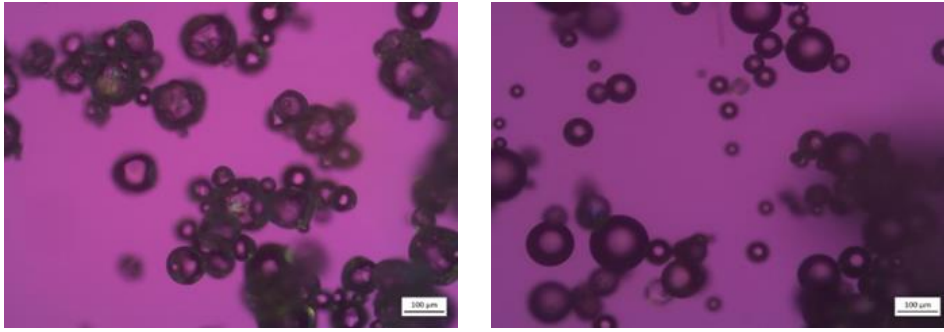
Figure 64 Microscopical appearance of microparticles after injection of a PLGA solution in methylene chloride into a heated 0.5 % PVA (left) and a 1.0 % PVA solution (right).

3.4.3 Influence of the preparation temperature on the particle size of PLGA microparticles

Blank and drug-loaded PLGA-based microparticles were prepared at various temperatures covering a range from ambient (25 °C), slightly above the theoretical boiling point of methylene chloride (55 °C), above the theoretical boiling point (75 °C) and above the limit of superheat (95 °C).
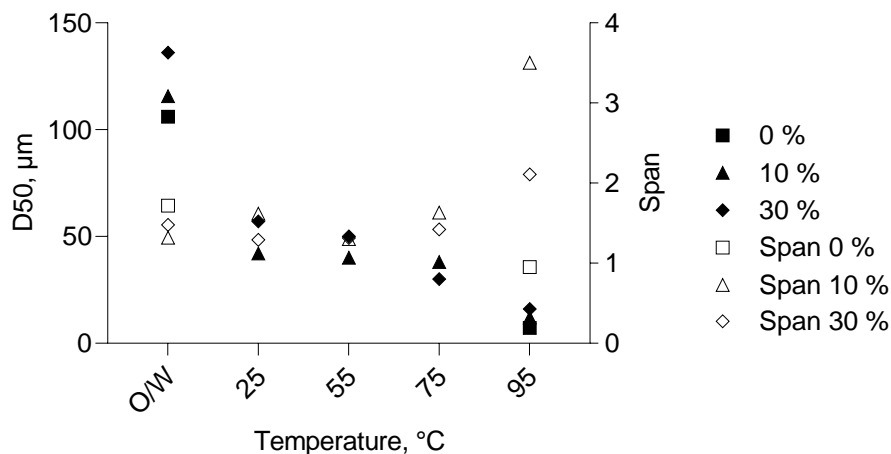
Figure 65 Influence of the preparation temperature on the mean particle size D50 for 0, 10 and 30 % w/w drug-loaded microparticles, and their respective primary emulsion droplet sizes (O/W) (n=100).

The droplet sizes of the primary O/W-emulsions increased with increasing solid content from 106 to 116 and 136 µm, respectively, which was due to an increasing viscosity of the organic phase (Figure 65).

When the hardening was performed at 25 °C, the mean diameter was reduced by factor 2.8 and 2.4 for the microparticles of the 10 and 30 % drug-loaded formulations, (D50 42 and 57 µm, respectively), which was assigned to droplet shrinkage by methylene chloride extraction known to occur in solvent evaporation processes.

When blank microparticles were prepared at 95 °C, the mean particle size was reduced about 15-fold from 106 to 7 µm, which was significantly higher than the shrinking observed at ambient temperature. This suggested the occurrence of a microexplosion due to an instant solvent vaporization, supported by the formation of bubbles after the injection into the heated aqueous phase, which was not observed at lower temperatures. The span of 0.953 indicated a microexplosion resulting in a homogeneous particle size distribution.

The same was observed for 10 % drug loaded particles, where at 95 °C, the particle size was decreased by factor 9.7 from about 116 µm to 12 µm, indicating the occurrence of a microexplosion above the limit of superheat. The vapor pressure was sufficiently high to disrupt the organic phase droplets, leaving hardened particles of low sizes. In contrast to blank microparticles, a high span of 3.5 indicated an inhomogeneous formation of the particles, with a high fraction of larger particles. This was attributed to the increasing viscosity by loading of a drug.

Although also showing a significant decrease, the size reduction at 30 % loading was not as pronounced as for the 10 %-drug loaded formulation at 95 °C. This was attributed to the higher viscosity of the dispersed phase, requiring higher energy to disrupt the droplets. Moreover, the higher solid content was accompanied by a lower methylene chloride content, which might have reduced the disruptive energy, as less solvent vapor was available to trigger the microexplosion. For the higher drug loading, a high span at 95 °C (2.110) indicated inhomogeneities upon formation of microparticles by microexplosion.

Increasing the temperature from 25 °C to 55 °C for the 10 % and 30 % drug-loaded formulations did not impact the particle size reduction with comparable size reduction factors (2.8 and 2.9 for 10 % drug loading, and 2.4 and 2.7 for 30 % drug loading, respectively, Figure 65). Compared to the lower drug loading, particle size reduction was already observed at 75 °C for the 30 % drug-loaded particles (reduction factor 4.5 *versus* 3.0). This indicated a dependence of the microexplosion character from the solid content of the dispersed phase where the boiling initiation depends on the presence of impurities, which most probably increased with increasing solid content.

3.4.4 Influence of the preparation temperature on the morphology of PLGA microparticles

The increased methylene chloride removal rate from the nascent microdroplets was expected to influence the morphology of the particle surface and cross-sections. However, independent of the preparation temperature and the drug loadings, the particle surface appeared smooth with very few pores and drug crystals (Figure 66, Figure 67). This was attributed to the preparation above the T_g and thus a possible pore closing.

Increasing the preparation temperature of the 10 % drug-loaded formulation from 25 to 55 °C led to an inner pore formation. Due to the increased evaporation rate (0.7 and 24.5 g/min for 25 and 55 °C, respectively, calculated from the linear section of the solvent removal study), the polymer precipitation occurred faster. Simultaneously, the state of equilibrium between dissolved solvent and gaseous methylene chloride was moved to the right with increasing temperature. As gaseous methylene chloride is not available as a polymer solvent anymore, a phase separation was induced, causing the formation of solvent bubbles. Despite the high diffusivity of gases compared to liquids, diffusion is hindered by the dense polymer shell wherein the solvent gas is not soluble. Upon heating at 55 °C, bubbles expanded and left bubble-like structures in the particle core before re-dissolving in the matrix and diffusing out of the particle. However, pores on the surface were not observed due to the direct contact of the particle surface to the heated aqueous phase above the T_g. The vapor pressure was not sufficient at this temperature to disrupt the precipitated polymer shell.

A further temperature increase from 55 °C to 75 °C led to microparticles without inner pores for the 10% drug-loaded formulation. A reason for this might be that a transition occurred at this temperature, where the diffusion of the organic solvent was faster than the polymer precipitation. The diffusivity was further increased by a higher temperature difference to the polymer T_g, decreasing the viscosity of the surrounding polymer matrix.

At 95 °C, small particles without internal voids were obtained. This suggests that a preparation above the emulsion-specific limit of superheat results in immediate droplet disruption and hardening. The absence of pores was due to a simultaneous occurrence of solvent vaporization, polymer precipitation and curing at a temperature above the T_g, leading to dense, small particles. In contrast to this, at lower temperatures, the

precipitation occurs before the gaseous solvent can escape from the polymer matrix, leaving pores inside the matrix. Due to a sufficient stabilization by PVA and a fast cooling, the risk of coalescence was low, and small particles sizes were maintained.

For the 30 % drug-loaded formulation, increasing the temperature from 25 to 55 °C also led to a pore formation. However, the observed pores were finely dispersed and showed a smaller mean pore diameter (0.30 µm) than the microparticles of the lower drug loading (1.70 µm), indicating a more homogeneous pore formation. This might be due to the higher solid content in the organic phase, leading to an increased boiling point and a slower, more controlled bubble formation. Again, no pores were observed on the particle surface, most probably due to preparation above the T_g of the polymer. A further temperature increase from 55 °C to 75 °C increased the mean pore size from 1.70 µm to 1.86 µm, which was due to a more pronounced gas expansion. Furthermore, pores were mainly located close to the particle surface. This indicated a high bubble agility and vapor pressure, but a hindered methylene chloride escape due to the higher viscosity of the matrix compared to the lower drug loading. Moreover, the formulations of higher drug loading contained less methylene chloride in the organic phase, thus accelerating the polymer precipitation and hindering methylene chloride escape, leaving voids close to the particle surface.

A further increase of the preparation temperature from 75 °C to 95 °C led to a similar cross-section appearance as observed for the 10 %-drug loaded formulation at 95 °C. The absence of pores was most probably due to a fast solvent vaporization and a processing above the T_g, leading to small and dense microparticles.

T, °C	Single microparticle	Surface	Cross-section
25			
55			
75			
95			
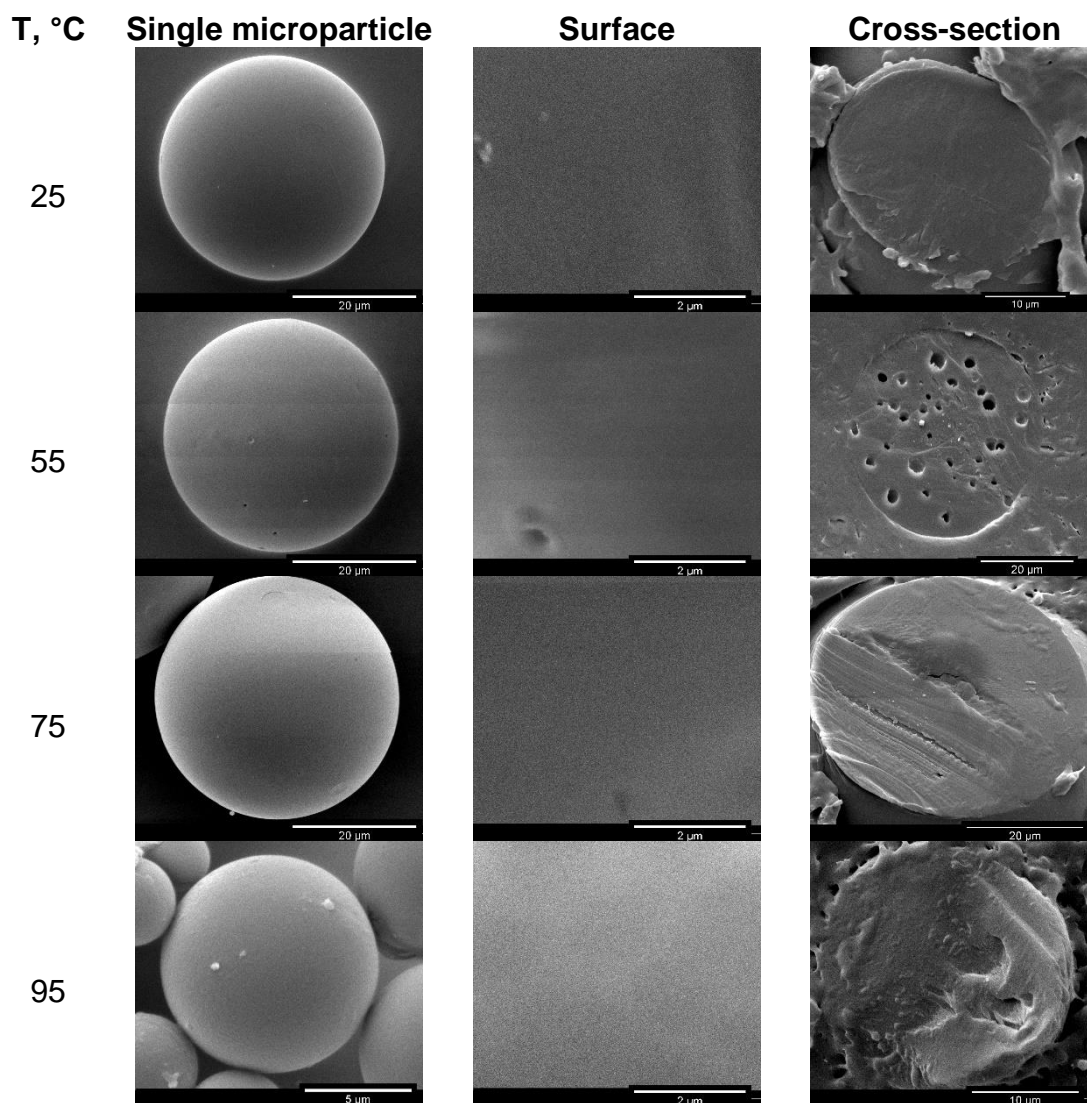
Figure 66 SEM-appearance of surface and cross-sections of microparticles with 10 % w/w drug loading prepared at different temperatures (25-95 °C).
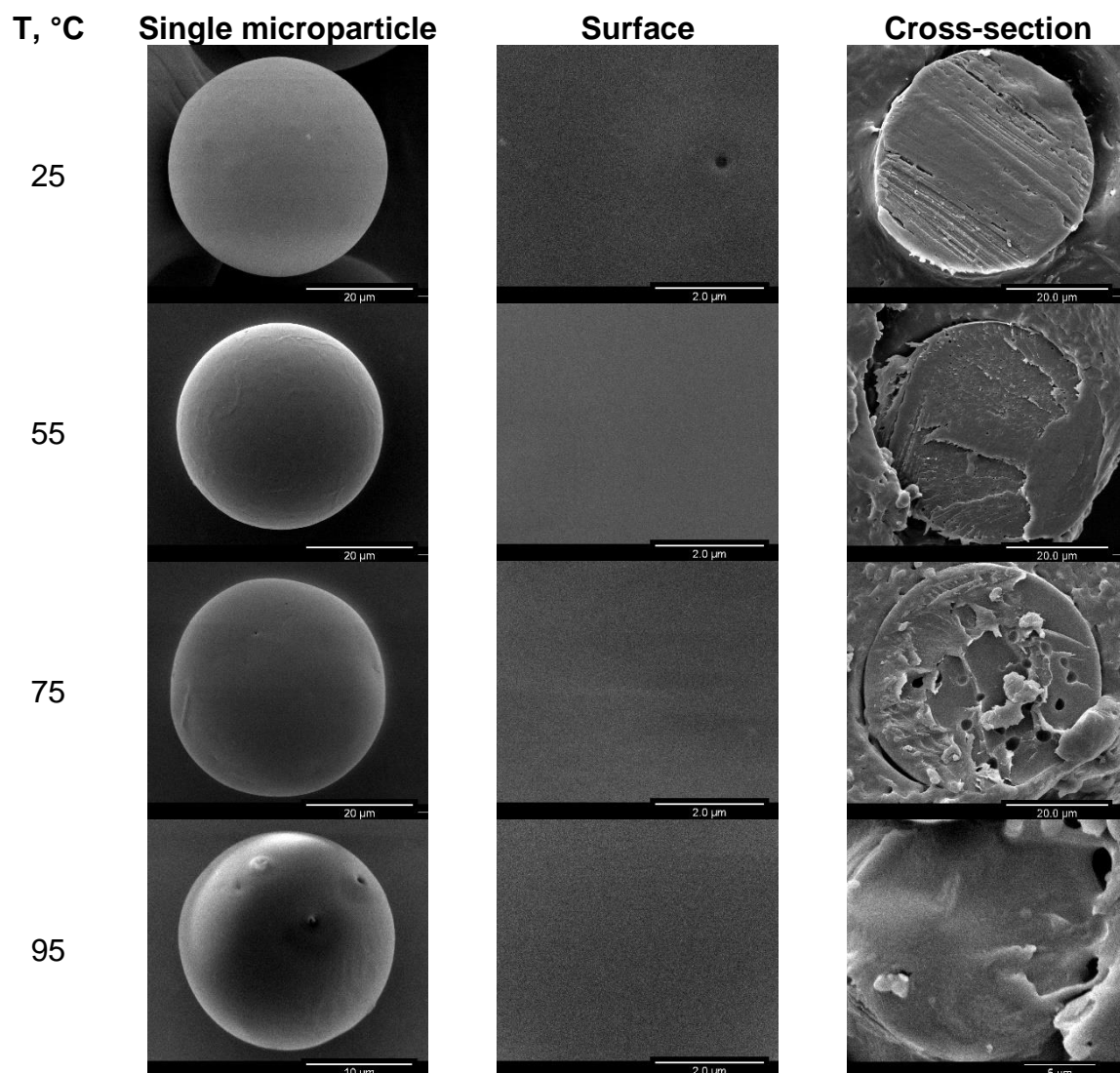
Figure 67 SEM-appearance of surface and cross-sections of microparticles with 30 % w/w drug loading prepared at different temperatures (25-95 °C).

3.4.5 Influence of the preparation temperature on assay and encapsulation efficiency of PLGA microparticles

Risperidone shows a 1500-fold higher solubility in methylene chloride than in water (Table 28). The solubility in the aqueous phase was slightly increased by the formulation and process parameters used in the solvent evaporation method: With increasing PVA concentrations and temperature, the drug solubility increased from 224 µg/mL to 579 µg/mL.

An effect of the preparation temperature on the encapsulation efficiency was expected due to changes of the solubility profiles, the increased methylene chloride removal rate and the polymer chain flexibility below or above the T_g.

Table 28 Risperidone solubilities in different media and different temperatures (n=3). Organic solvent methylene chloride (DCM), stabilizer polyvinyl alcohol (PVA).

Medium	Temperature, °C	Risperidone solubility, mg/mL
DCM	20	332.640
Water	20	0.224
0.5 % PVA in water	20	0.369
1.0 % PVA in water	20	0.530
1.0 % PVA in water	55	0.579
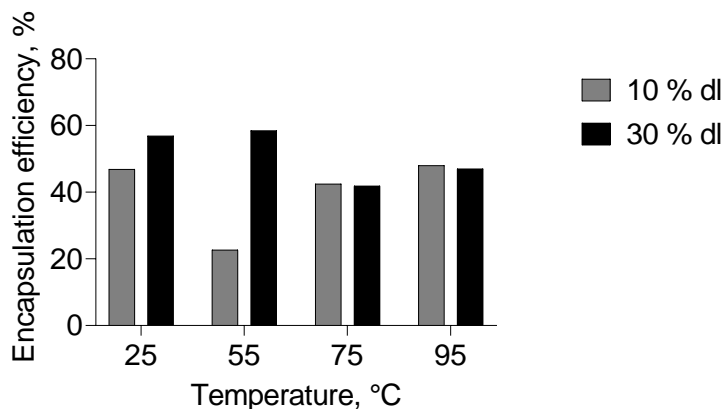
Figure 68 Effect of the preparation temperature on the mean encapsulation efficiency for 10 and 30 % w/w drug-loaded (dl) formulations.

For the 10 % drug-loading formulation, the encapsulation efficiency decreased from 46.9 % to 22.7 % with increasing temperature from 25 °C to 55 °C (Figure 68). This was due to the processing above the T_g in combination with a comparably long stirring time to remove methylene chloride (1 h).

A further temperature increase to 75 and 95 °C again increased the encapsulation efficiency to 42.5 and 48.0 %. This was most probably due to the increased methylene chloride extraction velocity, decreasing the time above the T_g from 1 h to 10 and 1 min. The encapsulation efficiency could, however, not be increased compared to the ambient preparation, which was most probably due to a high affinity of the dissolved drug to the organic solvent. The dissolved drug diffused together with methylene chloride to the aqueous phase, which was promoted when the viscosity of the matrix was decreased at temperatures above the T_g in combination with longer stirring times (55 and 75 °C) (Figure 68).

For the formulation at 30 % drug loading, encapsulation efficiency was higher for the preparation at 25 °C compared to the lower drug loading (56.9 % vs. 46.9 %). The faster drug and polymer precipitation upon methylene chloride evaporation caused a higher drug entrapment.

Increasing the temperature from 25 °C (56.9 %) to 55 °C (58.5 %) did practically not impact the encapsulation efficiency, despite the temperature was increased above the polymer T_g, which caused a decreased encapsulation efficiency for the lower drug loading. Due to the higher drug loading, less methylene chloride was present in the organic phase, leading to a faster polymer precipitation compared to the lower drug loading. Additionally, the higher drug loading caused an increased viscosity, hindering

the drug efflux to the outer aqueous phase, causing comparable encapsulation efficiencies.

A temperature increase from 55 °C to 75 °C reduced the encapsulation efficiency from 56.5 % to 41.9 %. The increased diffusivity above the T_g overweighed the increasing methylene chloride vaporization, causing a higher drug diffusion from the droplets to the aqueous phase.

A further temperature increase from 75 °C to 95 °C increased again the encapsulation efficiency from 41.9 % to 47.0 %, which was most probably due to a faster polymer precipitation and a lower processing time at temperatures above the glass transition temperature, thus reducing drug diffusion to the aqueous phase (Figure 68).

3.4.6 Influence of the preparation temperature on residual solvents of PLGA microparticles

The solvent removal efficiency during the solvent evaporation step is essential for the residual solvents in the microspheres. The influence of the processing temperature on the residual methylene chloride and water content in drug-loaded microparticles was investigated.
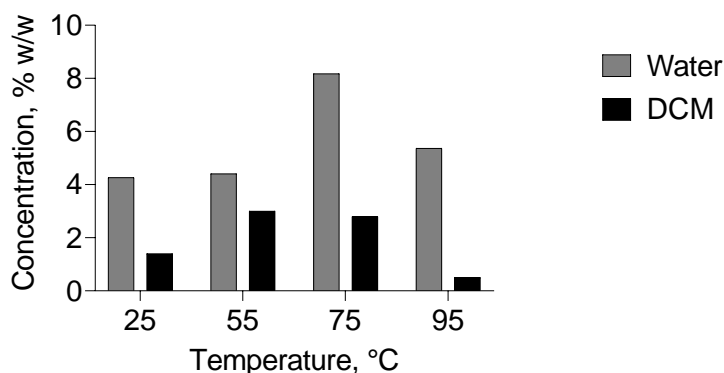
Figure 69 Effect of the preparation temperature on residual solvent levels in microparticles at 10 % w/w drug loading.
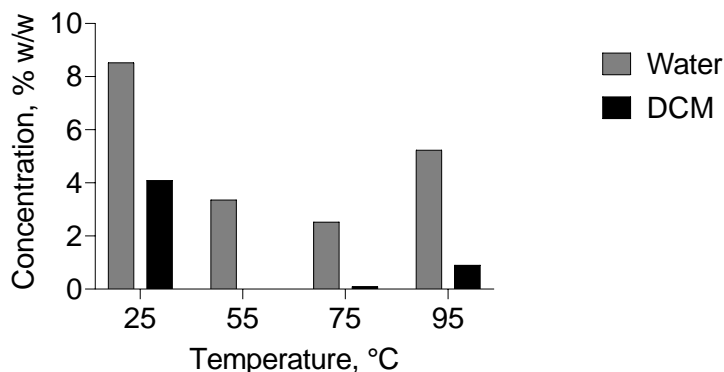
Figure 70 Effect of the preparation temperature on residual solvent levels in microparticles at 30 % w/w drug loading.

For both drug loadings, no connection between the preparation temperature and the residual solvent level for water or methylene chloride was established (Figure 69, Figure 70). Residual methylene chloride was maximum 4.1 %, indicating that the respective processing times allowed for complete solvent evaporation, which was supported by the observation that for all formulations free-flowing powders were obtained. The water content after the applied drying conditions was comparatively high, which would need further optimization in future studies. The water content of the microparticles was however assumed acceptable to test the impact of the preparation temperature on the drug release.

3.4.7 Influence of the preparation temperature on the drug release from PLGA microparticles

Prior to testing, the effect of the release test setup was investigated. The drug release from polymer-based matrix systems might be influenced by the applied release method [6]. To date, no compendial method is available for in vitro release-testing of microparticles. Drug release investigation with flow-through-cells was superior according to recent studies [197], but is characterized by large foot-print and extensive set-up. The comparatively long release periods of PLGA drug delivery systems over several weeks or months result in drawbacks regarding implementation especially at early stages of research and development. Thus, a minimization of the set-up seems beneficial. A "moved" method was compared to a small, "static" set-up for risperidone-

loaded microparticles, as the influence of local diffusion barriers by layers of high drug concentrations might influence the drug release.
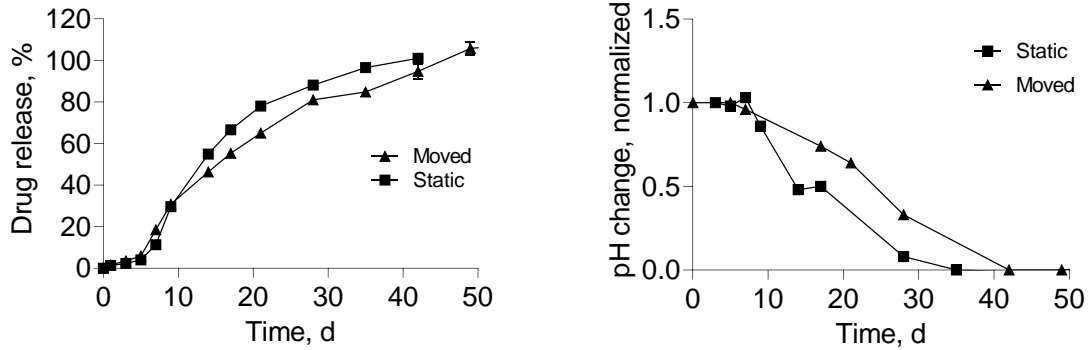
Figure 71 Influence of the release set-up on the drug release (left) and the pH change (right) as a function of time.

As an approach to assess the difference of the two release methods, the same formulation was released under the two stated conditions and the f_2-factor was calculated according to the following equation:

$$ f_2 = 50 * \log \left[\left\{ 1 + \frac{1}{n} \sum_{t=1}^{n} (R_t - T_t)^2 \right\}^{-0.5} * 100 \right] \tag{14} $$

with n the number of considered sampling time points, and R_t and T_t the cumulative percentage drug released at time point t.

Table 29 Drug release data used for the calculation of the similarity factor for comparison of two drug release methods (static *vs.* moved). Only one release value above 85% was used for the calculation.

Time, d	% Released		f_2
	Static	**Moved**	
0.04	0	0.27	
0.99	1.3	1.67	
3	2.4	3.56	
5	4.02	5.89	
7	11.33	18.58	
9	29.69	30.84	57.73
14	54.99	46.36	
17	66.69	55.33	
21	78.01	65.07	
28	88.13	81.02	

According to an f_2-factor of 57.73 (Table 29), release curves did not differ significantly. It was hence concluded that the static method is, in principle, suitable to test the risperidone release from microparticles prepared by the solvent evaporation method. However, the normalized pH change showed slight differences for the moved and static method (Figure 71). The pH decrease for the moved method was slightly delayed, which might be due to a higher local proton concentration under static conditions due to the formation of an acidic boundary layer. Despite the drug release was not influenced by the pH effect, the moved method was chosen as a higher discriminatory effect was expected.

Figure 72 Effect of the preparation temperature on the drug release (left) and pH change (right) from 10 % w/w drug-loaded PLGA microparticles (n=3, mean ± SD, PBS pH 6.8, 37 °C/80 rpm, sink conditions).

Despite the methylene chloride removal rate affected the microparticle size and morphology, which may impact the drug release [61], low impact was found regarding the drug release from microparticles prepared at different temperatures.

For the 10 % drug loaded formulations, the burst was unaffected by the preparation temperature (1.6, 2.3, 2.6 and 3.8 % for 25, 55, 75 and 95 °C, respectively) (Figure 72). After the burst, the lag-time of about 9 d was comparable for the formulations prepared at 25, 55 and 75 °C. Thereafter, drug release started simultaneously to a pH decrease, indicating a bulk-erosion. However, due to the slow drug release, a combination of diffusion and erosion was assumed to be the determining release mechanism.

Drug release onset of the formulation prepared at 95 °C occurred already after about 5 d. This was most probably due to the smaller particle size in combination with slightly higher encapsulation efficiency, increasing drug diffusion due to shorter diffusion pathways and increased concentration gradient.
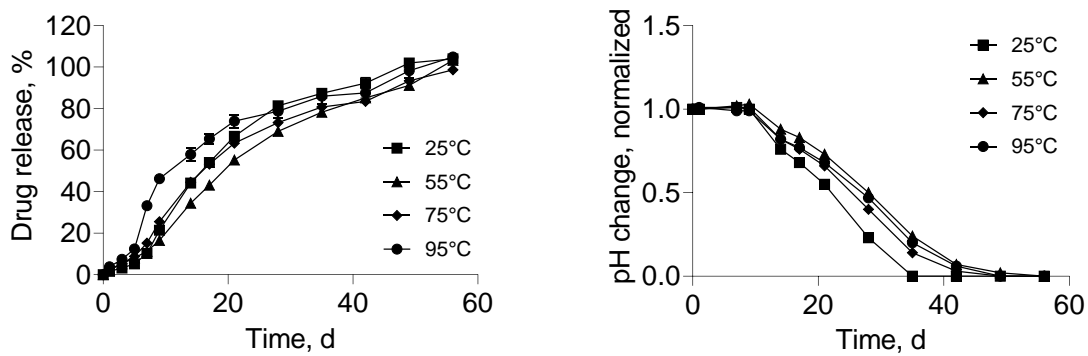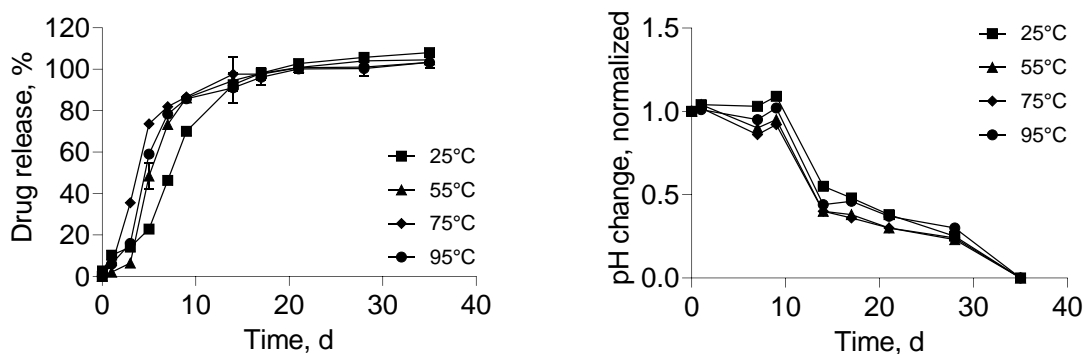
Figure 73 Effect of the preparation temperature on the drug release (left) and pH change (right) from 30 % drug-loaded PLGA microparticles (n=3, mean ± SD, PBS pH 6.8, 37 °C/80 rpm).

For the 30 % drug-loaded formulations, the microparticle preparation at 55 °C decreased the initial drug release compared to the other preparation temperatures (burst of about 10.3, 2.1, 5.3 and 6.0 % for 25, 55, 75 and 95 °C, respectively) (Figure 73), which was supported by an increased encapsulation efficiency at this temperature (Figure 68). However, the impact on drug release was minor, as the total amount of drug was released within 10 to 12 d for all formulations. Drug release patterns were comparable. After a short lag-time of about 1-2 d, the major drug fraction was released prior to a change in pH, indicating a drug release which was not controlled by the polymer erosion, but by drug diffusion through the matrix. Similar drug release patterns were observed for risperidone earlier [198]. For the same polymer grade, comparable encapsulation efficiencies were achieved, and risperidone was released within about 13 d. As the microparticle mean sizes were also comparable (about 39 µm), the release pattern was attributed to the drug substance diffusivity in the PLGA matrix.

The solvent evaporation step was significantly shortened from 12 hrs to less than 1 min with increasing processing temperatures from 25 °C to 95 °C and did not impact the drug release of a methylene chloride-soluble model drug. The existence of a limit of superheat explained the high energy needed to remove methylene chloride.

4. SUMMARY

The controlled parenteral drug delivery of drugs is advantageous due to lower fluctuations of drug plasma concentrations and reduced injection frequency, resulting in an improved safety and efficacy of the drug product for the patient. The incomparable biodegradability and biocompatibility of poly(lactide-*co*-glycolide) (PLGA) and the feasibility of controlling the drug release over days up to several months explains its common use as the polymeric matrix for such controlled parenteral drug delivery systems. Solid implants and microparticles represent common PLGA controlled drug delivery systems. In contrast to implants, microparticles can be administered without surgery, thus increasing the patient's compliance. The preparation methods, however, require high effort in terms of process development and control. There are two most common methods for the microparticle preparation: The organic phase separation method and the solvent evaporation method. The aim of this work was to study in detail the parameters which affect these processes at every stage to improve their robustness and to solve associated limitations.

The microparticle preparation process by organic phase separation was investigated in detail with the objective of improving the process robustness (Chapter 3.1). The preparation method mainly consists of three steps: First, the drug is dissolved, dispersed or emulsified in a polymer solution (i.e. PLGA in methylene chloride). To this, a non-solvent (e.g. polydimethylsiloxane) is added to induce a liquid-liquid phase separation, resulting in a polymer-rich (dispersed) and polymer-poor (continuous) phase. The polymer-rich (coacervate) droplets are then hardened in silicon oils (e.g. octamethylcyclotetrasiloxane) or alkanes (e.g. hexane or heptane) by methylene chloride extraction.

The formation of a stable coacervate phase is the core of the microparticle forming process, which is mainly characterized by the non-solvent concentration in the ternary mixture. The concentration of the non-solvent required to meet the stability window of coacervate droplets, where no sticking occurs, is commonly determined by optical microscopy. This study showed a lack of reproducibility of the conventional method due to occurrence of solvent evaporation, unstirred state, and a subjective evaluation of the microscopical appearance which lead to results highly dependent on the sample

preparation and/or the operator. To improve the method reliability, additional macroscopical investigations of the polymer-poor and polymer-rich phase and coacervate resuspendability as a function of the non-solvent concentration have been suggested, since both indicate the limits of the stability window.

A novel *in situ* method which allowed for the determination of the stability window under simulated process conditions was investigated. The closed, miniaturized system was equipped with an overhead stirrer, temperature control, camera (visualization probe) and an LED plus photosensor for real time transmission measurement. With the *in situ* method, the stability window was broader which was confirmed by the successful preparation of microparticles at non-solvent concentrations which were previously considered unfeasible based on the conventional stability window determination. Higher non-solvent concentrations were found in general to be advantageous to obtain a stable coacervate, leading to decreased collision frequency and coalescence efficiency. Increased mean theoretical distance between the coacervate droplets from 8 µm to 71 µm and 112 µm were calculated for 20, 40 and 45 % polydimethylsiloxane used. The theoretical calculations were confirmed by measurement of the actual distances between droplets obtained from the *in situ* appearances, and the transmissivity of the coacervate emulsion. Thus, by increasing the polydimethylsiloxane concentration from 36 % to 51 %, the stability of the emulsion was improved by factor 2.4 and 4.1 for 6 % and 3 % PLGA concentration, respectively. Finally, the dependencies of coacervate phase formation on temperature, polymer concentration and non-solvent addition rate could be established by applying the novel *in situ* method.

To improve the drug distribution of water-soluble drugs within the polymer matrix, a primary W/O-emulsion is commonly applied. The smaller the droplets of the primary emulsion, the lower the initial drug release from drug-loaded microparticles. Key parameters were identified influencing the droplet size distribution of the primary emulsion. To obtain small droplet sizes, reduced solid content of the aqueous phase, increased stirring efficiency, and increased solid content of the organic phase should be considered.

The effect of the hardening bath on the methylene chloride extraction was also investigated. With increasing methylene chloride affinity to the hardening agent and increasing hardening bath temperature, the methylene chloride extraction speed increased, thus shortening the hardening time.

Furthermore, the common step-wise transferal of the coacervate phase to the hardening phase is critical. With progressing transfer, the emulsion volume decreases, causing changes in stirring geometry and, thus, droplet sizes. The influence on the homogeneity of the batch is expected to increase with scale-up. Thus, a continuous production set-up for the coacervate phase by static mixing was developed and investigated. The particle size could be controlled by polymer concentration and total flow rate, while it was independent of the phase ratio between PLGA solution and non-solvent, and of the drug loading. A scale-up by factor 10 did not influence critical quality attributes of microparticles and thus demonstrated the suitability of the novel continuous coacervate production method.

A drawback of the microparticle preparation process by organic phase separation is the risk of volatile (methylene chloride, octamethylcyclotetrasiloxane) and non-volatile (polydimethylsiloxane) residual solvents, the monitoring of which is of high importance in process development and control due to the inherent toxicity for the patient, as well as the possible influence on critical quality attributes of the product. Gas chromatography (GC) is recommended for the quantification of residual volatile solvents in pharmaceutical products, but no method is currently available for the simultaneous quantification of the non-volatile silicon oil polydimethylsiloxane in presence of the volatile silicon oil octamethylcyclotetrasiloxane.

An H-NMR method was successfully developed and validated to simultaneously quantify volatile and non-volatile organic solvents and silicon oils appearing as residual solvents in microparticles prepared by organic phase separation (Chapter 3.2). Accuracy, precision, specificity, linearity, range, limit of detection and quantitation and robustness were investigated and agreed with validation requirements. The H-NMR method was less sensitive regarding the methylene chloride-, but more sensitive regarding the octamethylcyclotetrasiloxane-quantification compared to the compendial headspace gas chromatography. Additionally, with H-NMR it was possible to quantify volatile and non-volatile compounds simultaneously, at lower sample preparation effort and material consumption than with the compendial method. The method suitability is expected to apply for all excipients being soluble in deuterated solvents used for analysis, provided that obtained peaks do not overlap. Furthermore, the sample preparation for H-NMR measurement was simpler and less prone to systematical mistakes. The measurement by standard addition, needed for GC, increased the

sample preparation steps, thus increasing the effort in terms of time and costs and increasing the number of sources for mistakes. Due to the sample preparation based on weight (H-NMR) and not on volume (GC), a lower influence is expected for the processing of volatile organic compounds.

With the H-NMR method, the influence of formulation and process parameters on residual solvents in PLGA microparticles prepared by organic phase separation was studied (Chapter 3.3).

Microparticles were prepared by using the volatile methylene chloride as the organic solvent, the non-volatile silicon oil polydimethylsiloxane as the non-solvent and the volatile silicon oil octamethylcyclotetrasiloxane or heptane as the hardening agent. In particular, investigations on the simultaneous appearance of two silicon oils in PLGA drug delivery forms have, up to now, not been extensively discussed in the scientific literature.

Methylene chloride and polydimethylsiloxane residuals were reduced by decreasing the polymer concentration, increasing the hardening agent volume and increasing the hardening time, while they were increased by incorporation of a hydrophilic model drug. Additionally, methylene chloride residuals could be reduced by optimized drying conditions (vacuum, long drying times and drying temperature close to T_g). While methylene chloride residuals were independent of the hardening agent (octamethylcyclotetrasiloxane or heptane) and the polydimethylsiloxane addition rate, polydimethylsiloxane could be reduced by using octamethylcyclotetrasiloxane instead of heptane as the hardening agent and by decreasing the polydimethylsiloxane addition rate. Methylene chloride and polydimethylsiloxane residuals were independent of the coacervation temperature.

Octamethylcyclotetrasiloxane residuals were also independent of the coacervation temperature. However, for the other parameters octamethylcyclotetrasiloxane behaved contrary to methylene chloride and polydimethylsiloxane. Residuals were reduced by increasing the drug loading, and increased by decreasing the polymer concentration, increasing the hardening agent volume and increasing the hardening time. Despite its volatility, octamethylcyclotetrasiloxane could not be decreased even under severe drying conditions. Nevertheless, it was superior compared to heptane due to an improved polydimethylsiloxane extraction and significantly lower residuals in the microparticles.

Methylene chloride and polydimethylsiloxane are influenceable by comparable formulation and process parameters at the expense of octamethylcyclotetrasiloxane residuals, which were, however, acceptable for all investigated conditions showing residual levels of NMT 1 %.

For the preparation of microparticles by solvent evaporation, a drug-containing PLGA solution in methylene chloride is emulsified in an aqueous phase with a stabilizer. Methylene chloride is then evaporated to solidify microparticles. This method is advantageous due to lower organic solvent consumption, easier set-up and process control compared to the phase separation method, but drugs may diffuse out to the aqueous phase, causing low encapsulation efficiencies and high burst. Faster polymer precipitation by accelerated methylene chloride removal helps to solve these problems. Commonly, this is achieved by increasing the aqueous phase volume; however, large volumes are often unfavorable in industrial processes.

To accelerate the methylene chloride removal while maintaining the aqueous phase volume at a minimum, the preparation temperature was increased above the methylene chloride boiling point, and the influence of increased temperature on drug-loaded microparticles was studied (Chapter 3.4). Interestingly, emulsified methylene chloride in a 1 % poly(vinyl alcohol) (PVA) solution showed a metastable, superheated state above its boiling point (39.6 °C) until a limit of superheat was reached, referring to the temperature where instant methylene chloride vaporization occurs. Thus, methylene chloride evaporation was slower than expected around its actual boiling point, and boiling was delayed to a 2-fold higher temperature (74-79 °C) compared to the pure solvent. Addition of a polymer to the dispersed phase further increased the limit of superheat to 84 °C, which was unfavorable for an accelerated methylene chloride removal.

To test the influence of the solvent evaporation at elevated temperatures, PLGA microparticles were prepared at 25 °C, 55 °C, 75 °C and 95 °C and investigated in terms of particle size, appearance, encapsulation efficiency, residual solvents and drug release. The used model drug was soluble in methylene chloride.

By increasing the temperature, the process time decreased from 12 hrs (25°C) to less than 1 min (95°C) independent of the drug loading.

The particle size was only affected above the limit of superheat. Increasing the temperature to 95 °C decreased the particle size significantly by factors 15, 10 and 9

for 0, 10 and 30 % drug-loading due to an explosive methylene chloride vaporization sufficient for a droplet disruption.

The encapsulation efficiency was first decreased at temperatures above the polymer T_g (45-50 °C). However, a further temperature increase to 95 °C fastened the methylene chloride removal to such an extent that accelerated polymer precipitation caused encapsulation efficiency to raise again.

Residual solvents as well as the surface morphology were independent of the preparation temperature for all drug loadings. However, inner porosity depended on the preparation temperature. Increasing the temperature to 55 °C and 75 °C led to the formation of inner pores due to an expansion of gaseous bubbles which could not escape from the polymer matrix. In contrast to this, particles prepared at 95 °C were dense without inner voids.

Drug release from the 10 % drug-loaded formulations was comparable for the formulations prepared at 25 °C, 55 °C and 75 °C, while for the formulation prepared at 95 °C the initial drug release was faster. However, drug release was completed within about 60 d for all preparation temperatures.

Drug release from the 30 % drug-loaded formulations was completed within 10-12 d for all preparation temperatures and was independent of PLGA hydrolysis.

Results demonstrated that microparticles could be prepared at increased process temperatures, but that the accelerated methylene chloride removal is impeded by the presence of a metastable state and the limit of superheat, which influences critical quality attributes of the microparticles.

In conclusion, key formulation and process parameters affecting attributes of PLGA microparticles prepared by a phase separation method were identified, which are expected to improve the process robustness in future studies. Additionally, a novel analytical method was developed giving new insights on the effect of formulation and process parameters on residual solvent levels in these microparticles. Particularly, volatile and non-volatile silicon oils could be studied simultaneously. Furthermore, the methylene chloride removal rate during the preparation of microparticles by solvent evaporation increased with increasing temperature, but the energy needed to evaporate methylene chloride was much higher than expected due to the presence of a limit of superheat of the emulsion. Results contributed to the understanding of solvent

evaporation process, potentially serving as the basis for future process optimization approaches by accelerated methylene chloride removal.

5. ZUSAMMENFASSUNG

Die kontrollierte parenterale Arzneimittelabgabe von Arzneimittelsubstanzen ist aufgrund geringer Schwankungen der Arzneimittelplasmakonzentrationen und einer verringerten Injektionsfrequenz vorteilhaft, was zu einer verbesserten Sicherheit und Wirksamkeit des Arzneimittels für den Patienten führt. Die unvergleichliche biologische Abbaubarkeit und Biokompatibilität von Poly(lactid-co-glycolid) (PLGA) und die Machbarkeit der Kontrolle der Arzneimittelfreisetzung über Tage bis zu mehreren Monaten erklärt seine häufige Verwendung als Polymermatrix für solche kontrollierten parenteralen Arzneimittelabgabesysteme. Feste Implantate und Mikropartikel stellen übliche PLGA-basierte kontrollierte Arzneimittelabgabesysteme dar. Im Gegensatz zu Implantaten können Mikropartikel ohne Operation verabreicht werden, wodurch die Compliance des Patienten erhöht wird. Die Vorbereitungsmethoden erfordern jedoch einen hohen Aufwand in Bezug auf die Prozessentwicklung und -steuerung. Es gibt zwei gebräuchlichste Verfahren zur Herstellung von Mikropartikeln: das Verfahren zur Trennung der organischen Phase und das Verfahren zur Verdampfung des Lösungsmittels. Ziel dieser Arbeit war es, die Parameter, die diese Prozesse in jeder Phase beeinflussen, detailliert zu untersuchen, um ihre Robustheit zu verbessern und die damit verbundenen Einschränkungen zu lösen. Der Prozess der Herstellung von Mikropartikeln pro organischer Phasentrennung wurde eingehend untersucht, um die Robustheit des Prozesses zu verbessern (Kapitel 3.1). Das Herstellungsverfahren besteht hauptsächlich aus drei Schritten: Zunächst wird der Arzneistoff in einer Polymerlösung (z. B. PLGA in Methylenchlorid) gelöst, dispergiert oder emulgiert. Dazu wird ein Nichtlösungsmittel (z. B. Polydimethylsiloxan) gegeben, um eine Flüssig-Flüssig-Phasentrennung zu induzieren, was zu einer polymerreichen (dispergierten) und polymerarmen (kontinuierlichen) Phase führt. Die polymerreichen (Koazervat-) Tröpfchen werden dann durch Methylenchlorid-Extraktion in Silikonölen (z. B. Octamethylcyclotetrasiloxan) oder Alkanen (z. B. Hexan oder Heptan) gehärtet. Die Bildung eines stabilen Koazervats ist der Kern des Mikropartikelbildungsprozesses, der hauptsächlich durch die Nichtlösungsmittelkonzentration im ternären Gemisch gekennzeichnet ist. Die Konzentration des Nichtlösungsmittels, die erforderlich ist, um das Stabilitätsfenster von Koazervattropfen zu erreichen, bei denen keine Agglomeration auftritt, wird

üblicherweise durch optische Mikroskopie bestimmt. Diese Studie zeigte einen Mangel an Reproduzierbarkeit des herkömmlichen Verfahrens aufgrund des Auftretens von Lösungsmittelverdampfung, ungerührtem Zustand und einer subjektiven Bewertung des mikroskopischen Erscheinungsbilds, was zu Ergebnissen führte, die stark von der Probenvorbereitung und / oder dem Operator abhängen. Um die Zuverlässigkeit des Verfahrens zu verbessern, wurden zusätzliche makroskopische Untersuchungen der polymerarmen und polymerreichen Phase und der Koazervatresuspendierbarkeit als Funktion der Nichtlösungsmittelkonzentration vorgeschlagen, da beide die Grenzen des Stabilitätsfensters aufzeigen. Eine neuartige In-situ-Methode, mit der das Stabilitätsfenster unter simulierten Prozessbedingungen bestimmt werden konnte, wurde untersucht. Das geschlossene, miniaturisierte System war mit einem Überkopfrührer, einer Temperaturkontrolle, einer Kamera (Visualisierungssonde) und einem LED plus Photosensor zur Echtzeit-Transmissionsmessung ausgestattet. Mit der In-situ-Methode wurde ein breiteres Stabilitätsfenster gefunden, das durch die erfolgreiche Herstellung von Mikropartikeln bei Nichtlösungsmittelkonzentrationen bestätigt wurde, die zuvor aufgrund der herkömmlichen Bestimmung des Stabilitätsfensters als nicht durchführbar angesehen wurden. Höhere Nichtlösungsmittelkonzentrationen erwiesen sich im Allgemeinen als vorteilhaft, um ein stabiles Koazervat zu erhalten, da sie zu einer verringerten Kollisionsfrequenz und einer Koaleszenzeffizienz führen. Die mittleren theoretischen Abstände zwischen den Koazervattropfen wurden von 8 µm auf 71 µm und 112 µm für 20, 40 und 45 % Polydimethylsiloxane erhöht. Die theoretischen Berechnungen wurden durch Messung der tatsächlichen Abstände zwischen Tröpfchen, die aus den In-situ-Beobachtungen erhalten wurden, und der Transmission der Koazervatemulsion bestätigt. Durch Erhöhen der Polydimethylsiloxane-Konzentration von 36 % auf 51 % wurde die Stabilität der Emulsion für 6 % bzw. 3 % Polymer um den Faktor 2,4 und 4,1 verbessert. Schließlich konnten die Abhängigkeiten der Koazervatphasenbildung von Temperatur, Polymerkonzentration und Nichtlösungsmittel-Zugabegeschwindigkeit durch Anwendung des neuen In-situ-Verfahrens ermittelt werden.

Um die Arzneimittelverteilung wasserlöslicher Arzneistoffe innerhalb der Polymermatrix zu verbessern, wird üblicherweise eine primäre W/O-Emulsion angewendet. Je kleiner die Tröpfchen der primären Emulsion sind, desto geringer ist die anfängliche Arzneimittelfreisetzung aus mit Arzneimitteln beladenen Mikropartikeln. Es wurden Schlüsselparameter identifiziert, die die

Tröpfchengrößenverteilung der Primäremulsion beeinflussen. Um kleine Tröpfchengrößen zu erhalten, sollten ein verringerter Feststoffgehalt der wässrigen Phase, eine erhöhte Rühreffizienz und ein erhöhter Feststoffgehalt der organischen Phase in Betracht gezogen werden.

Der Einfluss des Härtebades auf die Methylenchlorid-Extraktion wurde ebenfalls untersucht. Mit zunehmender Methylenchlorid-Affinität zum Extraktionsmittel und zunehmender Härtebadtemperatur wurde die Methylenchlorid-Extraktionsgeschwindigkeit erhöht, wodurch die Härtezeit verkürzt wurde.

Darüber hinaus ist der übliche schrittweise Transfer der Koazervatphase in das Härtebad kritisch. Mit fortschreitendem Transfer nimmt das Volumen der verbleibenden Emulsion ab, was zu Änderungen der Rührgeometrie und damit der Tröpfchengröße führt. Es wird erwartet, dass der Einfluss auf die Homogenität der erhaltenen Charge mit dem Scale-up zunimmt. Daher wurde ein kontinuierlicher Produktionsaufbau für die Koazervatphasenherstellung mithilfe eines statischen Mischers entwickelt und untersucht. Die Partikelgröße konnte durch die Polymerkonzentration und die Gesamtflussrate gesteuert werden, während sie unabhängig vom Phasenverhältnis zwischen Polymerlösung und Nichtlösungsmittel und von der Wirkstoffbeladung war. Ein Scale-up um Faktor 10 hatte keinen Einfluss auf die kritischen Qualitätsmerkmale von Mikropartikeln und demonstrierte somit die Eignung des neuartigen kontinuierlichen Koazervat-Produktionsverfahrens.

Ein Nachteil des Mikropartikelherstellungsprozesses mithilfe der organischen Phasenseparation ist das Risiko von flüchtigen (Methylenchlorid, Octamethylcyclotetrasiloxane) und nichtflüchtigen (Polydimethylsiloxane) Restlösungsmitteln, deren Überwachung aufgrund der inhärenten Toxizität für den Patienten sowie der möglichen Auswirkungen auf kritische Qualitätsmerkmale des Produkts für die Prozessentwicklung und -kontrolle von großer Bedeutung ist. Die Gaschromatographie (GC) wird für die Quantifizierung von flüchtigen Restlösungsmitteln in pharmazeutischen Produkten empfohlen. Derzeit ist jedoch keine Methode zur gleichzeitigen Quantifizierung des nichtflüchtigen Silikonöls-Polydimethylsiloxane in Gegenwart des flüchtigen Silikonöls-octamethylcyclotetrasiloxane verfügbar. Eine neuartige H-NMR-Methode wurde erfolgreich entwickelt und validiert, um gleichzeitig flüchtige und nichtflüchtige organische Lösungsmittel und Silikonöle zu quantifizieren, die als Restlösungsmittel in

durch organische Phasenseparation hergestellten Mikropartikeln auftreten (Kapitel 3.2). Genauigkeit, Präzision, Spezifität, Linearität, Messbereich, Nachweis- und Bestimmungsgrenze sowie Robustheit wurden in Übereinstimmung mit den Validierungsanforderungen untersucht. Das neuartige H-NMR-Verfahren war in Bezug auf die Methylenchlorid-Quantifizierung weniger empfindlich, in Bezug auf die octamethylcyclotetrasiloxane-Quantifizierung jedoch empfindlicher als die Headspace-Gaschromatographie gemäß Arzneibuch. Zusätzlich war es mit H-NMR möglich, flüchtige und nichtflüchtige Verbindungen gleichzeitig zu quantifizieren, bei weniger umfangreichem Probenvorbereitungsaufwand und geringerem Materialverbrauch als mit der Vergleichsmethode. Es wird erwartet, dass die Eignung des Verfahrens für alle Hilfsstoffe gilt, die in deuterierten Lösungsmitteln löslich sind, die für die Analyse verwendet werden, vorausgesetzt, die erhaltenen Peaks interferieren nicht. Darüber hinaus wurde festgestellt, dass die Probenvorbereitung für die H-NMR-Messung weniger umfangreich und weniger anfällig für systematische Fehler ist. Die für die GC erforderliche Messung mithilfe des Standardadditionsverfahrens erhöhte die Probenvorbereitungsschritte, wodurch der Aufwand in Bezug auf Zeit und Kosten sowie die Anzahl der Fehlerquellen erhöht wurde. Aufgrund der Probenvorbereitung nach Gewicht (H-NMR) und nicht nach Volumen (GC) wird für die Verarbeitung flüchtiger organischer Verbindungen ein geringeres Risiko erwartet.

Mit der neuen H-NMR-Methode wurde der Einfluss von Formulierungs- und Prozessparametern auf Lösungsmittelreste in PLGA-basierten Mikropartikeln untersucht, die mithilfe der organischen Phasenseparation hergestellt wurden (Kapitel 3.3). Mikropartikel wurden unter Verwendung des flüchtigen Methylenchlorids als organisches Lösungsmittel, des nichtflüchtigen Silikonöls Polydimethylsiloxan als Nichtlösungsmittel und des flüchtigen Silikonöls Octamethylcyclotetrasiloxan oder Heptan als Extraktionsmittel hergestellt. Untersuchungen zum gleichzeitigen Auftreten von zwei Silikonölen in PLGA-basierten Arzneimittelformen wurden in der wissenschaftlichen Literatur bisher nicht ausführlich diskutiert. Methylenchlorid- und Polydimethylsiloxane-Rückstände wurden durch Verringern der Polymerkonzentration, Erhöhen des Härtungsmittelvolumens und Erhöhen der Härtezeit reduziert, während sie durch das Vorhandensein einer hydrophilen Modellarzneimittelsubstanz erhöht wurden. Zusätzlich konnten Methylenchlorid-Rückstände durch optimierte Trocknungsbedingungen (Vakuum, lange

Trocknungszeiten und Trocknungstemperatur nahe T_g) reduziert werden. Während Methylenchlorid-Rückstände unabhängig vom Härtungsmittel (Octamethylcyclotetrasiloxane oder Heptan) und der Polydimethylsiloxane-Zugaberate waren, konnte Polydimethylsiloxane durch Verwendung von Octamethylcyclotetrasiloxane anstelle von Heptan als Extraktionsmittel und durch Verringern der Polydimethylsiloxane-Zugaberate reduziert werden. Methylenchlorid- und Polydimethylsiloxane-Rückstände waren unabhängig von der Koazervationstemperatur.

Octamethylcyclotetrasiloxane-Rückstände waren ebenfalls unabhängig von der Koazervationstemperatur. Bei den anderen Parametern verhielt sich Octamethylcyclotetrasiloxane gegensätzlich zu Methylenchlorid und Polydimethylsiloxane. Die Rückstände wurden durch Erhöhen der Arzneimittelbeladung verringert, während sie durch Verringern der Polymerkonzentration, Erhöhen des Härtungsmittelvolumens und Verlängerung der Härtungszeit erhöht wurden. Trotz seiner Flüchtigkeit konnte Octamethylcyclotetrasiloxane selbst unter extremen Trocknungsbedingungen nicht verringert werden. Trotzdem war es im Vergleich zu Heptan aufgrund einer verbesserten Polydimethylsiloxane-Extraktion und signifikant geringerer Rückstände in den Mikropartikeln überlegen.

Methylenchlorid und Polydimethylsiloxane können so durch vergleichbare Formulierungs- und Prozessparameter auf Kosten von Octamethylcyclotetrasiloxane-Rückständen beeinflusst werden, die jedoch für alle untersuchten Bedingungen mit einem Restgehalt von weniger als 1 % akzeptabel waren.

Zur Herstellung von Mikropartikeln mithilfe der Lösungsmittelverdampfungsmethode wird eine arzneimittelhaltige Polymerlösung in Methylenchlorid in einer wässrigen Phase mit einem Stabilisator emulgiert. Methylenchlorid wird dann verdampft, um die Mikropartikel zu verfestigen. Dieses Verfahren ist aufgrund des geringeren Lösungsmittelverbrauchs, des einfacheren Aufbaus und der besseren Prozesskontrolle im Vergleich zum Phasenseparationsverfahren vorteilhaft; jedoch können Arzneimittel in die wässrige Phase diffundieren, was geringe Verkapselungseffizienzen und einen hohen Burst verursacht. Eine schnellere Polymerpräzipitation durch beschleunigte Methylenchlorid-Entfernung hilft, diese Probleme zu lösen. Üblicherweise wird dies durch Erhöhen des Volumens der

wässrigen Phase erreicht. Große Volumina sind jedoch in industriellen Prozessen oft unerwünscht. Um die Methylenchlorid-Entfernung zu beschleunigen und gleichzeitig das Volumen der wässrigen Phase auf einem Minimum zu halten, wurde die Herstellungstemperatur über den Methylenchlorid-Siedepunkt erhöht und der Einfluss einer erhöhten Temperatur auf arzneimittelbeladene Mikropartikel untersucht (Kapitel 3.4). Interessanterweise zeigte emulgiertes Methylenchlorid in einer 1%-igen Polyvinylalkohol (PVA)-Lösung durch das Auftreten von Siedeverzug einen metastabilen Zustand über seinem Siedepunkt (39,6 °C), bis ein „Limit of Superheat" erreicht wurde, welches die Temperatur darstellt, bei der eine sofortige Methylenchlorid-Verdampfung auftritt. Somit war die Methylenchlorid-Verdampfung am tatsächlichen Siedepunkt deutlich langsamer als erwartet, und der Siedepunkt in der Emulsion wurde auf eine etwa 2-fach höhere Temperatur (74-79ºC) im Vergleich zu dem reinen Lösungsmittel verlagert. Die Zugabe eines Polymers zu der dispergierten Phase erhöhte das „Limit of Superheat" weiter auf etwa 84ºC, was für eine beschleunigte Methylenchlorid-Entfernung ungünstig war. Um den Einfluss der Lösungsmittelverdampfung bei erhöhten Temperaturen zu testen, wurden PLGA-Mikropartikel bei 25°C, 55°C, 75°C und 95°C hergestellt und hinsichtlich Partikelgröße, Aussehen, Verkapselungseffizienz, Restlösungsmittel und Arzneimittelfreisetzung untersucht. Die verwendete Modellarzneimittelsubstanz war in Methylenchlorid löslich. Durch Erhöhen der Temperatur wurde die Prozesszeit unabhängig von der Wirkstoffbeladung von etwa 12 Stunden (25°C) auf weniger als 1 Minute (95° C) verringert. Die Partikelgröße wurde nur oberhalb des „Limit of Superheat" beeinflusst: Durch Erhöhen der Temperatur auf 95°C wurde die Partikelgröße aufgrund einer explosiven Methylenchlorid-Verdampfung, ausreichend für das Zerreißen von Tropfen, um die Faktoren 15, 10 und 9 für 0, 10 und 30 % Wirkstoffbeladung signifikant verringert.

Die Verkapselungseffizienz wurde bei Temperaturen oberhalb der Polymer-Tg (45-50ºC) zunächst verringert. Ein weiterer Temperaturanstieg auf 95°C beschleunigte jedoch die Methylenchlorid-Entfernung in einem solchen Ausmaß, dass eine beschleunigte Polymerpräzipitation dazu führte, dass die Verkapselungseffizienz wieder anstieg. Restlösungsmittel sowie die Oberflächenmorphologie waren für alle Arzneimittelbeladungen unabhängig von der Herstellungstemperatur.

Die innere Porosität hing jedoch von der Herstellungstemperatur ab. Das Erhöhen der Temperatur auf 55°C und 75°C führte zur Bildung innerer Poren aufgrund einer

Expansion von Gasblasen, die nicht aus der Polymermatrix entweichen konnten. Im Gegensatz dazu zeigten die bei 95 ° C hergestellte Partikel keine inneren Hohlräume.

Die Arzneimittelfreisetzung aus den mit 10 % Arzneistoff-beladenen Formulierungen war für die bei 25°C, 55°C und 75°C hergestellten Formulierungen vergleichbar, während für die bei 95°C hergestellte Formulierung die anfängliche Arzneimittelfreisetzung schneller war. Die Arzneimittelfreisetzung war jedoch für alle Herstellungstemperaturen innerhalb von etwa 60 Tagen abgeschlossen.

Die Arzneimittelfreisetzung aus den mit 30 % Arzneistoff-beladenen Formulierungen war für alle Herstellungstemperaturen innerhalb von 10 bis 12 Tagen abgeschlossen und unabhängig von der PLGA-Hydrolyse. Die Ergebnisse zeigten, dass Mikropartikel bei erhöhten Prozesstemperaturen hergestellt werden konnten, die beschleunigte Methylenchlorid-Entfernung jedoch durch das Vorhandensein eines metastabilen Zustands und des „Limit of Superheat" behindert wird, was sich auf die kritischen Qualitätsmerkmale der Mikropartikel auswirkt.

Zusammenfassend wurden wichtige Formulierungs- und Prozessparameter identifiziert, die die Eigenschaften von PLGA-basierten Mikropartikeln beeinflussen, die durch ein Phasentrennungsverfahren hergestellt wurden und die die Prozessrobustheit in zukünftigen Studien verbessern sollen. Zusätzlich wurde eine neuartige Analysemethode entwickelt, die neue Erkenntnisse über die Auswirkung von Formulierungs- und Prozessparametern auf den Restlösemittelgehalt in Mikropartikeln lieferte. Insbesondere konnten flüchtige und nichtflüchtige Silikonöle gleichzeitig untersucht werden. Darüber hinaus konnte die Methylenchlorid-Entfernungsrate während der Herstellung von Mikropartikeln per Lösungsmittelverdampfungsmethode mit zunehmender Temperatur erhöht werden. Die zum Verdampfen von Methylenchlorid erforderliche Energie war jedoch aufgrund des Auftretens eines Siedeverzugs der Emulsion deutlich höher als erwartet. Die Ergebnisse trugen zum Verständnis des Lösungsmittelverdampfungsprozesses bei und könnten als Grundlage für zukünftige Ansätze zur Prozessoptimierung durch beschleunigte Methylenchlorid-Entfernung dienen.

6. REFERENCES

1. Donovan, M.D., G.L. Flynn, and G.L. Amidon, *Absorption of polyethylene glycols 600 through 2000: the molecular weight dependence of gastrointestinal and nasal absorption.* Pharmaceutical research, 1990. **7**(8): p. 863-868.

2. Goldberg, M. and I. Gomez-Orellana, *Challenges for the oral delivery of macromolecules.* Nature reviews Drug discovery, 2003. **2**(4): p. 289-295.

3. Rojanasakul, Y., L.-Y. Wang, M. Bhat, D.D. Glover, C.J. Malanga, and J.K.H. Ma, *The Transport Barrier of Epithelia: A Comparative Study on Membrane Permeability and Charge Selectivity in the Rabbit.* Pharmaceutical Research, 1992. **9**(8): p. 1029-1034.

4. Scott, L.J., *Exenatide Extended-Release.* Drugs, 2012. **72**(12): p. 1679-1707.

5. Harrison, T.S. and K.L. Goa, *Long-Acting Risperidone.* CNS Drugs, 2004. **18**(2): p. 113-132.

6. Park, K., S. Skidmore, J. Hadar, J. Garner, H. Park, A. Otte, B.K. Soh, G. Yoon, D. Yu, Y. Yun, B.K. Lee, X. Jiang, and Y. Wang, *Injectable, long-acting PLGA formulations: Analyzing PLGA and understanding microparticle formation.* J Control Release, 2019. **304**: p. 125-134.

7. Thomasin, C., H. Nam-Trân, H.P. Merkle, and B. Gander, *Drug microencapsulation by PLA/PLGA coacervation in the light of thermodynamics. 1. Overview and theoretical considerations.* Journal of pharmaceutical sciences, 1998. **87**(3): p. 259-268.

8. Merck Sharp & Dohme GmbH. *SmPC of "Implanon NXT 68 mg, Implantat zur subkutanen Anwendung".* [26.04.2020]; Available from: www.fachinfo.de.

9. Cossé, A., C. König, A. Lamprecht, and K.G. Wagner, *Hot melt extrusion for sustained protein release: matrix erosion and in vitro release of PLGA-based implants.* AAPS PharmSciTech, 2017. **18**(1): p. 15-26.

10. Ramchandani, M., M. Pankaskie, and D. Robinson, *The influence of manufacturing procedure on the degradation of poly(lactide-co-glycolide) 85:15 and 50:50 implants.* Journal of Controlled Release, 1997. **43**(2): p. 161-173.

11. Kim, J.M., K.S. Seo, Y.K. Jeong, H.B. Lee, Y.S. Kim, and G. Khang, *Co-effect of aqueous solubility of drugs and glycolide monomer on in vitro release rates from poly(D,L-lactide- co-glycolide) discs and polymer degradation.* Journal of Biomaterials Science, Polymer Edition, 2005. **16**(8): p. 991-1007.

12. Rothen-Weinhold, A., K. Besseghir, E. Vuaridel, E. Sublet, N. Oudry, F. Kubel, and R. Gurny, *Injection-molding versus extrusion as manufacturing technique for the preparation of biodegradable implants.* European journal of pharmaceutics and biopharmaceutics, 1999. **48**(2): p. 113-121.

13. Ghalanbor, Z., M. Körber, and R. Bodmeier, *Improved Lysozyme Stability and Release Properties of Poly(lactide-co-glycolide) Implants Prepared by Hot-Melt Extrusion.* Pharmaceutical Research, 2010. **27**(2): p. 371-379.

14. Repka, M.A., S. Shah, J. Lu, S. Maddineni, J. Morott, K. Patwardhan, and N.N. Mohammed, *Melt extrusion: process to product.* Expert Opinion on Drug Delivery, 2012. **9**(1): p. 105-125.

15. *Rote Liste - Online.* 2020 [22.04.2020]; Available from: www.rote-liste.de.

16. Janssen-Cilag GmbH. *SmPC of "Risperdal Consta".* [26.04.2020]; Available from: www.fachinfo.de.

17. Kempe, S. and K. Mäder, *In situ forming implants — an attractive formulation principle for parenteral depot formulations.* Journal of Controlled Release, 2012. **161**(2): p. 668-679.

18. Kranz, H. and R. Bodmeier, *Structure formation and characterization of injectable drug loaded biodegradable devices: in situ implants versus in situ microparticles.* European journal of pharmaceutical sciences, 2008. **34**(2-3): p. 164-172.

19. Parent, M., C. Nouvel, M. Koerber, A. Sapin, P. Maincent, and A. Boudier, *PLGA in situ implants formed by phase inversion: critical physicochemical parameters to modulate drug release.* J Control Release, 2013. **172**(1): p. 292-304.

20. Camargo, J.A., A. Sapin, C. Nouvel, D. Daloz, M. Leonard, F. Bonneaux, J.L. Six, and P. Maincent, *Injectable PLA-based in situ forming implants for controlled release of Ivermectin a BCS Class II drug: solvent selection based on physico-chemical characterization.* Drug Development and Industrial Pharmacy, 2013. **39**(1): p. 146-155.

21. Vert, M., Y. Doi, K.-H. Hellwich, M. Hess, P. Hodge, P. Kubisa, M. Rinaudo, and F. Schué, *Terminology for biorelated polymers and applications (IUPAC Recommendations 2012).* Pure and Applied Chemistry, 2012. **84**.

22. Whitaker, M.A., P. Langston, A. Naylor, B.J. Azzopardi, and S.M. Howdle, *Particle size and shape effects in medical syringe needles: experiments and simulations for polymer microparticle injection.* Journal of Materials Science: Materials in Medicine, 2011. **22**(8): p. 1975-1983.

23. Birnbaum, D.T. and L. Brannon-Peppas, *Microparticle drug delivery systems*, in *Drug delivery systems in cancer therapy*. 2004, Springer. p. 117-135.

24. Singh, M.N., K.S.Y. Hemant, M. Ram, and H.G. Shivakumar, *Microencapsulation: A promising technique for controlled drug delivery.* Research in pharmaceutical sciences, 2010. **5**(2): p. 65-77.

25. Yow, H.N., X. Wu, A.F. Routh, and R.H. Guy, *Dye diffusion from microcapsules with different shell thickness into mammalian skin.* European Journal of Pharmaceutics and Biopharmaceutics, 2009. **72**(1): p. 62-68.

26. Vysloužil, J., P. Doležel, M. Kejdušová, E. Mašková, J. Mašek, R. Lukáč, V. Košťál, D. Vetchý, and K. Dvořáčková, *Influence of different formulations and process parameters during the preparation of drug-loaded PLGA microspheres evaluated by multivariate data analysis.* 2014. **64**(4): p. 403.

27. Luan, X., M. Skupin, J. Siepmann, and R. Bodmeier, *Key parameters affecting the initial release (burst) and encapsulation efficiency of peptide-containing poly(lactide-co-glycolide) microparticles.* International Journal of Pharmaceutics, 2006. **324**(2): p. 168-175.

28. Nykamp, G., U. Carstensen, and B.W. Müller, *Jet milling—a new technique for microparticle preparation.* International Journal of Pharmaceutics, 2002. **242**(1): p. 79-86.

29. Mueller, B.C., Ulrike, *Wirkstoffhaltige Mikropartikel und Verfahren zur Herstellung der Mikropartikel durch Abrasion.* 2000.

30. Edlund, U. and A.-C. Albertsson, *Degradable Polymer Microspheres for Controlled Drug Delivery*, in *Degradable Aliphatic Polyesters*. 2002, Springer Berlin Heidelberg: Berlin, Heidelberg. p. 67-112.

31. Park, T.G., *Degradation of poly(d,l-lactic acid) microspheres: effect of molecular weight.* Journal of Controlled Release, 1994. **30**(2): p. 161-173.

32. GÜMÜŞDERELİOĞLU, M. and G. DENİZ, *Synthesis, characterization and in vitro degradation of poly (dl-lactide)/poly (dl-lactide-co-glycolide) films.* Turkish Journal of Chemistry, 1999. **23**(2): p. 153-162.

33. Badi, N., D. Chan-Seng, and J.F. Lutz, *Microstructure control: an underestimated parameter in recent polymer design.* Macromolecular Chemistry and Physics, 2013. **214**(2): p. 135-142.

34. Washington, M.A., S.C. Balmert, M.V. Fedorchak, S.R. Little, S.C. Watkins, and T.Y. Meyer, *Monomer sequence in PLGA microparticles: Effects on acidic microclimates and in vivo inflammatory response.* Acta Biomaterialia, 2018. **65**: p. 259-271.

35. DeYoung, M.B., L. MacConell, V. Sarin, M. Trautmann, and P. Herbert, *Encapsulation of exenatide in poly-(D, L-lactide-co-glycolide) microspheres produced an investigational long-acting once-weekly formulation for type 2 diabetes.* Diabetes technology & therapeutics, 2011. **13**(11): p. 1145-1154.

36. Wang, J., L. Helder, J. Shao, J.A. Jansen, M. Yang, and F. Yang, *Encapsulation and release of doxycycline from electrospray-generated PLGA microspheres: Effect of polymer end groups.* International Journal of Pharmaceutics, 2019. **564**: p. 1-9.

37. Sanders, L.M., B.A. Kell, G.I. McRae, and G.W. Whitehead, *Prolonged Controlled-Release of Nafarelin, a Luteinizing Hormone-Releasing Hormone Analogue, from Biodegradable Polymeric Implants: Influence of Composition and Molecular Weight of Polymer.* Journal of Pharmaceutical Sciences, 1986. **75**(4): p. 356-360.

38. Nihant, N., S. Stassen, C. Grandfils, R. Jérǒme, and P. Teyssié, *Microencapsulation by coacervation of poly (lactide-co-glycolide)—II: Encapsulation of a dispersed aqueous phase.* Polymer international, 1993. **32**(2): p. 171-176.

39. Torza, S. and S. Mason, *Three-phase interactions in shear and electrical fields.* Journal of colloid and interface science, 1970. **33**(1): p. 67-83.

40. Altena, F.W. and C. Smolders, *Calculation of liquid-liquid phase separation in a ternary system of a polymer in a mixture of a solvent and a nonsolvent.* Macromolecules, 1982. **15**(6): p. 1491-1497.

41. Young, T.-H. and L.-W. Chen, *Pore formation mechanism of membranes from phase inversion process.* Desalination, 1995. **103**(3): p. 233-247.

42. Flory, P.J., *Principles of polymer chemistry.* 1953: Cornell University Press, Ithaca, NY.

43. Sauviat, M. and J.P. Cohen-Addad, *Polyisobutylene: fractional precipitation from binary solvent induced by non-solvent addition.* Polymer, 1981. **22**(4): p. 461-464.

44. Hansen, C.M., *The Three Dimensional Solubility Parameter and Solvent Diffusion Coefficient.* Copenhagen Danish Technical Press, 1967.

45. Nihant, N., C. Grandfils, R. Jérôme, and P. Teyssié, *Microencapsulation by coacervation of poly (lactide-co-glycolide) IV. Effect of the processing parameters on coacervation and encapsulation.* Journal of Controlled Release, 1995. **35**(2-3): p. 117-125.

46. Stassen, S., N. Nihant, V. Martin, C. Grandfils, R. Jérôme, and P. Teyssié, *Microencapsulation by coacervation of poly (lactide-co-glycolide): 1. Physicochemical characteristics of the phase separation process.* Polymer, 1994. **35**(4): p. 777-785.

47. Ruiz, J., B. Tissier, and J. Benoit, *Microencapsulation of peptide: a study of the phase separation of poly (D, L-lactic acid-co-glycolic acid) copolymers 50/50 by silicone oil.* International journal of Pharmaceutics, 1989. **49**(1): p. 69-77.

48. Mitchell, N., C. Brown, and S. Bermingham, *Micro-scale process development and optimization for crystallization processes.* 2017.

49. Freitas, S., H.P. Merkle, and B. Gander, *Microencapsulation by solvent extraction/evaporation: reviewing the state of the art of microsphere preparation process technology.* Journal of controlled release, 2005. **102**(2): p. 313-332.

50. Li, M., O. Rouaud, and D. Poncelet, *Microencapsulation by solvent evaporation: State of the art for process engineering approaches.* International Journal of pharmaceutics, 2008. **363**(1-2): p. 26-39.

51. Leo, E., S. Pecquet, J. Rojas, P. Couvreur, and E. Fattal, *Changing the pH of the external aqueous phase may modulate protein entrapment and delivery*

from poly(lactide-co-glycolide) microspheres prepared by a w/o/w solvent evaporation method. Journal of Microencapsulation, 1998. **15**(4): p. 421-430.

52. Freytag, T., A. Dashevsky, L. Tillman, G. Hardee, and R. Bodmeier, *Improvement of the encapsulation efficiency of oligonucleotide-containing biodegradable microspheres.* Journal of controlled release, 2000. **69**(1): p. 197-207.

53. Herrmann, J. and R. Bodmeier, *Somatostatin containing biodegradable microspheres prepared by a modified solvent evaporation method based on W/O/W-multiple emulsions.* International journal of pharmaceutics, 1995. **126**(1-2): p. 129-138.

54. Bao, W., J. Zhou, J. Luo, and D. Wu, *PLGA microspheres with high drug loading and high encapsulation efficiency prepared by a novel solvent evaporation technique.* Journal of Microencapsulation, 2006. **23**(5): p. 471-479.

55. Mehta, R.C., B.C. Thanoo, and P.P. Deluca, *Peptide containing microspheres from low molecular weight and hydrophilic poly(d,l-lactide-co-glycolide).* Journal of Controlled Release, 1996. **41**(3): p. 249-257.

56. Bodmeier, R. and J. McGinity, *Solvent selection in the preparation of poly (DL-lactide) microspheres prepared by the solvent evaporation method.* International journal of pharmaceutics, 1988. **43**(1-2): p. 179-186.

57. Rafati, H., A.G.A. Coombes, J. Adler, J. Holland, and S.S. Davis, *Protein-loaded poly(dl-lactide-co-glycolide) microparticles for oral administration: formulation, structural and release characteristics.* Journal of Controlled Release, 1997. **43**(1): p. 89-102.

58. Li, X., X. Deng, M. Yuan, C. Xiong, Z. Huang, Y. Zhang, and W. Jia, *Investigation on process parameters involved in preparation of poly-dl-lactide-poly(ethylene glycol) microspheres containing Leptospira Interrogans antigens.* International Journal of Pharmaceutics, 1999. **178**(2): p. 245-255.

59. Mehta, R.C., R. Jeyanthi, S. Calls, B.C. Thanoo, K.W. Burton, and P.P. DeLuca, *Biodegradable microspheres as depot system for patenteral delivery of peptide drugs.* Journal of Controlled Release, 1994. **29**(3): p. 375-384.

60. Jeyanthi, R., B. Thanoo, R. Metha, and P. DeLuca, *Effect of solvent removal technique on the matrix characteristics of polylactide/glycolide microspheres for peptide delivery.* Journal of Controlled Release, 1996. **38**(2-3): p. 235-244.

61. Klose, D., F. Siepmann, K. Elkharraz, S. Krenzlin, and J. Siepmann, *How porosity and size affect the drug release mechanisms from PLGA-based microparticles.* International Journal of Pharmaceutics, 2006. **314**(2): p. 198-206.

62. Siepmann, J., K. Elkharraz, F. Siepmann, and D. Klose, *How Autocatalysis Accelerates Drug Release from PLGA-Based Microparticles: A Quantitative Treatment.* Biomacromolecules, 2005. **6**(4): p. 2312-2319.

63.   Heller, J., *Controlled drug release from poly(ortho esters) — A surface eroding polymer.* Journal of Controlled Release, 1985. **2**: p. 167-177.

64.   Burkersroda, F.v., L. Schedl, and A. Göpferich, *Why degradable polymers undergo surface erosion or bulk erosion.* Biomaterials, 2002. **23**(21): p. 4221-4231.

65.   Fredenberg, S., M. Wahlgren, M. Reslow, and A. Axelsson, *The mechanisms of drug release in poly(lactic-co-glycolic acid)-based drug delivery systems—A review.* International Journal of Pharmaceutics, 2011. **415**(1): p. 34-52.

66.   Wang, J., B.M. Wang, and S.P. Schwendeman, *Characterization of the initial burst release of a model peptide from poly (D, L-lactide-co-glycolide) microspheres.* Journal of controlled release, 2002. **82**(2-3): p. 289-307.

67.   Batycky, R.P., J. Hanes, R. Langer, and D.A. Edwards, *A Theoretical Model of Erosion and Macromolecular Drug Release from Biodegrading Microspheres.* Journal of Pharmaceutical Sciences, 1997. **86**(12): p. 1464-1477.

68.   Alexis, F., S.S. Venkatraman, S.K. Rath, and F. Boey, *In vitro study of release mechanisms of paclitaxel and rapamycin from drug-incorporated biodegradable stent matrices.* Journal of Controlled Release, 2004. **98**(1): p. 67-74.

69.   Chen, X., C.P. Ooi, and T.H. Lim, *Effect of Ganciclovir on the Hydrolytic Degradation of Poly(lactide-co-glycolide) Microspheres.* Journal of Biomaterials Applications, 2006. **20**(3): p. 287-302.

70.   Kang, J. and S.P. Schwendeman, *Determination of Diffusion Coefficient of a Small Hydrophobic Probe in Poly(lactide-co-glycolide) Microparticles by Laser Scanning Confocal Microscopy.* Macromolecules, 2003. **36**(4): p. 1324-1330.

71.   Janoria, K.G. and A.K. Mitra, *Effect of lactide/glycolide ratio on the in vitro release of ganciclovir and its lipophilic prodrug (GCV-monobutyrate) from PLGA microspheres.* International Journal of Pharmaceutics, 2007. **338**(1): p. 133-141.

72.   Makino, K., T. Mogi, N. Ohtake, M. Yoshida, S. Ando, T. Nakajima, and H. Ohshima, *Pulsatile drug release from poly (lactide-co-glycolide) microspheres: how does the composition of the polymer matrices affect the time interval between the initial burst and the pulsatile release of drugs?* Colloids and Surfaces B: Biointerfaces, 2000. **19**(2): p. 173-179.

73.   Qin, C., C. Chen, Q. Xiao, N. Yang, C. Yuan, C. Kunkelmann, M. Cetinkaya, and K. Muelheims, *CFD-PBM simulation of droplets size distribution in rotor-stator mixing devices.* Chemical Engineering Science, 2016. **155**: p. 16-26.

74.   Capek, I., *Degradation of kinetically-stable o/w emulsions.* Advances in Colloid and Interface Science, 2004. **107**(2): p. 125-155.

75.   McClements, D., E. Decker, and J. Weiss, *Emulsion-based delivery systems for lipophilic bioactive components.* Journal of food science, 2007. **72**(8): p. R109-R124.

76. Schuchmann, H.P. and T. Danner, *Emulgieren: mehr als nur Zerkleinern.* Chemie Ingenieur Technik, 2004. **76**(4): p. 364-375.

77. Chesters, A., *Modelling of coalescence processes in fluid-liquid dispersions: a review of current understanding.* Chemical engineering research and design, 1991. **69**(A4): p. 259-270.

78. Liao, Y. and D. Lucas, *A literature review on mechanisms and models for the coalescence process of fluid particles.* Chemical Engineering Science, 2010. **65**(10): p. 2851-2864.

79. Bazhlekov, I.B., A.K. Chesters, and F.N. van de Vosse, *The effect of the dispersed to continuous-phase viscosity ratio on film drainage between interacting drops.* International Journal of Multiphase Flow, 2000. **26**(3): p. 445-466.

80. Frising, T., C. Noïk, and C. Dalmazzone, *The liquid/liquid sedimentation process: from droplet coalescence to technologically enhanced water/oil emulsion gravity separators: a review.* Journal of dispersion science and technology, 2006. **27**(7): p. 1035-1057.

81. Kuboi, R., I. Komasawa, and T. Otake, *COLLISION AND COALESCENCE OF DISPERSED DROPS IN TURBULENT LIQUID FLOW.* Journal of Chemical Engineering of Japan, 1972. **5**(4): p. 423-424.

82. Verhoff, F.H., S.L. Ross, and R.L. Curl, *Breakage and Coalescence Processes in an Agitated Dispersion. Experimental System and Data Reduction.* Industrial & Engineering Chemistry Fundamentals, 1977. **16**(3): p. 371-377.

83. Ross, S.L., F.H. Verhoff, and R.L. Curl, *Droplet Breakage and Coalescence Processes in an Agitated Dispersion. 2. Measurement and Interpretation of Mixing Experiments.* Industrial & Engineering Chemistry Fundamentals, 1978. **17**(2): p. 101-108.

84. Stokes, G.G., *On the effect of the internal friction of fluids on the motion of pendulums.* Vol. 9. 1851: Pitt Press Cambridge.

85. Maa, Y.-F. and C. Hsu, *Liquid-liquid emulsification by rotor/stator homogenization.* Journal of Controlled Release, 1996. **38**(2-3): p. 219-228.

86. Saadevandi, B.A. and J.L. Zakin, *A STUDY OF SILICONE OIL-IN-WATER EMULSIONS.* Chemical Engineering Communications, 1997. **156**(1): p. 227-246.

87. Scholz, P. and C.M. Keck, *Nanoemulsions produced by rotor–stator high speed stirring.* International Journal of Pharmaceutics, 2015. **482**(1): p. 110-117.

88. Kim, H.K. and T.G. Park, *Microencapsulation of dissociable human growth hormone aggregates within poly(d,l-lactic-co-glycolic acid) microparticles for sustained release.* International Journal of Pharmaceutics, 2001. **229**(1): p. 107-116.

89. Håkansson, A., *Rotor-stator mixers: from batch to continuous mode of operation—a review.* Processes, 2018. **6**(4): p. 32.

90. Mortensen, H.H., F. Innings, and A. Håkansson, *The effect of stator design on flowrate and velocity fields in a rotor-stator mixer—An experimental investigation.* Chemical Engineering Research and Design, 2017. **121**: p. 245-254.

91. van der Schaaf, U.S. and H.P. Karbstein, *Chapter 6 - Fabrication of Nanoemulsions by Rotor-Stator Emulsification*, in *Nanoemulsions*, S.M. Jafari and D.J. McClements, Editors. 2018, Academic Press. p. 141-174.

92. Jasińska, M., J. Bałdyga, S. Hall, and A.W. Pacek, *Dispersion of oil droplets in rotor–stator mixers: Experimental investigations and modeling.* Chemical Engineering and Processing: Process Intensification, 2014. **84**: p. 45-53.

93. Hall, S., M. Cooke, A. El-Hamouz, and A. Kowalski, *Droplet break-up by in-line Silverson rotor–stator mixer.* Chemical Engineering Science, 2011. **66**(10): p. 2068-2079.

94. Adler-Nissen, J., S.L. Mason, and C. Jacobsen, *Apparatus for Emulsion Production in Small Scale and Under Controlled Shear Conditions.* Food and Bioproducts Processing, 2004. **82**(4): p. 311-319.

95. Higashitani, K., K. Yoshida, N. Tanise, and H. Murata, *Dispersion of coagulated colloids by ultrasonication.* Colloids and Surfaces A: Physicochemical and Engineering Aspects, 1993. **81**: p. 167-175.

96. Sivakumar, M., S.Y. Tang, and K.W. Tan, *Cavitation technology – A greener processing technique for the generation of pharmaceutical nanoemulsions.* Ultrasonics Sonochemistry, 2014. **21**(6): p. 2069-2083.

97. Sumitomo, S., H. Koizumi, M.A. Uddin, and Y. Kato, *Comparison of dispersion behavior of agglomerated particles in liquid between ultrasonic irradiation and mechanical stirring.* Ultrasonics sonochemistry, 2018. **40**: p. 822-831.

98. Gaikwad, S.G. and A.B. Pandit, *Ultrasound emulsification: effect of ultrasonic and physicochemical properties on dispersed phase volume and droplet size.* Ultrasonics Sonochemistry, 2008. **15**(4): p. 554-563.

99. Maa, Y.-F. and C.C. Hsu, *Performance of sonication and microfluidization for liquid–liquid emulsification.* Pharmaceutical development and technology, 1999. **4**(2): p. 233-240.

100. Abismaïl, B., J.P. Canselier, A.M. Wilhelm, H. Delmas, and C. Gourdon, *Emulsification by ultrasound: drop size distribution and stability.* Ultrasonics Sonochemistry, 1999. **6**(1): p. 75-83.

101. Tabata, Y., S. Gutta, and R. Langer, *Controlled Delivery Systems for Proteins Using Polyanhydride Microspheres.* Pharmaceutical Research, 1993. **10**(4): p. 487-496.

102. Reich, G., *Ultrasound-induced degradation of PLA and PLGA during microsphere processing: influence of formulation variables.* European journal of pharmaceutics and biopharmaceutics, 1998. **45**(2): p. 165-171.

103. Freitas, S., G. Hielscher, H.P. Merkle, and B. Gander, *Continuous contact-and contamination-free ultrasonic emulsification—a useful tool for pharmaceutical development and production.* Ultrasonics sonochemistry, 2006. **13**(1): p. 76-85.

104. Myers, K.J., R.W. Ward, and A. Bakker, *A Digital Particle Image Velocimetry Investigation of Flow Field Instabilities of Axial-Flow Impellers.* Journal of Fluids Engineering, 1997. **119**(3): p. 623-632.

105. Joshi, J.B., N.K. Nere, C.V. Rane, B. Murthy, C.S. Mathpati, A.W. Patwardhan, and V.V. Ranade, *CFD simulation of stirred tanks: Comparison of turbulence models. Part I: Radial flow impellers.* The Canadian Journal of Chemical Engineering, 2011. **89**(1): p. 23-82.

106. Khang, S.J. and O. Levenspiel, *New scale-up and design method for stirrer agitated batch mixing vessels.* Chemical Engineering Science, 1976. **31**(7): p. 569-577.

107. Kumaresan, T. and J.B. Joshi, *Effect of impeller design on the flow pattern and mixing in stirred tanks.* Chemical engineering journal, 2006. **115**(3): p. 173-193.

108. Maa, Y.F. and C. Hsu, *Microencapsulation reactor scale-up by dimensional analysis.* Journal of Microencapsulation, 1996. **13**(1): p. 53-66.

109. Kiss, N., G. Brenn, H. Pucher, J. Wieser, S. Scheler, H. Jennewein, D. Suzzi, and J. Khinast, *Formation of O/W emulsions by static mixers for pharmaceutical applications.* Chemical Engineering Science, 2011. **66**(21): p. 5084-5094.

110. Kraume, M., *Mischen und Rühren*, in *Transportvorgänge in der Verfahrenstechnik: Grundlagen und apparative Umsetzungen*. 2012, Springer Berlin Heidelberg: Berlin, Heidelberg. p. 555-601.

111. Tozzi, E.J., L.A. Bacca, W.H. Hartt, M.J. McCarthy, and K.L. McCarthy, *Study of multi-lamination of a non-Newtonian fluid in a split and recombine static mixer using magnetic resonance imaging.* Chemical Engineering Science, 2013. **93**: p. 140-149.

112. Jaffer, S.A. and P.E. Wood, *Quantification of laminar mixing in the Kenics static mixer: an experimental study.* The Canadian Journal of Chemical Engineering, 1998. **76**(3): p. 516-521.

113. Maa, Y.F. and C. Hsu, *Liquid-liquid emulsification by static mixers for use in microencapsulation.* Journal of Microencapsulation, 1996. **13**(4): p. 419-433.

114. Rauline, D., P.A. Tanguy, J.M. Le Blévec, and J. Bousquet, *Numerical investigation of the performance of several static mixers.* The Canadian Journal of Chemical Engineering, 1998. **76**(3): p. 527-535.

115. Chabanon, E., N. Sheibat-Othman, O. Mdere, J.-P. Valour, S. Urbaniak, and F. Puel, *Drop size distribution monitoring of oil-in-water emulsions in SMX+ static*

mixers: Effect of operating and geometrical conditions. International Journal of Multiphase Flow, 2017. **92**: p. 61-69.

116. Das, P.K., J. Legrand, P. Morançais, and G. Carnelle, *Drop breakage model in static mixers at low and intermediate Reynolds number.* Chemical engineering science, 2005. **60**(1): p. 231-238.

117. Bayer, T., K. Himmler, and V. Hessel, *Don't be baffled by static mixers: how to select and size the correct static mixer. (Feature Report)*, in *Chemical Engineering.* 2003. p. 50+.

118. Jeffery, H., S.S. Davis, and D.T. O'Hagan, *The preparation and characterisation of poly(lactide-co-glycolide) microparticles. I: Oil-in-water emulsion solvent evaporation.* International Journal of Pharmaceutics, 1991. **77**(2): p. 169-175.

119. Rosca, I.D., F. Watari, and M. Uo, *Microparticle formation and its mechanism in single and double emulsion solvent evaporation.* Journal of Controlled Release, 2004. **99**(2): p. 271-280.

120. Thomasin, C., H.P. Merkle, and B. Gander, *Drug microencapsulation by PLA/PLGA coacervation in the light of thermodynamics. 2. Parameters determining microsphere formation.* Journal of Pharmaceutical Sciences, 1998. **87**(3): p. 269-275.

121. Stassen, S., N. Nihant, V. Martin, C. Grandfils, R. Jérôme, and P.J.P. Teyssié, *Microencapsulation by coacervation of poly (lactide-co-glycolide): 1. Physicochemical characteristics of the phase separation process.* 1994. **35**(4): p. 777-785.

122. Thomasin, C., P. Johansen, R. Alder, R. Bemsel, G. Hottinger, H. Altorfer, A.D. Wright, G. Wehrli, H. Merkle, and B. Gander, *A contribution to overcoming the problem of residual solvents in biodegradable microspheres prepared by coacervation.* European Journal of Pharmaceutics and Biopharmaceutics, 1996. **42**: p. 16-24.

123. EMA, *ICH guideline Q3C (R6) on impurities: guideline for residual solvents.* 2019. **Step 5**.

124. Passerini, N. and D. Craig, *An investigation into the effects of residual water on the glass transition temperature of polylactide microspheres using modulated temperature DSC.* Journal of Controlled Release, 2001. **73**(1): p. 111-115.

125. Vay, K., W. Frieß, and S. Scheler, *A detailed view of microparticle formation by in-process monitoring of the glass transition temperature.* European Journal of Pharmaceutics and Biopharmaceutics, 2012. **81**(2): p. 399-408.

126. Devotta, I., M.V. Badiger, P.R. Rajamohanan, S. Ganapathy, and R.A. Mashelkar, *Unusual retardation and enhancement in polymer dissolution: Role of disengagement dynamics.* Chemical Engineering Science, 1995. **50**(16): p. 2557-2569.

127. Wyzgoski, M.G. and G.S.Y. Yeh, *Origin of Impact Strength in Polycarbonate: I. Effect of Crystallization and Residual Solvent.* International Journal of Polymeric Materials and Polymeric Biomaterials, 1974. **3**(2): p. 133-148.

128. Benoit, J., F. Courteille, and C. Thies, *A physicochemical study of the morphology of progesterone-loaded poly (d, l-lactide) microspheres.* International journal of pharmaceutics, 1986. **29**(2-3): p. 95-102.

129. United States Pharmacopeial Convention, *USP 41 <467> Residual Solvents.*

130. Katou, H., A.J. Wandrey, and B. Gander, *Kinetics of solvent extraction/evaporation process for PLGA microparticle fabrication.* International Journal of Pharmaceutics, 2008. **364**(1): p. 45-53.

131. Ruchatz, F., P. Kleinebudde, and B.W. Müller, *Residual solvents in biodegradable microparticles. Influence of process parameters on the residual solvent in microparticles produced by the aerosol solvent extraction system (ASES) process.* Journal of Pharmaceutical Sciences, 1997. **86**(1): p. 101-105.

132. WHO, *Protocol to conduct equilibrium solubility experiments for the purpose of biopharmaceutical classification system-based classifications for active pharmaceutical ingredients for biowaiver.* 2018. **Revised Draft for Discussion**.

133. O'Donnell, P.B. and J.W. McGinity, *Preparation of microspheres by the solvent evaporation technique.* Advanced drug delivery reviews, 1997. **28**(1): p. 25-42.

134. Iqbal, M., N. Zafar, H. Fessi, and A. Elaissari, *Double emulsion solvent evaporation techniques used for drug encapsulation.* International journal of pharmaceutics, 2015. **496**(2): p. 173-190.

135. Yeo, Y. and K. Park, *Control of encapsulation efficiency and initial burst in polymeric microparticle systems.* Arch Pharm Res, 2004. **27**(1): p. 1-12.

136. Sanders, L.M., G.I. McRae, K.M. Vitale, and B.A. Kell, *Controlled delivery of an LHRH analogue from biodegradable injectable microspheres.* Journal of Controlled Release, 1985. **2**: p. 187-195.

137. Pettit, D.K., J.R. Lawter, W.J. Huang, S.C. Pankey, N.S. Nightlinger, D.H. Lynch, J.A.C. Schuh, P.J. Morrissey, and W.R. Gombotz, *Characterization of poly (glycolide-co-D, L-lactide)/poly (D, L-lactide) microspheres for controlled release of GM-CSF.* Pharmaceutical research, 1997. **14**(10): p. 1422-1430.

138. Ruiz, J.-M., J.-P. Busnel, and J.-P. Benoît, *Influence of average molecular weights of poly (DL-lactic acid-co-glycolic acid) copolymers 50/50 on phase separation and in vitro drug release from microspheres.* Pharmaceutical research, 1990. **7**(9): p. 928-934.

139. Kim, S.S. and D.R. Lloyd, *Microporous membrane formation via thermally-induced phase separation. III. Effect of thermodynamic interactions on the structure of isotactic polypropylene membranes.* Journal of Membrane Science, 1991. **64**(1): p. 13-29.

140. Anton Paar GmbH [20.03.2020]; Available from: https://wiki.anton-paar.com/de-de/dichlormethan/.

141. DowCorning, *Product Information on "Dow Corning® 360 Medical Fluid".* 2015.

142. Williams, Y.O.N., N. Roas-Escalona, G. Rodríguez-Lopez, A. Villa-Torrealba, and J. Toro-Mendoza, *Modeling droplet coalescence kinetics in microfluidic devices using population balances.* Chemical Engineering Science, 2019. **201**: p. 475-483.

143. Xia, L., S. Lu, and G. Cao, *Stability and demulsification of emulsions stabilized by asphaltenes or resins.* Journal of colloid and interface science, 2004. **271**(2): p. 504-506.

144. Bouwmans, I., A. Bakker, and H. Van den Akker, *Blending liquids of differing viscosities and densities in stirred vessels.* Chemical Engineering Research and Design, 1997. **75**(8): p. 777-783.

145. Dinarvand, R., S.H. Moghadam, A. Sheikhi, and F. Atyabi, *Effect of surfactant HLB and different formulation variables on the properties of poly-D,L-lactide microspheres of naltrexone prepared by double emulsion technique.* J Microencapsul, 2005. **22**(2): p. 139-51.

146. Nihant, N., C. Schugens, C. Grandfils, R. Jérôme, and P. Teyssié, *Polylactide Microparticles Prepared by Double Emulsion/Evaporation Technique. I. Effect of Primary Emulsion Stability.* Journal of Pharmaceutical Research, 1994. **11**(10): p. 1479-1484.

147. Maa, Y.F. and C.C. Hsu, *Effect of primary emulsions on microsphere size and protein-loading in the double emulsion process.* J Microencapsul, 1997. **14**(2): p. 225-41.

148. Blanco, D. and M.J. Alonso, *Protein encapsulation and release from poly(lactide-co-glycolide) microspheres: effect of the protein and polymer properties and of the co-encapsulation of surfactants.* Eur J Pharm Biopharm, 1998. **45**(3): p. 285-94.

149. Cai, C., S. Mao, O. Germershaus, A. Schaper, E. Rytting, D. Chen, and T. Kissel, *Influence of morphology and drug distribution on the release process of FITC-dextran-loaded microspheres prepared with different types of PLGA.* J Microencapsul, 2009. **26**(4): p. 334-45.

150. Johnson, K.A., *Preparation of peptide and protein powders for inhalation.* Advanced Drug Delivery Reviews, 1997. **26**(1): p. 3-15.

151. Ma, G., *Microencapsulation of protein drugs for drug delivery: Strategy, preparation, and applications.* Journal of Controlled Release, 2014. **193**: p. 324-340.

152. van der Walle, C.F., G. Sharma, and M.N.V. Ravi Kumar, *Current approaches to stabilising and analysing proteins during microencapsulation in PLGA.* Expert Opinion on Drug Delivery, 2009. **6**(2): p. 177-186.

153. Baker, M.R., *Droplet breakup using in-line mixers located in recirculation loops around batch vessels.* Chemical Engineering Science, 1993. **48**(22): p. 3829-3833.

154. Pandolfe, W.D., *Effect of dispersed and continuous phase viscosity on droplet size of emulsions generated by homogenization.* Journal of Dispersion Science and Technology, 1981. **2**(4): p. 459-474.

155. Farah, M.A., R.C. Oliveira, J.N. Caldas, and K. Rajagopal, *Viscosity of water-in-oil emulsions: Variation with temperature and water volume fraction.* Journal of Petroleum Science and Engineering, 2005. **48**(3-4): p. 169-184.

156. Yang, Y.-Y., H.-H. Chia, and T.-S. Chung, *Effect of preparation temperature on the characteristics and release profiles of PLGA microspheres containing protein fabricated by double-emulsion solvent extraction/evaporation method.* Journal of controlled release, 2000. **69**(1): p. 81-96.

157. Nihant, N., S. Stassen, C. Grandfils, R. Jérôme, P. Teyssié, and G. Goffinet, *Microencapsulation by coacervation of poly (lactide-co-glycolide). III. Characterization of the final microspheres.* Polymer international, 1994. **34**(3): p. 289-299.

158. Carrasquillo, K.G., A.M. Stanley, J.C. Aponte-Carro, P. De Jésus, H.R. Costantino, C.J. Bosques, and K. Griebenow, *Non-aqueous encapsulation of excipient-stabilized spray-freeze dried BSA into poly (lactide-co-glycolide) microspheres results in release of native protein.* Journal of Controlled Release, 2001. **76**(3): p. 199-208.

159. Blanco-Príeto, M.a.J., M.A. Campanero, K. Besseghir, F. Heimgatner, and B. Gander, *Importance of single or blended polymer types for controlled in vitro release and plasma levels of a somatostatin analogue entrapped in PLA/PLGA microspheres.* Journal of controlled release, 2004. **96**(3): p. 437-448.

160. Lee, S.L., T.F. O'Connor, X. Yang, C.N. Cruz, S. Chatterjee, R.D. Madurawe, C.M.V. Moore, L.X. Yu, and J.J.J.o.P.I. Woodcock, *Modernizing Pharmaceutical Manufacturing: from Batch to Continuous Production.* 2015. **10**(3): p. 191-199.

161. Freitas, S., A. Walz, H. Merkle, and B. Gander, *Solvent extraction employing a static micromixer: a simple, robust and versatile technology for the microencapsulation of proteins.* Journal of microencapsulation, 2003. **20**(1): p. 67-85.

162. Herbert, P.H., Azar, *Preparation of biodegradable microparticles containing a biologically active agent* US5654008.

163. Kumar, R.T., Gregory; Ramstack, Michael; Herbert, Paul; Figa, Michael, *Coacervation Process.* 2008. US20080233199A1.

164. Lyons, S.W., Steven, *Apparatus and method for preparing microparticles* US6331317B1.

165. Bitz, C. and E. Doelker, *Influence of the preparation method on residual solvents in biodegradable microspheres.* International journal of pharmaceutics, 1996. **131**(2): p. 171-181.

166. Witschi, C. and E. Doelker, *Residual solvents in pharmaceutical products: acceptable limits, influences on physicochemical properties, analytical methods and documented values.* European Journal of Pharmaceutics and Biopharmaceutics, 1997. **43**(3): p. 215-242.

167. Nogueira, R., B.C. Garrido, R.M. Borges, G.E. Silva, S.M. Queiroz, and V.S. Cunha, *Development of a new sodium diclofenac certified reference material using the mass balance approach and 1H qNMR to determine the certified property value.* European Journal of Pharmaceutical Sciences, 2013. **48**(3): p. 502-513.

168. Monakhova, Y.B., M. Kohl-Himmelseher, T. Kuballa, and D.W. Lachenmeier, *Determination of the purity of pharmaceutical reference materials by 1H NMR using the standardless PULCON methodology.* Journal of pharmaceutical and biomedical analysis, 2014. **100**: p. 381-386.

169. Shen, S., X. Yang, and Y. Shi, *Application of quantitative NMR for purity determination of standard ACE inhibitors.* Journal of pharmaceutical and biomedical analysis, 2015. **114**: p. 190-199.

170. Hou, Z., X. Liang, L. Du, F. Su, and W. Su, *Quantitative determination and validation of avermectin B1a in commercial products using quantitative nuclear magnetic resonance spectroscopy.* Magnetic Resonance in Chemistry, 2014. **52**(9): p. 480-485.

171. Liang, X., L. Du, F. Su, H.S. Parekh, and W. Su, *The application of quantitative NMR for the facile, rapid and reliable determination of clindamycin phosphate in a conventional tablet formulation.* Magnetic Resonance in Chemistry, 2014. **52**(4): p. 178-182.

172. Garner, J., S. Skidmore, H. Park, K. Park, S. Choi, and Y. Wang, *A protocol for assay of poly (lactide-co-glycolide) in clinical products.* International journal of pharmaceutics, 2015. **495**(1): p. 87-92.

173. Wahl, O. and U. Holzgrabe, *Impurity profiling of carbocisteine by HPLC-CAD, qNMR and UV/vis spectroscopy.* Journal of pharmaceutical and biomedical analysis, 2014. **95**: p. 1-10.

174. EMA, *Validation of analytical procedures: Text and Methodology Q2 (R1).* 2005.

175. Johnson, L., L. Gao, C. Shields Iv, M. Smith, K. Efimenko, K. Cushing, J. Genzer, and G. López, *Elastomeric microparticles for acoustic mediated bioseparations.* Journal of nanobiotechnology, 2013. **11**: p. 22.

176. Lo, C.-H., M.-H. Lin, K.-S. Liao, M. De Guzman, H.-A. Tsai, V. Rouessac, T.-C. Wei, K.-R. Lee, and J.-Y. Lai, *Control of pore structure and characterization of plasma-polymerized SiOCH films deposited from octamethylcyclotetrasiloxane (OMCTS).* Journal of Membrane Science, 2010. **365**(1): p. 418-425.

177. Blasi, P., A. Schoubben, S. Giovagnoli, L. Perioli, M. Ricci, and C.J.A.P. Rossi, *Ketoprofen poly(lactide-co-glycolide) physical interaction.* 2007. **8**(2): p. E78-E85.

178. *Residual solvents, chapter 5.4*, in *Ph. Eur. 9.5.*

179. Mumper, R.J. and M. Jay, *Poly(L-lactic Acid) Microspheres Containing Neutron-Activatable Holmium-165: A Study of the Physical Characteristics of Microspheres Before and After Irradiation in a Nuclear Reactor.* Pharmaceutical Research, 1992. **9**(1): p. 149-154.

180. Spenlehauer, G., M. Veillard, and J.-P. Benoit, *Formation and characterization of cisplatin loaded poly(d,l-lactide) microspheres for chemoembolization.* Journal of Pharmaceutical Sciences, 1986. **75**(8): p. 750-755.

181. Petersen, H.L., Olivier; Loeffler, Rolf; Ausborn, Michael; Bonny, Jean-Daniel, *Organic compounds.* 2007.

182. Lawter, J.R.L., Michael Gerard, *Hardening agent for phase separation microencapsulation* 1987. EP0292710B1.

183. Ramstack, M., *Method for preparing microparticles unsing liquid-liquid extraction.* 2005. US6884372B2.

184. Lewis, D.S., DJ, *Low residual solvent microspheres and microencapsulation process.* 1987. WO1989003678A1.

185. Komen, J.G., Jan W., *Process for microencapsulation.* US5066436A.

186. SigmaAldrich [01.02.2019]; Available from: https://www.sigmaaldrich.com/technical-documents/articles/chemistry/pressure-temperature-nomograph.html.

187. Li, X., X. Deng, M. Yuan, C. Xiong, Z. Huang, Y. Zhang, and W. Jia, *Investigation on process parameters involved in preparation of poly-DL-lactide-poly (ethylene glycol) microspheres containing Leptospira Interrogans antigens.* International journal of pharmaceutics, 1999. **178**(2): p. 245-255.

188. Mehta, R.C., B. Thanoo, and P.P. Deluca, *Peptide containing microspheres from low molecular weight and hydrophilic poly (d, l-lactide-co-glycolide).* Journal of Controlled Release, 1996. **41**(3): p. 249-257.

189. Wang, J. and S.P. Schwendeman, *Mechanisms of solvent evaporation encapsulation processes: Prediction of solvent evaporation rate.* Journal of Pharmaceutical Sciences, 1999. **88**(10): p. 1090-1099.

190. Chung, T.W., Y.Y. Huang, and Y.Z. Liu, *Effects of the rate of solvent evaporation on the characteristics of drug loaded PLLA and PDLLA microspheres.* Int J Pharm, 2001. **212**(2): p. 161-9.

191. Yang, Y.Y., H.H. Chia, and T.S. Chung, *Effect of preparation temperature on the characteristics and release profiles of PLGA microspheres containing*

protein fabricated by double-emulsion solvent extraction/evaporation method. J Control Release, 2000. **69**(1): p. 81-96.

192. Yang, Y.-Y., T.-S. Chung, X.-L. Bai, and W.-K. Chan, *Effect of preparation conditions on morphology and release profiles of biodegradable polymeric microspheres containing protein fabricated by double-emulsion method.* Chemical Engineering Science, 2000. **55**(12): p. 2223-2236.

193. Bosselmann, S., M. Nagao, K.T. Chow, and R.O. Williams, *Influence of formulation and processing variables on properties of itraconazole nanoparticles made by advanced evaporative precipitation into aqueous solution.* AAPS PharmSciTech, 2012. **13**(3): p. 949-960.

194. Morozumi, Y. and Y. Saito, *Effect of Physical Properties on Microexplosion Occurrence in Water-in-Oil Emulsion Droplets.* Energy & Fuels, 2010. **24**(3): p. 1854-1859.

195. Bulanov, N. and B. Gasanov, *Peculiarities of boiling of emulsions with a low-boiling disperse phase.* International Journal of Heat and Mass Transfer, 2008. **51**(7-8): p. 1628-1632.

196. Ivanov, V.M., Nefedov, P. I., *Experimental investigation of the combustion process of natural and emulsified liquid fuels*, P.I. Nefedov, Editor. 1965, National Aeronautics and Space Administration: [Washington, D.C. :].

197. Andhariya, J.V. and D.J. Burgess, *Recent advances in testing of microsphere drug delivery systems.* Expert Opinion on Drug Delivery, 2016. **13**(4): p. 593-608.

198. Su, Z.-X., Y.-N. Shi, L.-S. Teng, X. Li, L.-x. Wang, Q.-F. Meng, L.-R. Teng, and Y.-X. Li, *Biodegradable poly (D, L-lactide-co-glycolide)(PLGA) microspheres for sustained release of risperidone: Zero-order release formulation.* Pharmaceutical Development and Technology, 2011. **16**(4): p. 377-384.

7. LIST OF PUBLICATIONS

Publications

Besslich, L; Koerber, M; Bodmeier, R. Quantification and reduction of volatile and non-volatile residual solvents in poly(lactide-*co*-glycolide) microparticles prepared by an organic phase separation method. *In preparation*

Besslich, L; Koerber, M; Bodmeier, R. Study of the microparticle preparation by organic phase separation – I. Role of the phase separation process. *In preparation*

Besslich, L; Koerber, M; Bodmeier, R. Study of the microparticle preparation by organic phase separation – II. Coacervate stability and incorporation of a water-soluble peptide drug. *In preparation*

Besslich, L; Bodmeier, R. Influence of the aqueous phase temperature during the preparation of PLGA microparticles by solvent evaporation. *In preparation*

Poster presentations

Besslich, L; Koerber, M.; Bodmeier, R. Simultaneous determination and quantification of residual solvents in PLGA microparticles by H-NMR. Poster #242, PBP 11th World Meeting 2018, March 2018, Granada, Spain

Besslich, L; Koerber, M.; Bodmeier, R. Residual organic solvent content of PLGA microparticles prepared by an organic phase separation method. 21st International Symposium on Microencapsulation, September 2017, Faro-Algarve, Portugal

Besslich, L; Koerber, M.; Bodmeier, R. Simultaneous Quantitative Determination of Silicon Oils and Organic Solvent in PLGA Microparticles using H-NMR. Poster #T2251, AAPS annual meeting, October 2015, Orlando, Florida, US

8. CURRICULUM VITAE

For reasons of data protection, the curriculum vitae is not published in the electronic version.